Role of RANKL in the differentiation of B cell associated stroma in secondary lymphoid organs

Farouk Allouche

UNIVERSITÉ DE STRASBOURG

ÉCOLE DOCTORALE DES SCIENCES DE LA VIE ET DE LA SANTÉ

IBMC-CNRS UPR3572 – IMMUNOPATHOLOGIE ET CHIMIE THÉRAPEUTIQUE

THÈSE présentée par :

Farouk ALLOUCHE

Soutenue le : **12 janvier 2018**

pour obtenir le grade de : **Docteur de l'université de Strasbourg**

Discipline/ Spécialité : Aspects moléculaires et cellulaires de la biologie/Immunologie

Role of RANKL in the differentiation of B cell associated stroma in secondary lymphoid organs

THÈSE dirigée par :

Dr MUELLER Christopher DR2, CNRS, IBMC, UPR3572, Université de Strasbourg

---

RAPPORTEUR-E-S :

Dr RIZZI Marta Department of Rheumatology and Clinical Immunology
University of Freiburg, Germany

Dr WAKKACH Abdelilah DR2, CNRS, Laboratoire de PhysioMédecine Moléculaire
UMR7370, Université Nice Sophia Antipolis

EXAMINATRICE :

Pr FOURNEL Sylvie Laboratoire de Conception et Applications de Molécules Bioactives
UMR7199, Université de Strasbourg

Ad familiam, sempre fidelis

Remerciements

Je voudrais remercier les membres du jury de thèse, M^me^ le Professeur Sylvie Fournel, M^me^ le Docteur Marta Rizzi et M^r^ le Docteur Abdelilah Wakkach d'avoir accepté d'évaluer mon travail de thèse.

Je tiendrais également à remercier l'université de Strasbourg, mon université dont je suis particulièrement fier, pour tout le travail déployé avec et pour les doctorants. Merci notamment à toute l'équipe de l'ED414 : Pr. Serge Potier, Dr. Catherine Schuster, Mme. Mélanie Muser et Mme. Géraldine Schverer. Votre sympathie, efficacité et disponibilité sont plus qu'appréciables.

Je souhaiterais remercier Madame le professeur Sylviane Mueller, notre directrice, de m'avoir admis au sein de son institut. Je vous suis reconnaissant pour votre empathie et votre soutien. Votre engagement scientifique et votre parcours me seront toujours une grande source d'inspiration.

Je voudrais notamment remercier le Dr. Christopher Mueller, Chris, mon directeur de thèse de m'avoir choisi pour mener ce projet. J'ai toujours été impressionné par tes qualités scientifiques, tes connaissances et ton savoir-faire. Grâce à toi, je comprends mieux la "Deutsche Qualität". Les barbecues à la Robertsau, les longues mais fructueuses réunions d'équipe et le stress des deadlines improbables vont certainement me manquer. Je tiens particulièrement à te remercier de ton aide et ton soutien infaillibles dans mes projets associatifs et extracurriculaires.

J'aimerais également remercier Monique et Delphine pour leur travail laboureux, leur gestion des lignées de souris et des différentes vagues d'immunisation assez longues et interminables. Je voudrais surtout leur remercier de m'avoir appris à travailler avec la souris. Vous étiez bien patientes et ça a fini par payer.

Merci à tous les membres de l'équipe d'avoir rendu cette expérience agréable et enrichissante. Merci Vincent pour ton aide précieuse en cytométrie en flux. Merci Janina pour les nombreuses manips effectuées ensemble. Merci à Evelyne, Astrid, Mélanie, Olga, Adrien, Quentin et Abdou.

Merci également à Jean-Daniel de ton aide en microscopie, en analyse d'image, et surtout ta disponibilité.

Merci à Isabelle de son aide pour toutes les démarches administratives qui resteront toujours un mystère pour moi.

Je tiendrais particulièrement à remercier Hélène Dumortier, Diane, Laurie et Matthieu qui étaient présents au moment le plus difficile. Votre soutien et votre aide m'ont été d'un grand secours, je m'en souviendrai toujours.

Ma reconnaissance s'adresse aussi au Dr. Laurent Miguet, mon encadrant de master. Sans ton soutien, ton aide, tes conseils et ton appui, je n'aurais jamais pu continuer mon parcours en doctorat.

Merci aux jumelles : Janina et Sophia pour leur soutien et leur disponibilité tout au long de la thèse. Votre bonté et votre ouverture d'esprit ont toujours été mon refuge et mon point d'appoint. Je ne saurais jamais vous remercier assez.

Merci à Astrid qui a été une deuxième maman pour moi pendant ma thèse. Son affection et sa disponibilité m'ont toujours été d'une grande aide.

Merci à Cécilia pour tous ces moments culturels enrichissants qu'on a passé ensemble et de m'avoir fait découvrir des nouveaux styles de théâtre à Strasbourg.

Merci à toute l'armada : Diane, Janina, Sophia, Mathieu, Adriano, Flora, Giacomo, Maud et Cécile pour les innombrables moments hilarants passés ensemble. Les barbecues à Hartmannswiller, Noël au Luxembourg, les Cheese and Wine evenings, et les soirées improvisées vont sans doute me manquer. Vous avez rendu mon passage dans le labo bien agréable, j'en suis sorti avec des amitiés inestimables.

Merci Romain et Alexandre pour tous vos conseils scientifiques et culinaires. Je me souviendrai certainement des cours de méditation à 6h le matin à Mittelwihr, des réunions préparatoires de la commission recherche et des posters spéciaux.

Merci au programme doctoral international de l'université, à son coordinateur, Dr. Christopher Mueller, ses gestionnaires administratifs Virginie Herbasch et Florian Fritsch qui ont été particulièrement à l'écoute ainsi que les doctorant-e-s membres de ma promotion « Hellen Keller » et des autres promotions. Notre solidarité a toujours payé et notre aventure continuera après la thèse.

Merci à toutes les équipes associatives à Strasbourg, Paris et Bruxelles, avec qui j'ai mené une aventure extraordinaire et à qui je dois toute ma reconnaissance.

Merci à Béchara, Calvin, Stefanos, Najwa, Elsa, Shree, Antoine, Marie-Belle, Adrien, Garen, Lydia, Matteo, Gabriella, Laura, Marta, Francesca, Thomas, Giorgios, Sébastien, Agatha, Frangiska, Elisabetta, Giannis, Charchit, et tous ceux que j'ai pu oublier d'avoir été présents à mes côtés ; vous êtes une deuxième famille pour moi. Je sais que je peux toujours compter sur votre soutien.

Ma reconnaissance éternelle s'adresse à mes parents et ma sœur. Ensemble nous avons parcouru un long chemin parsemé de difficultés et d'obstacles, mais votre foi en moi et votre soutien indéfectible m'ont toujours rendu plus fort. Ayez l'assurance de mon amour filial et fraternel inconditionnel. Petite sœur, tu es la prochaine !

Table of contents

Résumé en Français

Introduction

Stroma associé aux lymphocytes *B*

Notre laboratoire étudie le rôle du stroma dans le contrôle et le fonctionnement du système immunitaire (cf. schéma ci-contre). En plus de son rôle structural dans la mobilité et le positionnement cellulaires, le stroma fournit également des signaux régulateurs pour la viabilité, la prolifération et la différenciation des cellules. Ainsi, dans les organes lymphoïdes secondaires, à savoir les ganglions lymphatiques et la rate, les cellules fibroblastiques dendritiques folliculaires (FDC) organisent les lymphocytes B dans les follicules primaires et les centres germinatifs, présentent les antigènes pour l'activation des récepteurs des lymphocytes B (BCR) et des signaux de survie et favorisent ainsi la différenciation et la maturation de l'affinité des lymphocytes B (*1*). Les cellules réticulaires marginales récemment découvertes (MRC), qui sont également des cellules fibroblastiques, sont localisées dans la zone marginale ; elles tapissent la région corticale des follicules de lymphocytes B (cf. figure 1). Ces cellules expriment RANKL et la chémokine CXCL13 (*2*). Une lignée cellulaire de type MRC favorise la migration des lymphocytes B (*2*), suggérant que les MRCs pourraient jouer un rôle important dans la biologie des lymphocytes B. Or, jusqu'à présent, la fonction des MRCs *in vivo* reste méconnue. Récemment, il a été suggéré que les MRCs sont des cellules précurseurs pour les FDCs (*3*).

Stroma → Cellules Immunitaires

Fibroblastes
Cellules endothéliales
Cellules épithéliales
Cellules nerveuses
Cellules Souches

RANKL, un régulateur du système immunitaire

RANKL (ligand de l'activateur récepteur de NF-kB) est un membre de la super famille (SF) du facteur de nécrose tumorale (TNF) ; son interaction avec son récepteur RANK permet la transduction du signal. RANKL joue un rôle important pour les cellules immunitaires en favorisant l'hématopoïèse dans la moelle osseuse (en induisant la différenciation des ostéoclastes qui dégradent la matrice osseuse), la mobilisation des cellules souches hématopoïétiques et le développement des ganglions lymphatiques (*4*). Chez l'adulte, RANKL est exprimé de manière constitutive par les MRCs, alors que, dans des conditions d'inflammation, les kératinocytes et les lymphocytes T l'expriment également. Le récepteur RANK est exprimé par les macrophages et les cellules dendritiques, mais aussi par les cellules épithéliales et les cellules endothéliales. La fonction de RANKL exprimé par les MRCs n'a pas été étudiée.

Objectifs de la thèse

Les objectifs de la thèse sont de mieux comprendre le rôle de RANKL exprimé par les MRC dans la régulation de l'activité des cellules B. Étant donné que les MRCs sont positionnés à proximité des lymphocytes B et peuvent être des précurseurs des FDCs, il est probable que les MRCs jouent un rôle dans le recrutement des lymphocytes B ainsi que dans leur activation (cf. la figure 1).

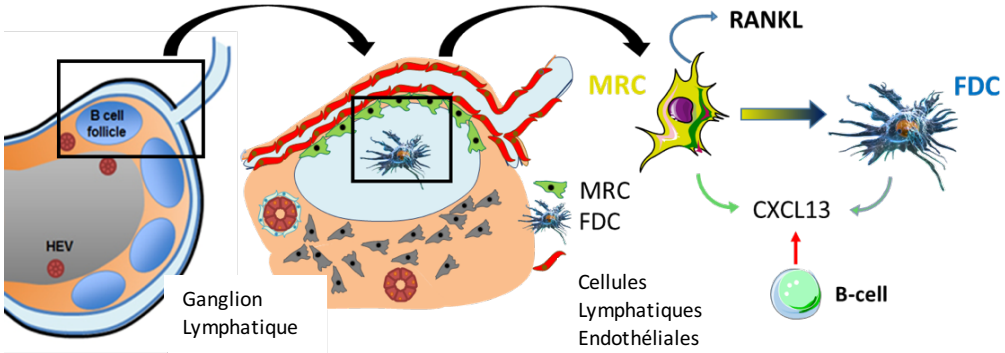

Figure 1. *À gauche : Les organes lymphoïdes secondaires tels que les ganglions lymphatiques comprennent des cellules B assemblées dans des follicules. Centre : les FDCs résident dans les follicules tandis que les MRCs forment la bordure à côté des cellules endothéliales lymphatiques. A droite : les MRCs expriment RANKL et peuvent être des précurseurs de FDCs. Les MRCs et les FDCs produisent CXCL13, une chimokine qui attire les cellules B.*

Pour aborder ces questions, j'ai étudié des souris présentant une déficience conditionnelle pour RANKL dans les MRCs. Mes résultats me permettent de conclure que RANKL produit par les MRCs réglemente la production CXCL13 et la formation de FDCs. De plus, RANKL semble jouer un rôle dans le recrutement des lymphocytes B aux organes lymphoïdes secondaires et leur prolifération.

Résultats

Le rôle concomitant de RANKL dans les MRCs et dans la fonction des FDCs

Le stroma immunitaire est régulé par des membres de la superfamille des TNFs tels que TNFα et lymphotoxine αβ (5). Notre laboratoire avait montré ont montré que RANKL joue également un rôle dans la régulation du stroma immunitaire. Dans un modèle souris où RANKL est surexprimé, Hess et al. (6) ont montré que les cellules stromales étaient activées pour proliférer et pour recruter un grand nombre de lymphocytes conduisant à une hyperplasie des ganglions lymphatiques. Grâce à un consortium financé par l'Union Européenne, C. Mueller et la doctorante Olga Cordeiro ont généré un knock-out conditionnel de RANKL dans les MRC ($RANKL^{\Delta ccl19}$) et pouvaient montrer que MRC RANKL fonctionne pour activer les cellules endothéliales lymphatiques juxtaposées (figure 1) (7). J'ai contribué à cette publication :

> Cordeiro OG, Chypre M, Brouard N, Rauber S, **Alloush F**, Romera-Hernandez M, Benezech C, Li Z, Eckly A, Coles MC, Rot A, Yagita H, Leon C, Ludewig B, Cupedo T, Lanza F, Mueller CG (2016) Integrin-Alpha IIb Identifies Murine Lymph Node Lymphatic Endothelial Cells Responsive to RANKL. PLoS ONE 11: e0151848.

J'ai étudié ces souris $RANKL^{\Delta CCL19}$ et j'ai constaté qu'en l'absence de RANKL spécifique aux MRCs, l'expression de CXCL13 et le nombre des FDCs étaient fortement réduits, entraînant une formation anormale de follicules de lymphocytes B (Figure 2-B, D). J'ai montré que le nombre de MRCs ne changeait pas (data non montrée) et j'ai confirmé par qRT-PCR que l'expression de CXCL13 était considérablement diminuée (figure 2-C).

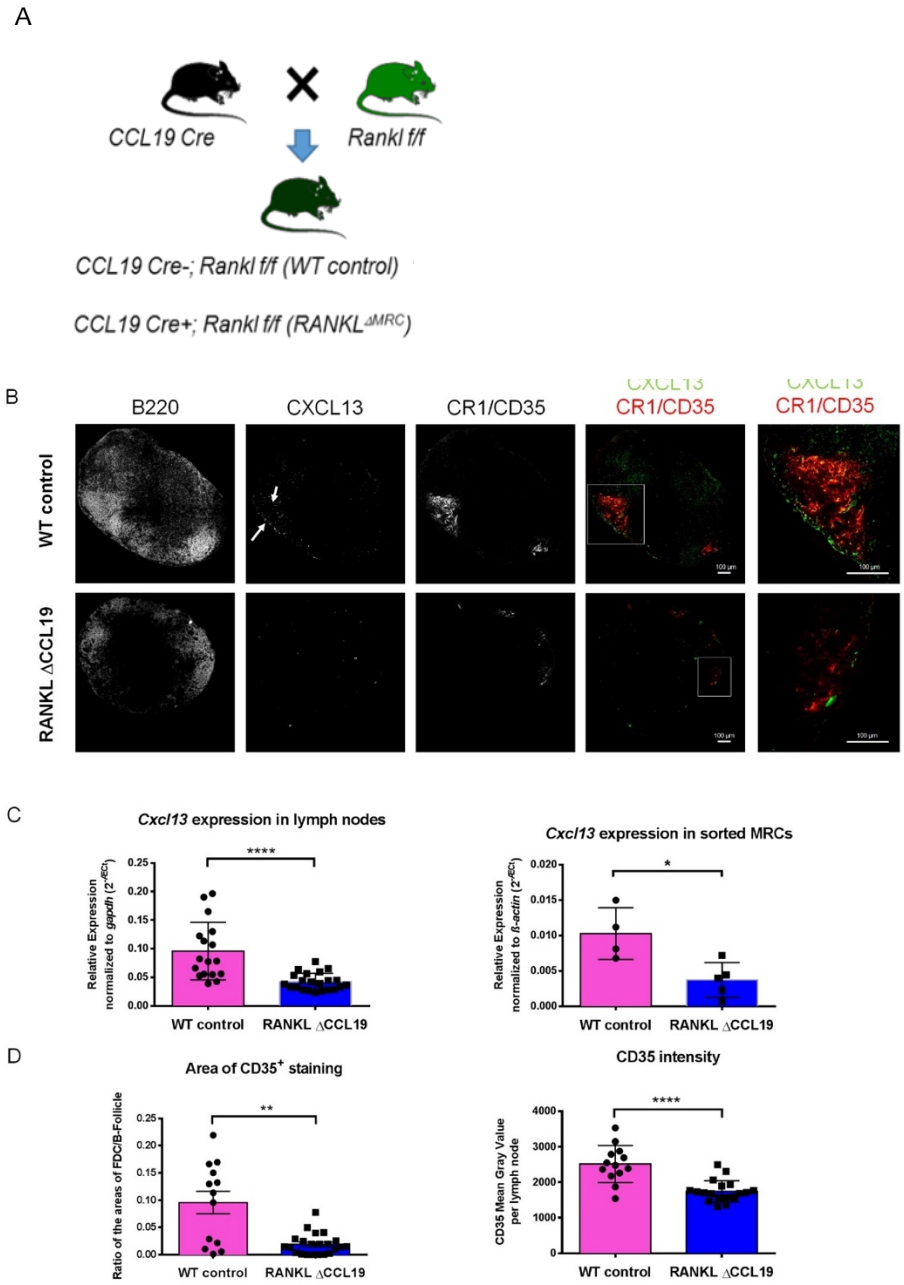

Figure 2. *(A) : Les souris portant la recombinase Cre sous le contrôle du promoteur CCL19 ont été croisées avec celles portant RANKL floxé pour générer les souris contrôles et celles RANKL$^{\Delta CCL19}$. (B) : leurs ganglions lymphatiques poplités ont été marqués pour FDC (CD35) et CXCL13. Il semble que les souris RANKL$^{\Delta CCL19}$ manquent de FDCs et de CXCL13. Echelle : 100 µm. (C) : A gauche - l'expression de Cxcl13 a été mesurée par qRT-PCR dans les différents ganglions (poplités, axillaires, inguinaux et brachiaux) de différentes souris (n>5). Chaque point représente le niveau d'expression d'un ganglion lymphatique. A droite – Le niveau d'expression de Cxcl13 dans les MRCs triés d'un pool de ganglions périphériques. Chaque point représente le niveau d'expression d'ARNm d'une expérience. Les barres horizontales représentent les valeurs moyennes ±SED. (D) : A gauche – la formation du réseau FDC dans les follicules B des coupes de ganglions poplités a été calculée en rapportant la surface de la zone CD35+ à celle B220+. Chaque point représente une valeur correspondant à un follicule B d'un ganglion des différentes coupes de ganglions de plus que 3 souris différentes. A droite – L'intensité du marquage CD35 a été déterminée dans la zone marquée CD35+. Chaque point représente la valeur d'une zone CD35 d'un follicule B des différentes coupes de ganglions poplités. Les barres horizontales représentent les valeurs moyennes ±SED. Significativité : *=p<0.05 ; **=p<0.01 ; ****=p<0.0001 ; ns = non significatif.*

Ces résultats montrent que RANKL exprimé constitutivement par les MRCs contrôle positivement la transcription de CXCL13 par les MRCs et la différenciation des FDCs.

Ainsi, RANKL peut constituer une nouvelle stratégie thérapeutique pour contrecarrer simultanément la production CXCL13 et la formation FDC.

Mécanisme sous-jacent de RANKL lors de l'activation des MRCs

Il a été montré que TNFR1 est nécessaire pour la formation de FDCs (*8*) et que la co-signalisation TNFR1 et LTβR est requise pour la production maximale de CXCL13 (9). Pour comprendre le mécanisme sous-jacent à l'activation des MRCs et à la formation du réseau des FDCs par RANKL, j'ai donc mesuré l'expression de LTα, LTβ, TNFα et leurs récepteurs respectifs TNFR1, TNFR2 et LTβR par qRT-PCR dans les ganglions lymphatiques entiers. De manière frappante, j'ai constaté que seule l'expression de TNFR1 était considérablement réduite, alors que l'expression de tous les autres gènes était normale (Figure 3-A). J'ai pu également montrer que les cellules concernées par cette baisse de TNFR1 sont bien les MRCs (Figure 3-B).

Par ailleurs, j'ai montré par qRT-PCR que les MRCs elles-mêmes n'expriment pas RANK et que les souris RANK knock-out dans les MRCs ne montrent aucun phénotype (données non montrées). Par conséquent, RANKL ne transduit pas le signal cellulaire de manière autonome et à ce stade, l'identité de la cellule sensible au RANKL n'est pas claire.

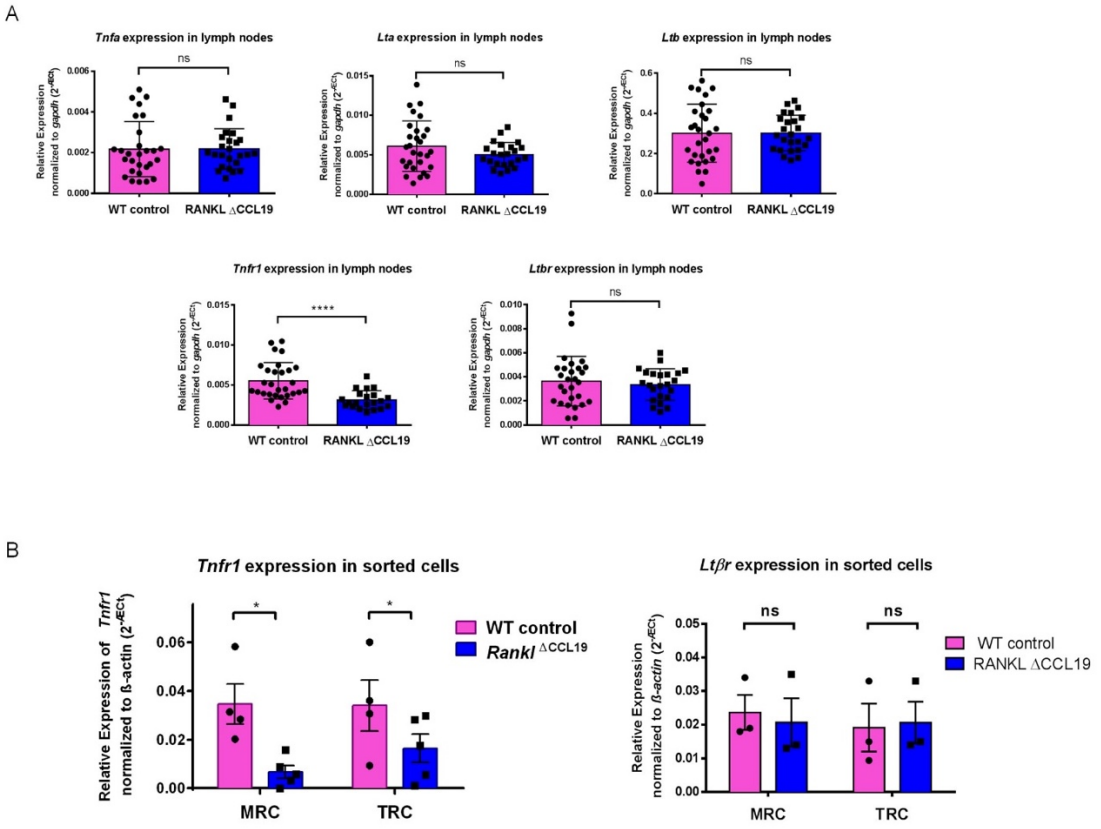

Figure 3. *(A) : l'expression de Tnfa, Lta, Ltb, Tnfr1 et Ltbr a été mesurée par qRT-PCR dans différents ganglions lymphatiques (axiaux, brachiaux et inguinaux) de différentes souris (n>5 Chaque point représente le niveau d'expression d'un ganglion lymphatique (B) : Le niveau d'expression de Tnfr1 et Ltbr dans les MRCs et TRCs triés d'un pool de ganglions périphériques. Chaque point représente le niveau d'expression d'ARNm d'une expérience. Les barres horizontales représentent les valeurs moyennes ±SED. Significativité : *=p<0.05 ; **=p<0.01 ; ****=p<0.0001 ; ns = non significatif.*

Rôle de RANKL dans l'activation des lymphocytes B

Parce que CXCL13 et les FDCs jouent un rôle important dans la réaction du centre germinatif qui conduit à la production de lymphocytes B, nous avons évalué l'impact de la déficience de RANKL sur la réponse immunitaire humorale. Les souris RANKL$^{\Delta CCL19}$ et les souris contrôles étaient immunisées avec de l'ovalbumine, de l'alun et *B. pertussis* inactivée par la chaleur. Le sang a été prélevé après chaque immunisation et le taux d'IgG et d'IgM anti-OVA a été mesuré par ELISA. A la fin de l'expérience, les souris ont été sacrifiées et les ganglions poplités drainantes ont été analysés (figure 4A). La production d'IgG n'a montré aucune différence significative entre les souris témoins WT et les KO à n'importe quel stade

pendant l'immunisation (Figure 4B). Cependant, de manière surprenante, aucune IgM n'a été détectée dans les souris KO tandis que certaines souris WT ont fortement produit cet isotype (Figure 4B). Les ganglions poplités ont été analysés pour l'expression de l'ARNm Cxcl13 (Figure 4C), ou, en marquage immunofluorescent pour B220, CXCL13 et CD35, et l'étendue du réseau CD35 + FDC et l'intensité de l'expression CD35 a été déterminée (Figure 4D, E). Il n'y avait pas de différence dans le niveau de Cxcl13 et l'étendue et l'intensité du marquage CD35 étaient similaires. Enfin, les sections ont également été colorées pour les cellules B du centre germinal GL7+ (figure 4F). Le marquage GL7 était présent dans les deux génotypes. Par conséquent, l'inflammation peut surmonter l'expression de CXCL13 restreinte par RANKL et la formation de FDC pour générer une réaction normale du centre germinatif. Nous avons ensuite testé si ce soulagement s'accompagnait d'une normalisation de l'expression de *Tnfr1*. Bien que les niveaux aient augmenté chez les deux génotypes par rapport aux ganglions non immunisés, l'expression de *Tnfr1* est restée significativement plus faible chez les souris RANKLCCL19, montrant que l'expression réduite de TNFR1 résiste au stimulus inflammatoire.

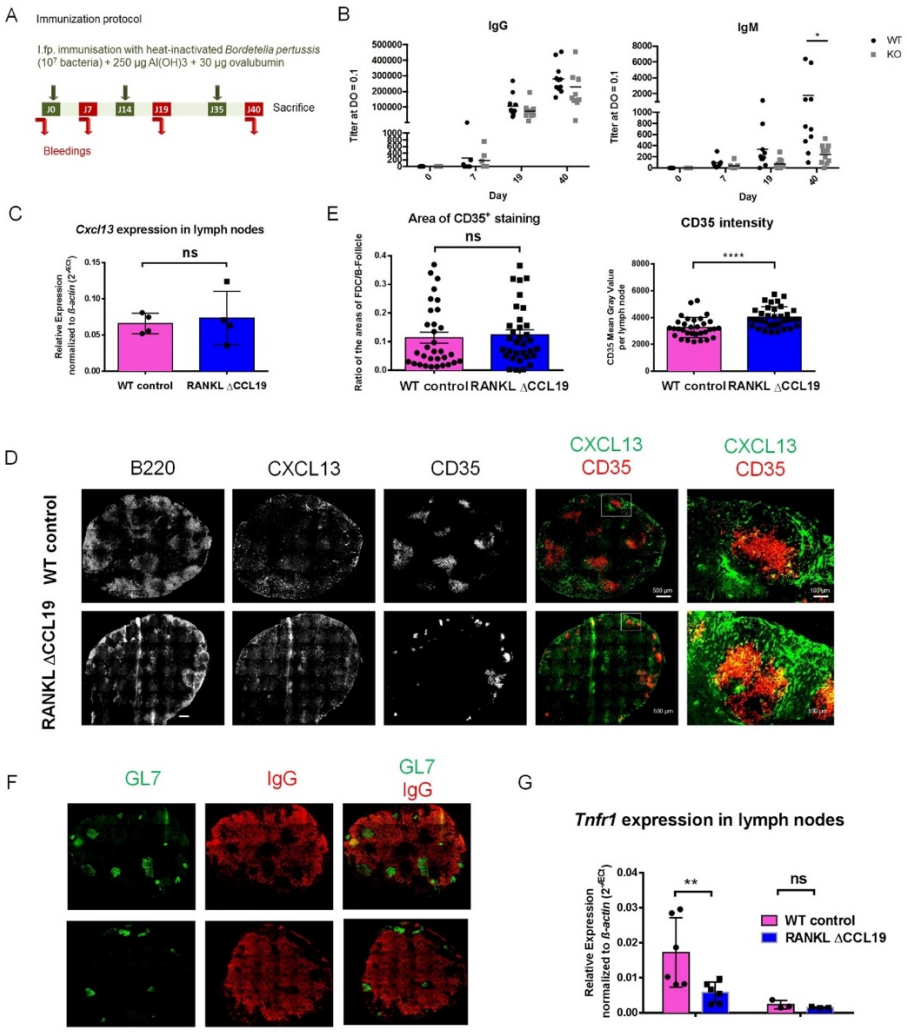

Figure 4. *(A) : Protocole d'immunisation. Les souris étaient immunisées dans les cuisses des pates postérieures et ont été saignées aux temps indiqués. Après la saignée finale, les souris ont été sacrifiées et les ganglions poplités drainant ont été analysés. (B) Mesure par ELISA des niveaux d'immunoglobuline IgG et IgM sériques spécifiques de l'ovalbumine de poulet. Chaque point représente une souris et le Les barres horizontales représentent les valeurs moyennes. (C) : Expression de l'ARNm de Cxcl13 mesurée par qRT-PCR dans les ganglions poplités. Chaque point représente une valeur obtenue d'une souris. Les barres horizontales représentent les valeurs moyennes ±SED. (D) : coupes de ganglions poplités marquées par immunofluorescence pour FDC (CD35) et CXCL13. Echelle : 100 µm. (E) : A gauche – la formation du réseau FDC dans les follicules B des coupes de ganglions poplités a été calculée en rapportant la surface de la zone CD35+ à celle B220+. Chaque point représente une valeur correspondant à un follicule B d'un ganglion des différentes coupes de ganglions de plus que 5 souris différentes. A droite – L'intensité du marquage CD35 a été déterminée dans la zone marquée CD35+. Chaque point représente la valeur d'une zone CD35 d'un follicule B des différentes coupes de ganglions poplités (N>5). Les barres horizontales représentent les valeurs moyennes ±SED. (F) : Coupes de ganglions poplités marqués par immunofluorescence pour les centres germinatifs (GL7) et les IgG. Echelle : 100 µm. (G) Expression de Tnfr1 et Ltbr dans les ganglions poplités. Chaque point représente le niveau d'expression d'ARNm d'un ganglion lymphatique différent. Les barres horizontales représentent les valeurs moyennes ±SED. Significativité : *=p<0.05 ; **=p<0.01 ; ****=p<0.0001 ; ns = non significatif.*

Conclusion et Perspectives

RANKL joue un rôle clé dans l'organogenèse des organes lymphoïdes secondaires durant l'embryogenèse. Cependant, son rôle à l'âge adulte reste peu connu. Lors de ma thèse, j'ai pu montré qu'en plus du rôle de RANKL dans l'activation des LECs (7), il est également indispensable pour la différenciation des FDCs, la sécrétion de CXCL13 et ainsi l'organisation des lymphocytes B dans le follicule.

Dans le but de vérifier si le rôle de RANKL dans cette organisation folliculaire fait intervenir la signalisation TNFα/TNFR1, il serait intéressant, dans la suite de cette étude, injecter du TNFα et suivre l'expression de CXCL13 ainsi que la formation des FDCs dans les souris $MRC^{\Delta RANKL}$.

Afin d'élucider la cascade de signalisation cellulaire qui permet à RANKL de réguler la formation de follicules de lymphocytes B, et étant donné que RANKL exprimé par les MRCs active les LECs, nous avons généré un modèle de souris où RANK est knock-out dans les LECs. Ceci nous permettra de savoir si RANKL contrôle la formation des follicules de lymphocytes B ainsi que l'expression de CXCL13 à travers l'activation des LECs.

References

1. M. E. M. El Shikh, C. Pitzalis, Follicular dendritic cells in health and disease. *Front. Immunol.* **3**, 292 (2012).
2. T. Katakai *et al.*, Organizer-like reticular stromal cell layer common to adult secondary lymphoid organs. *J. Immunol. Baltim. Md 1950.* **181**, 6189–6200 (2008).
3. M. Jarjour *et al.*, Fate mapping reveals origin and dynamics of lymph node follicular dendritic cells. *J. Exp. Med.* **211**, 1109–1122 (2014).
4. C. G. Mueller, E. Hess, Emerging Functions of RANKL in Lymphoid Tissues. *Front. Immunol.* **3**, 261 (2012).
5. J. H. Fritz, J. L. Gommerman, Cytokine/stromal cell networks and lymphoid tissue environments. *J. Interferon Cytokine Res. Off. J. Int. Soc. Interferon Cytokine Res.* **31**, 277–289 (2011).
6. E. Hess *et al.*, RANKL induces organized lymph node growth by stromal cell proliferation. *J. Immunol. Baltim. Md 1950*. **188**, 1245–1254 (2012).
7. O. G. Cordeiro *et al.*, Integrin-Alpha IIb Identifies Murine Lymph Node Lymphatic Endothelial Cells Responsive to RANKL. *PloS One*. **11**, e0151848 (2016).
8. M. Pasparakis *et al.*, Peyer's patch organogenesis is intact yet formation of B lymphocyte follicles is defective in peripheral lymphoid organs of mice deficient for tumor necrosis factor and its 55-kDa receptor. *Proc. Natl. Acad. Sci. U. S. A.* **94**, 6319–6323 (1997).
9. R. Gräbner *et al.*, Lymphotoxin beta receptor signaling promotes tertiary lymphoid organogenesis in the aorta adventitia of aged ApoE-/- mice. *J. Exp. Med.* **206**, 233–248 (2009).

List of Abbreviations

Ag	antigen
Aire	Autoimmune regulatory element
AP-1	activator protein 1
APC	antigen presenting cells
BAFF	B cell survival factor
BALT	bronchial-associated lymphoid tissue
BCR	B cell receptor
BCMA	B cell maturation antigen
BEC	blood endothelial cells
bHLH	basic Helix-Loop-Helix
BM	bone marrow
CCL	chemokine (C-C motif) ligand
CCR	chemokine (C-C motif) receptor
CD	cluster of differentiation
Cl2MDP	dichloromethylene diphosphonate
CLCA	Chloride channel accessory 1
CXCL	chemokine (C-X-C motif) ligand
CXCR	chemokine (C-X-C motif) receptor
DC	dendritic cell
Dll1	Notch ligands Delta-like 1
DN	double negative cells
DNA	deoxyribonucleic acid
DZ	Dark Zone
EGF	epidermal growth factor
ELISA	enzyme-linked immunosorbent assay
EpCAM	epithelial cell adhesion molecule
ER	endoplasmic reticulum
Fc	Fragment crystallizable region
FCRγ	Fc receptor common γ subunit
FDC	follicular dendritic cells
FRC	fibroblastic reticular cells
GC	Germinal Center
gp38	Glycoprotein 38
HEV	high endothelial venules (HEV)

IC	Immune Complex
ICAM	InterCellular Adhesion Molecule
IFN	interferon
Ig	immunoglobulin
IKK	IκB kinase
IL	interleukin
I.P.	Intraperitoneal
ISL	insulin gene enhancer protein
ITGA2b	integrin alpha-IIb
ITIM	tyrosine-based inhibitory motif
I.V.	Intravenously
Jg1	Jagged1
KO	knockout
LCK	lymphocyte specific protein tyrosine kinase
LEC	lymphatic endothelial cells
LFA-1	Lymphocyte function-associated antigen 1
LN	lymph node
LPS	lipopolysaccharide
LT	lymphotoxin
LTi	Lymphoid tissue inducer
LTo	lymphoid tissue organizer
LYVE1	lymphatic vessel endothelial hyaluronan receptor 1
LZ	light zone
mAb	monoclonal antibody
MAdCAM-1	mucosal vascular addressin cell adhesion molecule 1
MALT	mucosal associated lymphoid tissues
MFGE8	Milk fat globule-EGF-factor 8
MHC	major histocompatibility complex
MRC	marginal reticular cells
mRNA	messenger RNA
NALT	nasal-associated lymphoid tissue
NF-κB	nuclear factor-kappa B
NK	natural-killer
NKX	NK2 homeobox 5 protein
NRP2	neuropilin 2
OPG	osteoprotegerin
PD	programmed death protein
PD-L1	programmed death protein – ligand 1
PDGFR	platelet-derived growth factor receptor 1
PECAM	platelet endothelial cell adhesion molecule

PNAd	peripheral node adressin
PNAD	Protein NH_2-Terminal Asparagine Deamidase
PP	Peyer's patches
preFDC	ubiquitous perivascular precursor of FDC
Prox1	prospero homeobox 1
PTA	peripheral tissue restricted antigens
qRT-PCR	quantitative real time – polymerase chain reaction
RA	retinoic acid
RANK	receptor activator of NF-κB
RANKL	receptor activator of NF-κB ligand
RAR	retinoic acid receptor
ROR	retinoic acid receptor-related orphan receptor
RNA	ribonucleic acid
SCID	severe combined immunodeficiency
SCS	subcapsular sinus
SHM	somatic hypermutation
SLO	secondary lymphoid organs
SMA	alpha smooth muscle actin
SSM	subcapsular sinus macrophages
TACI	transmembrane activator and calcium modulator and cyclophilin-ligand interactor
TBM	tingible-body macrophage
TCR	T cell receptor
T_{FH}	follicular helper T cell
TGF-β	transforming growth factor β
TLR	toll-like receptor
TNF	tumor necrosis factor
TNFRSF	tumor necrosis factor receptor super family
TNFSF	tumor necrosis factor super family
TRAF	TNF receptor associated factor
TRC	T cell zone reticular cells
Treg	regulatory T cells
VCAM-1	Vascular cell adhesion protein 1
VE-cadherin	vascular endothelial cadherin
VEGF	vascular endothelial growth factor
VEGF-C	vascular endothelial growth factor C
VEGFR	vascular endothelial growth factor receptor
wt	wild type

INTRODUCTION

Introduction

The immune system is a host defense system that ensures organism protection. It comprises different structures that we can classify into 2 categories: primary lymphoid organs including bone marrow and thymus, and secondary lymphoid organs (SLOs) including lymph nodes (LNs), spleen and mucosal associated lymphoid tissues such as Peyer's Patches (PPs), tonsils, nasal-associated lymphoid tissue (NALTs) and bronchial-associated lymphoid tissue (BALTs). SLOs form together with the lymphatic vascular network what we call the lymphatic system. During my thesis, I focused on the organization and function of one of the SLOs, namely lymph nodes, in immune response and homeostasis.

1. Ontogeny of lymph nodes

Histological and molecular studies show that LN development starts in the embryo and continues several weeks after birth (1). Five stages of LN organogenesis have been identified (2). The initial stage occurs at E10.5 with the formation of the lymph sac which sprouts to form lymphatic vessels during the second stage at E14.5-15.5 (3, 4). Then, mesenchymal connective tissue infiltrates the lymph sac to form the primary LN anlagen where stromal cells, some leukocytes, capillaries and vascular loops can be identified (Figure 1-1) (1, 2). Even though some LNs develop earlier than others, the achievement of the LN morphogenesis is completed during embryogenesis at around E17.5-18 (5). During the fourth stage, $CD45^+$ $CD4^+$ $CD3^-$ $IL7R\alpha^+$ Lymphoid Tissue inducer cells (LTis) are recruited and interacts with the stromal organizer cells (2, 6). The ultimate stage is marked by B and T cell recruitment and the expansion of the LN (6).

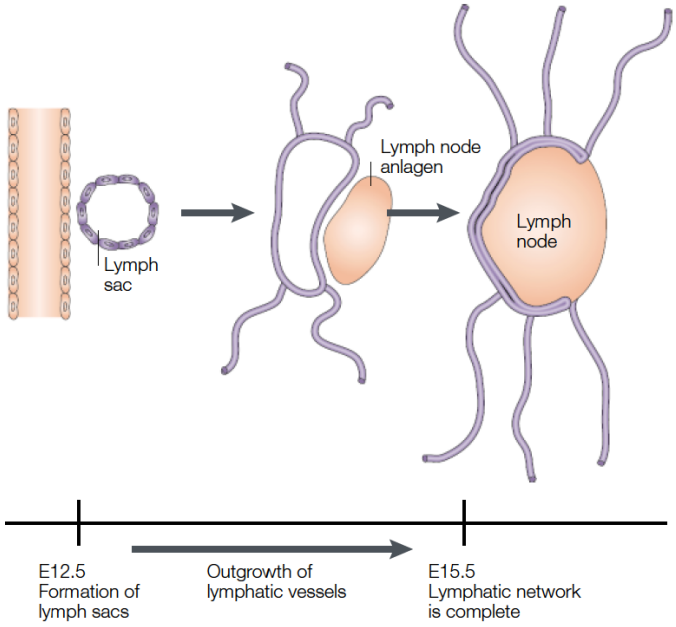

Figure 1-1 - LN anlagen genesis. *Following its formation, the lymph sac is infiltrated by mesenchymal tissue in order to form the lymph node anlagen. Modified after reference* **(2)**.

1.1. Cellular actors: LTis and LTos

1.1.1. Lymphoid Tissue inducer cells (LTis)

LTis are the first hematopoietic cells to colonize the LN anlagen and are detected in mouse as a cluster of IL7Rα/CD127-positive cells (7). They were described as part of the innate lymphoid cell family like Natural Killers (NK); they are negative for lymphoid, myeloid and erythroid markers except for CD4 (7–10). Chemokines like CXCL13 (Chemokine C-X-C motif ligand 13) and CCL21 (Chemokine C-C motif ligand 21) expressed by stromal cells are required for initial clustering of LTis that express their respective receptors CXCR5 (chemokine C-X-C motif receptor 5) and CCR7 (chemokine C-C motif receptor 7) (6, 11). In addition, a negative regulator of basic helix-loop-helix (bHLH) protein signaling Id2 and the nuclear retinoic acid (RA) receptor-related orphan receptor RORγt are required for CXCL13 production. LTi survival and differentiation require interleukin-7 (IL-7) signaling. The lymphotoxin α1β2 (LTα1β2) ensures their function via its interaction with LTβR expressed by stromal cells. LTα1β2 expression is dependent on RANK and IL7R signaling (10, 12–16). Thus, LTis are characterized as $CD45^{+}CD3^{-}CD4^{+}IL7R\alpha^{+}$ and they further express CD25 (IL-

2Rα), CD132 (IL-2Rγ), CD44, CD90, CD117 (c-kit), MHC-II, integrins α4β7 and α4β1, RANK, RANKL and LTα1β2 (Table 1-1) (*2*, *6–8*, *13*).

1.1.2. Lymphoid Tissue organizer cells (LTos)

Another cell subset, the Lymphoid Tissue organizer cells (LTos), has been shown to co-localize with the clusters of LTis (*11*). These CD45-negative LTos interact with LTis in order to induce LN organogenesis (*17*). LTos express adhesion molecules: ICAM-1 (InterCellular Adhesion Molecule-1), VCAM-1 (Vascular Cells Adhesion Molecule-1) and MAdCAM-1 (Mucosal Addressin Cell Adhesion Molecule-1). Furthermore, following the expression level of those molecules, we distinguish two subpopulations of LTos. Indeed, their expression levels reveal the maturation stage of LTos: the LTo precursors (ICAM-1$^-$ VCAM-1$^-$) first become ICAM-1^{int} VCAM-1^{Int}, and this independently of Lymphotoxin signaling by LTis; then, they differentiate into ICAM1^{high}VCAM1^{high}MAdCAM1$^+$ organizer cells, this process depends on both LTis and Lymphotoxin signaling (*8*, *17*). LTos express different genes that are required for LN development like RANKL and LTβR (Table 1-1).

	TNFS(R)F members	Chemokines and their receptors	Adhesion molecules	Other Surface antigens	Soluble Molecules
LTis	LTα1β2 RANK RANKL	CXCR4 CXCR5 CCR7	Integrin α4β7 Integrin α4β1 ICAM-1	CD45, CD4, CD16/32, CD25, CD32, CD44, CD90 (Thy1), CD127 (IL7Rα), CD132 (IL2Rγ), MHC class II (±50%), CD117 (c-kit, low)	RANKL
LTos	RANKL LTβR	CXCL12 CXCL13 CCL19 CCL21	VCAM-1 ICAM-1 MAdCAM-1	PDGF-receptor α, CD117 (c-kit)	TGFβ, IL6

Table 1-1: Murine LTi and LTo principal molecules (2, 6–8, 10).

1.1.3. LTo-LTi cross-talk

LNs always emerge at the same location, i.e. around large veins and blood vessels branching sites; this LN development depends on the LTo-LTi interaction. However, we still do not have evidence about the triggering signal (*11*, *17*). LTi clusters seem to be formed next to local sources of CXCL13, a molecule expressed by LTos and that could be triggered by vagal nerve stimulation (*18*, *19*). After LTi clustering in the developing LN, RANKL induces

the expression of LTα1β2 by LTis; interaction with the LTβR expressed by surrounding LTos stimulates these cells to express adhesion molecules (VCAM1, ICAM1, MAdCAM1), chemokines (CXCL13, CCL19, CCL21) and other cytokines leading to cell attraction to the LN anlagen (*20*, *21*). Subsequently, LTos express RANKL and IL-7, which together further induce the expression of LTα1β2 by the newly arriving LTis. A positive feedback loop is ensured by LTα1β2 expressed by LTis via their interaction with stromal LTβR (*16*, *17*, *21*). Furthermore, Lymphotoxin signaling induces the expression of the lymphangiogenic factor VEGF-C (vascular endothelial growth factor C) by LTos and hence ensure the connection of the developing LN to the lymphatic vasculature (*21*). The differentiation of blood vessels into High Endothelial Venules (HEVs) occurs at the final stage of the LN which permits cell entry from the bloodstream. Then B and T cells start replacing LTi to ensure the differentiation and survival of the LTβR+ stromal cells (Figure 1-2) (*1*, *17*).

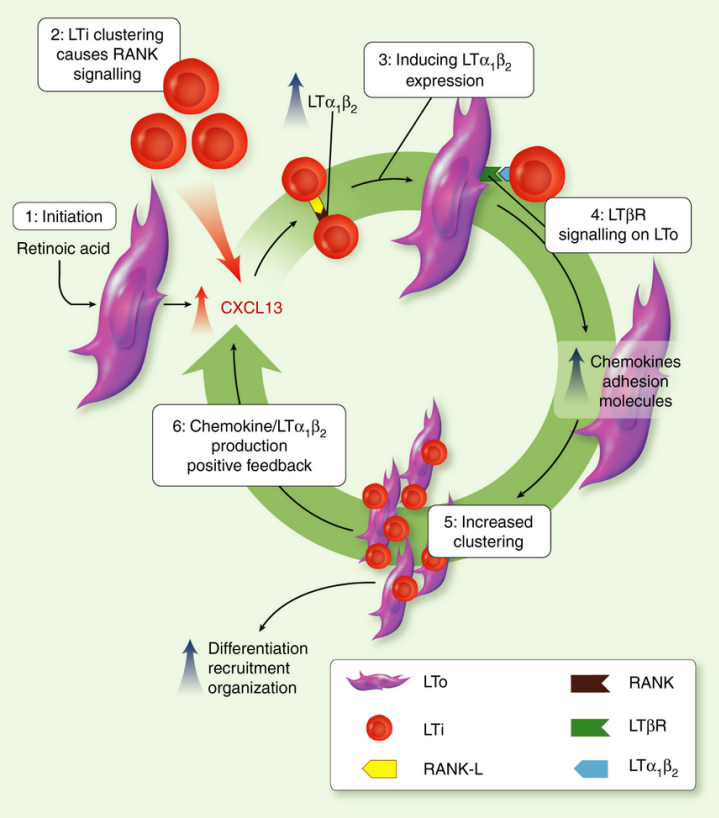

Figure 1-2: LTi-LTo cross-talk ensures LN development during embryogenesis. *LN organogenesis is initiated after retinoic acid induces CXCL13 expression by LTos (1) leading to CXCR5$^+$ LTi attraction and clustering. RANK and RANKL expressed simultaneously by LTis for a brief period stimulate each other in an autocrine way (2) leading to LTα1β2 expression (3). The signal is transduced by LTβR expressed by LTos leading to chemokine and adhesion molecules expression (4), thus, more LTis are attracted and clustered (5) resulting in further LTα1β2 production and therefore LN expansion* **(19)**.

1.2. Molecular actors: TNF(R)SF and other Chemokines

The role of Tumor Necrosis Factor (TNF) Super Family (SF) and TNF-Receptor SF members in LN development has been studied in genetically modified mice, the first model was LTα-deficient mice were the loss of LTα prevents LN formation (22). In other genetic studies, it was found that both RANKL and LTβR signaling play an essential role for LN development while TNFR1 is not required for LN organogenesis (Table 1-2).

Mutation	Signalling Pathway	Affected Cells	LNs	PPs	NALTs
LTα-/-, LTβr-/-, Nik-/-, Aly/aly, Rela x Tnfr-/-	LTβR	Stromal	-	-	-
Nfκb2-/-, Relb-/-	LTβR	Stromal	±*	-	ND
LTβ-/-	LTβR	Stromal	cLNs, mLNs	-	+
Light-/-	LTβR	Stromal	+	+	+
Light-/- x LTβ-/-	LTβR	Stromal	Less mLNs than LTβ-/-	-	ND
Ikkα-/-	LTβR	Stromal	-	-	+
Tnfr1-/-	TNFR1	Stromal	+	Reduced number	+
Tnf-/-	TNFR1 AND 2	Stromal	+	Reduced number	+
IL7rα-/-, Jak3-/-, γc-/-	IL-7R	LTis	bLN, aLN, mLN	-	+
IL7-/-	IL-7R	LTis	mLN	-	-
RANK-/-, RANKL-/-, Traf6-/-	RANK	LTis	-	Smaller	+
Rorγ-/-		LTis	-	-	+
Id2-/-		LTis	-	-	-
Ikaros-/-		LTis	-	-	ND
Cxcl13-/-, Cxcr5-/-	CXCR5	LTis	cLN, fLN, mLN	Reduced number	-
Plt/plt, Ccr7-/-	CCR7	LTis	+	+	+
Cxcr5x Ccr7-/-	CXCR5/CCR7	LTis	+	-	ND
Plt/plt/Cxcl13-/-	CXCR5/CCR7	LTis	-	-	-

Table 1-2: Incidence of gene deficiency on lymphoid organogenesis. *Symbols and abbreviations: + normal lymphoid organ development; - impaired development; ND not determined; * development was reported normal at day P0 but at P10 lymphoid depletion was observed; aLN, axillary LN; bLN brachial LN, cLN, cervical LN, fLN, facial LN; mLN mesenteric LN; NALT, nasal-associated lymphoid tissue; PPs, Peyer's Patches; aly, alymphoplasia; γc, common cytokine receptor γ-chain; CCR7, chemokine receptor for CCL19 and CCL21; CXCL13, chemokine (C-X-C motif) ligand 13; CXCR5, CXCL13 receptor; IKK, inhibitor of κb kinase; IL-7, interleukine-7; Jak3, Janus kinase 3; LT, lymphotoxin; NIK, nuclear-factor- κb-inducing kinase; Plt, paucity of LN T cells; RORγ, retinoid-related orphan receptor γ; TNF, tumo-necrosis factor; Traf6, TNF-receptor-associated factor 6* **(2, 22, 23)**.

1.2.1. RANK/RANKL Signaling in LN development

The role of RANK/RANKL signaling in LN development has been discovered first in RANKL-deficient mice where LN do not develop, while spleen is not affected; PPs and NALTs form but are smaller (*24*). Similar observations have been made in RANK- and TRAF6-deficient mice (*15*, *24*). Indeed, this absence of LNs in RANKL-deficient mice is not the result of a defective cellular homing but is due to the decrease in LTis numbers that seem unable to cluster and then to interact with LTos (*16*, *24*). These results have been confirmed by administrating RANK-Fc antagonist (*9*). Nevertheless, the subsistence of LTis suggests that RANK/RANKL signaling is required for LTi survival and/or proliferation but not their generation (*16*). The partial recovery of LTi numbers and LN development in RANKL-deficient mice with RANKL-transgenic overexpression in T and B cells support this role of RANK/RANKL signaling (*11*).

In addition to RANK expression by LTis during embryogenesis, LTis express briefly RANKL (E14.5-15.5), which would engage an autocrine activation of LTis and lead to LTα1β2 expression that activates LTβR signaling on LTo precursor and their maturation into LTos (*13*, *21*, *25*, *26*). A positive feedback loop by LTo-RANKL, 10-fold higher in LTos than in LTis, may then ensure LTi expansion (*26*, *27*). The existence of another autocrine loop RANK/RANKL on LTos has been also suspected (Figure 1-3) (*25*).

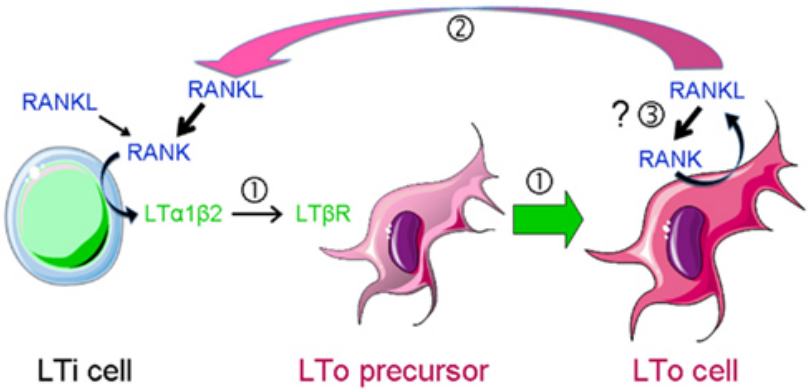

Figure 1-3: Molecular Signaling during LN development. *LN organogenesis is initiated by LTi recruitment to a rudimentary anlagen of mesenchymal Lymphoid Tissue organizer (LTos) cell progenitors. (1) The cross-talk between LTi cells in clusters via RANK/RANKL signaling leads to LTα1β2 expression by LTis and LTβR signal transduction in LTo precursor cells leading to their maturation. (2) Mature LTo cells express RANKL that amplifies signaling on LTis leading to their expansion and thus, LN development. (3) The question whether a comparable autocrine loop RANK/RANKL exists on LTos to induce their own activation has been raised* **(25–28)**.

1.2.2. LTα1β2/LTβR Signaling in LN development

LTα-deficient mice was the first genetic model in which the role of a TNFSF member in LN development has been discovered: both LNs and PPs are absent even though rudimentary mLNs appear in some mice (<5%) (22, 25). Similar observations have been made for LTβR-deficient mice while in LTβ-deficient mice, cLN, mLN and NALT are still able to emerge (29, 30). It has also been shown that both NF-κB classical and alternative signaling pathways of LTβR are crucial for LN organogenesis *via* the promotion of different sets of chemokines (31–34). Moreover, LTβR signaling is essential for HEV development in order to facilitate lymphocyte transmigration into the LN; it also influences B cell follicle micro-architecture (13, 35, 36).

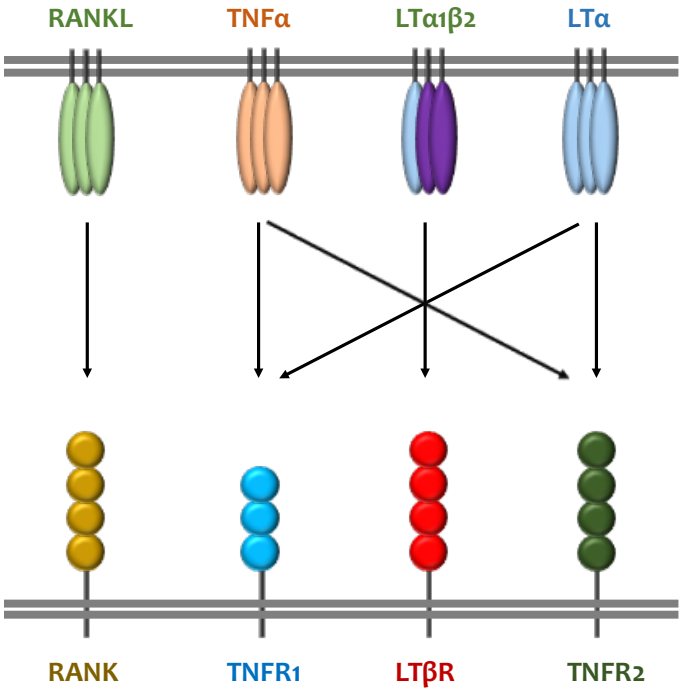

Figure 1-4: Interactions between TNF(R)SF members important in SLO development. *Schematic representation of the interactions between TNF, LTα and β and their receptors. Abbreviations: RANK: Receptor Activator of NF-κB ; RANKL, RANK Ligand; TNF, tumor necrosis factor; LT, lymphotoxin; TNFR, TNF receptor; LTβR, LTβ receptor* **(37)**.

1.2.3. TNF/TNFR Signaling is not required for LN organogenesis

The similarities in structure and function between TNFα and LTα, and the ability of LTα to bind TNF-Receptors 1 and 2, raised the question of TNF signaling role in LN organogenesis (*38*). However, TNFα, TNFR1 or TNFR2 deficiency in mice do not affect LN or PP development but only B cell follicle structure (*39–41*). This difference is explained by the fact that the signal transduction is ensured by the heterotrimer LTα1β2 interaction specifically with LTβR and not with TNFR1 or TNFR2 (Figure 1-4) (*37*, *42*, *43*). Nevertheless, TNFα contribution to LN development, even minor, has been highlighted in mice where administration of LTβR blocking antibody to embryos induces the loss of several LN except cLN and mLN, and the combination of this antibody with TNF-Ig leads to the loss of also those LNs (*13*).

1.2.4. Other Chemokines: CXCL13 and IL7

The role of mesenchymal CXCL13 in LN initiation has been described during the early stages as essential for LTi clustering and then LN development. Mice deficient for CXCL13 lack several LN except mLN (*44*). Furthermore, IL-7 has been shown as another required molecule for LTi maintenance and development. Even though IL-7 is mainly required for PP and not for LN development, it has been demonstrated that in TRAF6-deficient embryos presenting an impaired RANK signaling cascade, the application of ectopic IL-7 could rescue early phases of LN development and discrete mLNs were recovered (*11*, *14*). In addition, it has been shown that mice where both CXCL13 and IL7Rα are deficient fail to form all LNs, even mLNs that are normally present in CXCL13-mice (*23*, *44*, *45*). Further, CXCL13 seems also to be important during late stages of LN development especially for Follicular Dendritic Cells (FDCs) formation and B cell follicle organization (*23*, *44*).

1.3. Cellular organization during LN development

Once sufficient LTi and LTo clustering has taken place, endothelial cells start to differentiate into specialized cell called HEVs; those cells are responsible for lymphocyte transmigration into lymphoid organ (*2*, *46*). HEVs express MAdCAM-1 during embryonic development till day 1 postnatally (P1) and to a certain extend till the 4th week after birth (peripheral LN), thus, they attract the LTis (α4β7+); then a switch occurs and they start expressing PNAd (Peripheral Node Addressin) allowing the recruitment of L-selectin+ B

and T cells. Only after B and T cell recruitment and segregation, B cell follicle formation starts. Functional tests showed that HEV function is regulated by LTβR signaling (36). The transmigration of other leukocytes through HEVs depends on other molecular partners e.g. CCR7, CXCR4 and CXCL13 (47–49). The main cells entering the LNs through HEVs are naïve B cells, naïve and central memory T cells (Figure 1-5).

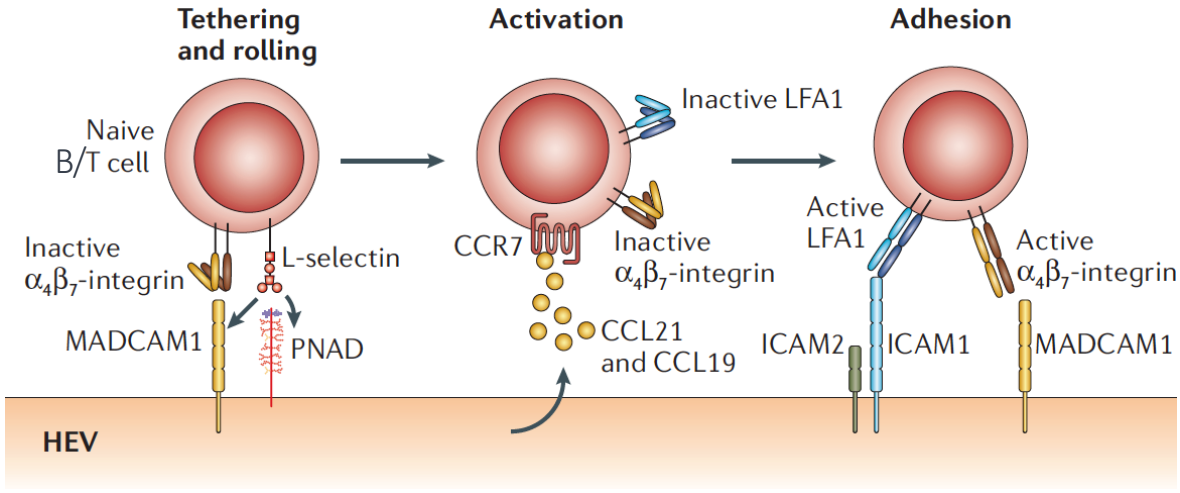

Figure 1-5: HEVs regulate leukocyte (T cell) homing in LN. *Rolling and tethering is initiated by naïve B and T cells and central memory T cells through L-selectin/PNAd interaction. Rolling can also take place thanks to MAdCAM-1 / α4β7interaction. HEV express CCL21 and to a lower extend CCL19 and CXCL12 inducing rapid integrin signaling and then the Lymphocyte function associated antigen 1 (LFA1)-mediated arrest on ICAM and MAdCAM leading to cell transmigration across HEVs* **(1, 50)**.

The transmigration of lymphocytes into LN is orchestrated by different chemokines (CCL19, CCL21, CXCL12, CXCL13) that lead B and T cells to their specific regions and are essential for the compartmentalization of the lymphocytes within the LN (51). Genetic studies showed that B cell follicle formation is dependent on CXCL13 expressed by B cell zone associated stroma, and its receptor CXCR5 expressed by recirculating B cells (45, 52). On the other hand, T cell area organization depends on CCL19/CCL21 expressed by T cell-stromal cells and their receptor CCR7 expressed by DCs and resting T cells (53–55). The expression of these homing chemokines by stromal cells is governed by LTα1β2 and TNFα (Figure 1-6) (56). Interestingly, B cell migration to the LN is CXCL13-independent till P4, since at that time B cells are LTα1β2- and CXCR5-low. B cells start to express LTα1β2 at P2 and

then CXCR5 at P4 and become CXCL13-sensitive, and so the LTi replacement starts in LN architecture maintenance (57, 58).

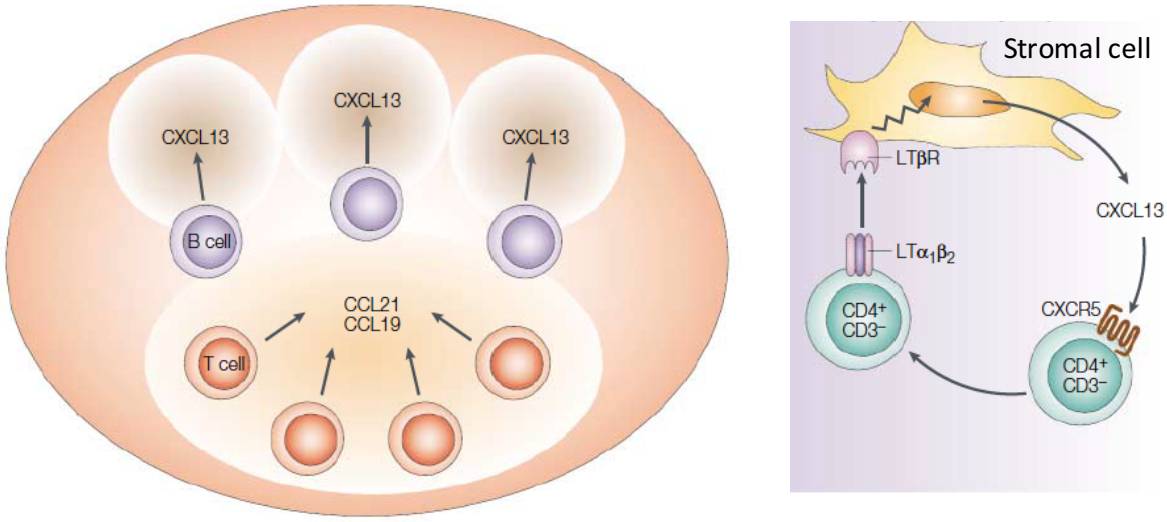

Figure 1-6: Role of lymphoid chemokines in the organization of LN. *Left - The compartmentalization of LNs is ensured by chemokines: CXCL13 expressed in the follicles attracts CXCR5-expressing B cells; CCL19 and CCL21 expressed in the T cell area attracts CCR7-expressing T cells and DC. Right - In LNs, the CXCL13/CXCR5 axis is regulated by LTβR signaling. Modified after* **(2)**.

1.4. Bibliography

1. P. Eikelenboom, J. J. Nassy, J. Post, J. C. Versteeg, H. L. Langevoort, The histogenesis of lymph nodes in rat and rabbit. *Anat. Rec.* **190**, 201–215 (1978).

2. R. E. Mebius, Organogenesis of lymphoid tissues. *Nat. Rev. Immunol.* **3**, 292–303 (2003).

3. G. Oliver, Lymphatic vasculature development. *Nat. Rev. Immunol.* **4**, 35–45 (2004).

4. M. F. Vondenhoff *et al.*, Lymph sacs are not required for the initiation of lymph node formation. *Dev. Camb. Engl.* **136**, 29–34 (2009).

5. P. D. Rennert, J. L. Browning, R. Mebius, F. Mackay, P. S. Hochman, Surface lymphotoxin alpha/beta complex is required for the development of peripheral lymphoid organs. *J. Exp. Med.* **184**, 1999–2006 (1996).

6. T. D. Randall, D. M. Carragher, J. Rangel-Moreno, Development of secondary lymphoid organs. *Annu. Rev. Immunol.* **26**, 627–650 (2008).

7. R. E. Mebius, P. Rennert, I. L. Weissman, Developing lymph nodes collect CD4+CD3- LTbeta+ cells that can differentiate to APC, NK cells, and follicular cells but not T or B cells. *Immunity*. **7**, 493–504 (1997).

8. T. Cupedo *et al.*, Presumptive lymph node organizers are differentially represented in developing mesenteric and peripheral nodes. *J. Immunol. Baltim. Md 1950*. **173**, 2968–2975 (2004).

9. G. Eberl *et al.*, An essential function for the nuclear receptor RORgamma(t) in the generation of fetal lymphoid tissue inducer cells. *Nat. Immunol.* **5**, 64–73 (2004).

10. A. Brendolan, J. H. Caamaño, Mesenchymal cell differentiation during lymph node organogenesis. *Front. Immunol.* **3**, 381 (2012).

11. H. Yoshida *et al.*, Different cytokines induce surface lymphotoxin-alphabeta on IL-7 receptor-alpha cells that differentially engender lymph nodes and Peyer's patches. *Immunity*. **17**, 823–833 (2002).

12. M. D. Boos, Y. Yokota, G. Eberl, B. L. Kee, Mature natural killer cell and lymphoid tissue-inducing cell development requires Id2-mediated suppression of E protein activity. *J. Exp. Med.* **204**, 1119–1130 (2007).

13. P. D. Rennert, D. James, F. Mackay, J. L. Browning, P. S. Hochman, Lymph node genesis is induced by signaling through the lymphotoxin beta receptor. *Immunity*. **9**, 71–79 (1998).

14. D. Meier *et al.*, Ectopic lymphoid-organ development occurs through interleukin 7-mediated enhanced survival of lymphoid-tissue-inducer cells. *Immunity*. **26**, 643–654 (2007).

15. W. C. Dougall *et al.*, RANK is essential for osteoclast and lymph node development. *Genes Dev.* **13**, 2412–2424 (1999).

16. D. Kim *et al.*, Regulation of peripheral lymph node genesis by the tumor necrosis factor family member TRANCE. *J. Exp. Med.* **192**, 1467–1478 (2000).

17. S. A. van de Pavert, R. E. Mebius, New insights into the development of lymphoid tissues. *Nat. Rev. Immunol.* **10**, 664–674 (2010).

18. S. A. van de Pavert *et al.*, Chemokine CXCL13 is essential for lymph node initiation and is induced by retinoic acid and neuronal stimulation. *Nat. Immunol.* **10**, 1193–1199 (2009).

19. M. J. W. Kain, B. M. J. Owens, Stromal cell regulation of homeostatic and inflammatory lymphoid organogenesis. *Immunology*. **140**, 12–21 (2013).

20. K. Honda *et al.*, Molecular basis for hematopoietic/mesenchymal interaction during initiation of Peyer's patch organogenesis. *J. Exp. Med.* **193**, 621–630 (2001).

21. M. F. Vondenhoff *et al.*, LTbetaR signaling induces cytokine expression and up-regulates lymphangiogenic factors in lymph node anlagen. *J. Immunol. Baltim. Md 1950*. **182**, 5439–5445 (2009).

22. P. De Togni *et al.*, Abnormal development of peripheral lymphoid organs in mice deficient in lymphotoxin. *Science*. **264**, 703–707 (1994).

23. S. A. Luther, K. M. Ansel, J. G. Cyster, Overlapping roles of CXCL13, interleukin 7 receptor alpha, and CCR7 ligands in lymph node development. *J. Exp. Med.* **197**, 1191–1198 (2003).

24. Y. Y. Kong *et al.*, OPGL is a key regulator of osteoclastogenesis, lymphocyte development and lymph-

node organogenesis. *Nature*. **397**, 315–323 (1999).

25. C. G. Mueller, E. Hess, Emerging Functions of RANKL in Lymphoid Tissues. *Front. Immunol.* **3**, 261 (2012).

26. M. Sugiyama *et al.*, Expression pattern changes and function of RANKL during mouse lymph node microarchitecture development. *Int. Immunol.* **24**, 369–378 (2012).

27. J. J. Koning, R. E. Mebius, Interdependence of stromal and immune cells for lymph node function. *Trends Immunol.* **33**, 264–270 (2012).

28. R. Roozendaal, R. E. Mebius, Stromal cell-immune cell interactions. *Annu. Rev. Immunol.* **29**, 23–43 (2011).

29. P. A. Koni *et al.*, Distinct roles in lymphoid organogenesis for lymphotoxins alpha and beta revealed in lymphotoxin beta-deficient mice. *Immunity*. **6**, 491–500 (1997).

30. A. Fütterer, K. Mink, A. Luz, M. H. Kosco-Vilbois, K. Pfeffer, The lymphotoxin beta receptor controls organogenesis and affinity maturation in peripheral lymphoid tissues. *Immunity*. **9**, 59–70 (1998).

31. S. Miyawaki *et al.*, A new mutation, aly, that induces a generalized lack of lymph nodes accompanied by immunodeficiency in mice. *Eur. J. Immunol.* **24**, 429–434 (1994).

32. R. Shinkura *et al.*, Alymphoplasia is caused by a point mutation in the mouse gene encoding Nf-kappa b-inducing kinase. *Nat. Genet.* **22**, 74–77 (1999).

33. S. Fagarasan *et al.*, Alymphoplasia (aly)-type nuclear factor kappaB-inducing kinase (NIK) causes defects in secondary lymphoid tissue chemokine receptor signaling and homing of peritoneal cells to the gut-associated lymphatic tissue system. *J. Exp. Med.* **191**, 1477–1486 (2000).

34. E. Dejardin *et al.*, The lymphotoxin-beta receptor induces different patterns of gene expression via two NF-kappaB pathways. *Immunity*. **17**, 525–535 (2002).

35. L. Onder *et al.*, Endothelial cell-specific lymphotoxin-β receptor signaling is critical for lymph node and high endothelial venule formation. *J. Exp. Med.* **210**, 465–473 (2013).

36. J. L. Browning *et al.*, Lymphotoxin-beta receptor signaling is required for the homeostatic control of HEV differentiation and function. *Immunity*. **23**, 539–550 (2005).

37. R. M. Locksley, N. Killeen, M. J. Lenardo, The TNF and TNF receptor superfamilies: integrating mammalian biology. *Cell*. **104**, 487–501 (2001).

38. B. B. Aggarwal, T. E. Eessalu, P. E. Hass, Characterization of receptors for human tumour necrosis factor and their regulation by gamma-interferon. *Nature*. **318**, 665–667 (1985).

39. S. L. Erickson *et al.*, Decreased sensitivity to tumour-necrosis factor but normal T cell development in TNF receptor-2-deficient mice. *Nature*. **372**, 560–563 (1994).

40. M. Pasparakis *et al.*, Peyer's patch organogenesis is intact yet formation of B lymphocyte follicles is defective in peripheral lymphoid organs of mice deficient for tumor necrosis factor and its 55-kDa receptor. *Proc. Natl. Acad. Sci. U. S. A.* **94**, 6319–6323 (1997).

41. M. Pasparakis, L. Alexopoulou, V. Episkopou, G. Kollias, Immune and inflammatory responses in TNF alpha-deficient mice: a critical requirement for TNF alpha in the formation of primary B cell follicles, follicular dendritic cell networks and germinal centers, and in the maturation of the humoral immune response. *J. Exp. Med.* **184**, 1397–1411 (1996).

42. J. L. Browning *et al.*, Lymphotoxin beta, a novel member of the TNF family that forms a heteromeric complex with lymphotoxin on the cell surface. *Cell*. **72**, 847–856 (1993).

43. P. D. Crowe *et al.*, A lymphotoxin-beta-specific receptor. *Science*. **264**, 707–710 (1994).

44. K. M. Ansel *et al.*, A chemokine-driven positive feedback loop organizes lymphoid follicles. *Nature*. **406**, 309–314 (2000).

45. R. Förster *et al.*, A putative chemokine receptor, BLR1, directs B cell migration to defined lymphoid organs and specific anatomic compartments of the spleen. *Cell*. **87**, 1037–1047 (1996).

46. R. E. Mebius, P. R. Streeter, J. Brevé, A. M. Duijvestijn, G. Kraal, The influence of afferent lymphatic vessel interruption on vascular addressin expression. *J. Cell Biol.* **115**, 85–95 (1991).

47. R. E. Mebius, P. R. Streeter, S. Michie, E. C. Butcher, I. L. Weissman, A developmental switch in lymphocyte homing receptor and endothelial vascular addressin expression regulates lymphocyte homing and permits CD4+ CD3- cells to colonize lymph nodes. *Proc. Natl. Acad. Sci. U. S. A.* **93**, 11019–11024 (1996).

48. N. Kanemitsu *et al.*, CXCL13 is an arrest chemokine for B cells in high endothelial venules. *Blood*. **106**, 2613–2618 (2005).

49. U. H. von Andrian, T. R. Mempel, Homing and cellular traffic in lymph nodes. *Nat. Rev. Immunol.* **3**, 867–878 (2003).

50. W. W. Agace, Tissue-tropic effector T cells: generation and targeting opportunities. *Nat. Rev. Immunol.* **6**, 682–692 (2006).

51. J. G. Cyster, Chemokines and cell migration in secondary lymphoid organs. *Science*. **286**, 2098–2102 (1999).

52. D. F. Legler *et al.*, B cell-attracting chemokine 1, a human CXC chemokine expressed in lymphoid tissues, selectively attracts B lymphocytes via BLR1/CXCR5. *J. Exp. Med.* **187**, 655–660 (1998).

53. S. Mori *et al.*, Mice lacking expression of the chemokines CCL21-ser and CCL19 (plt mice) demonstrate delayed but enhanced T cell immune responses. *J. Exp. Med.* **193**, 207–218 (2001).

54. M. D. Gunn *et al.*, Mice lacking expression of secondary lymphoid organ chemokine have defects in lymphocyte homing and dendritic cell localization. *J. Exp. Med.* **189**, 451–460 (1999).

55. R. Förster *et al.*, CCR7 coordinates the primary immune response by establishing functional microenvironments in secondary lymphoid organs. *Cell*. **99**, 23–33 (1999).

56. V. N. Ngo *et al.*, Lymphotoxin alpha/beta and tumor necrosis factor are required for stromal cell expression of homing chemokines in B and T cell areas of the spleen. *J. Exp. Med.* **189**, 403–412 (1999).

57. M. C. Coles *et al.*, Role of T and NK cells and IL7/IL7r interactions during neonatal maturation of lymph nodes. *Proc. Natl. Acad. Sci. U. S. A.* **103**, 13457–13462 (2006).

58. T. Cupedo *et al.*, Initiation of cellular organization in lymph nodes is regulated by non-B cell-derived signals and is not dependent on CXC chemokine ligand 13. *J. Immunol. Baltim. Md 1950*. **173**, 4889–4896 (2004).

*****

2. Organization of adult LNs: role of stromal cells

2.1. Overview of structure and function in adult LN

Lymph nodes are part of the lymphatic system, and therefore of the circulatory system to which they are connected by lymphatic vessels. Thus, they play a crucial role in filtration of lymph and its immune surveillance. Twenty-two LNs have been described in mice, they are present at different strategic positions in the body to detect antigens (Ags) and prevent systemic infection. Lymph arrives in LN via afferent lymphatic vessels, is channeled through the LN sinuses to the parenchyma and finally exits via efferent vessel. LN consists of a collecting point hence it usually has several afferent vessels and one efferent vessel. These SLOs act as filters where all needed factors and cells for the initiation of the immune response are in close contact. Furthermore, they also play a role in resolution of immune responses and maintenance of tolerance.

LNs are organized into lobules which are separated by open communicating sinus in small animals like rate; in mice, they are generally formed of one single lobule. LNs are organized into 3 major compartments: the cortex, the paracortex and the medulla (Figure 2-1) (*1*). Each compartment contains different cell types of both hematopoietic and non-hematopoietic origin that form the complex microarchitecture of a functional LN. Non-hematopoietic cells comprise endothelial and mesenchymal cells while hematopoietic cells include lymphocytes, DCs and macrophages. LN is encapsulated in a dense irregular connective tissue with some collagen fibers. Under this capsule, afferent lymphatic vessels, bring tissue derived antigens (Ags) and immune cells to the lymph node subcapsular sinus (SCS), which consists of a double layer of lymphatic endothelial cells (LECs). Beneath the SCS lies the cortex where B cell follicles are located. On the outer side they are lined by Marginal Reticular cells (MRCs) that express RANKL. MRCs together with FDCs are the B cell follicle organizers secreting the chemokine CXCL13 to attract B cells and keep them in close contact which ensures their immunocompetence (2–5). High Endothelial Venules (HEV) are also present in the cortex. They are specialized vascular endothelial cells that express Protein NH2-Terminal Asparagine Deamidase (PNAD) and CCL21, facilitating lymphocyte entry into the LN (*3*). In the paracortex, T cells are guided to the lymph node by CCL19 and CCL21, which are both secreted by fibroblastic reticular cells in the T zone

(TRCs). TRCs form also conduits that allows the flow of small soluble molecule through the lymph node parenchyma (3). Finally, Blood Endothelial cells (BECs) form the High Endothelial Venules (HEVs) that are the main entry site for naïve leucocytes. Medullary sinus and efferent lymphatic vessels allow lymphocyte exit from the LN and their return to the blood stream (Figure 2-1).

Different types of antigens arrive into LN either through the lymph flow or actively transported by cells. Self-antigens carried by tissue-resident antigen-presenting cells (APCs) are then presented to lymphocytes to maintain tolerance. Resident APCs can also capture soluble antigens that passively reach the LN via the lymph (6, 7).

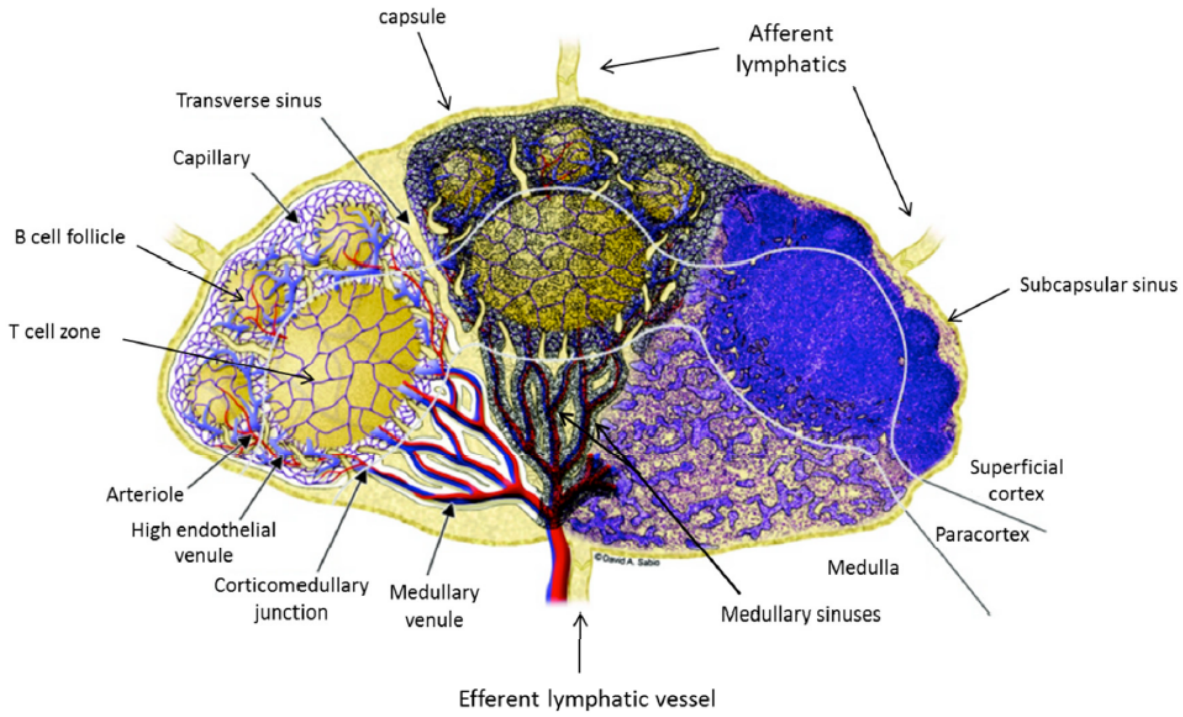

Figure 2-1: Schematic representation of LN organization. *Representation of a LN with 3 lobules showing the organization in cortex, paracortex and medulla areas. Each lobule has one afferent lymphatic vessel and a single efferent vessel. Left lobule: schematic representation of the blood vascular network. Arterioles (Red) arborize in the paracortical cords and interfollicular cortex and give rise to capillary beds (purple) that empty into high endothelial venules (blue). Center lobule: blood vascular network together with the reticular network formed by non-hematopoietic cells. Right lobule: section from a rat mesenteric LN. Densely packed basophilic lymphocytes fill the lobular reticular meshwork. Five cortical follicles give the superficial cortex a lumpy appearance. Small empty paracortical sinuses are easily visible in the peripheral DCU. The medullary sinuses contain macrophages, lymphocytes and erythrocytes. Modified after reference* ***(1)****.*

2.2. LN Stroma

For a long time in the past, stromal cells have been considered cells that only provide support within the organ, however the involvement of these cells in immune response is now starting to be considered. Indeed, stromal cells form the cellular structures necessary for the initiation of the immune response in LNs by insuring its expansion (*3*, *8*). Thus, LN stroma and immune response are strongly interdependent. Stroma is constituted of a heterogeneous group of non-hematopoietic cells in the LN identified as CD45-negative cells. LN stromal cells could be divided into two groups following their origin: endothelial cells and those derived from mesenchymal progenitors called Fibroblastic Reticular Cells (FRCs) (*2*, *9*). Endothelial cells are constituted of Lymphatic Endothelial Cells (LECs) and Blood Endothelial Cells (BECs) that include the Highly Endothelial Venules (HEVs). According to their location in the LN, the FRCs could be subdivided into: T cell Zone Reticular Cells (TRCs), B cells zone FDCs and Marginal Reticular Cells (MRCs) (*9*–*12*).

The stromal subsets can be discriminated based on their differential expression of podoplanin a.k.a. glycoprotein 38 (gp38) and the platelet endothelial cell adhesion molecule (PECAM-1) a.k.a. CD31 (*13*). CD31 is a classical marker of all endothelial cells; nevertheless, it is also carried by platelets and some blood leukocytes (*14*). Gp38 is a mucin-type transmembrane protein that binds the C-type lectin receptor CLEC-2 on platelets and immune cells (*15*, *16*). While LECs express both CD31 and gp38, BECs are only CD31+. FRCs carry only gp38 and another population lacking both CD31 and gp38 constitutes the Double Negative Cells (DNs) that include the Integrin α7 pericytes (*8*). FRCs can further be characterized by ICAM-1, VCAM-1 and the production of the following chemokines: CCL19, CC21 and IL-7. FDCs are characterized with their own markers FDC-M1 and FDC-M2 and produce CXCL13 and the B cell survival factor (BAFF) (*17*). MRCs, that are located beneath the Subcapsular Sinus (SCS) in the outer edge of B cell follicles express MAdCAM-1 and RANKL and produce CXCL13 (*5*). Another population of B cell zone reticular cells has been also identified as $BAFF^{+}$ but $FDC\text{-}M2^{-}$ (*18*, *19*).

Stromal cell subtype	Features	Location	Functions
Follicular Dendritic Cell (FDC)	gp38+ CD31- ER-TR7- CD35+ FDC-M1+ FDC-M2+ VCAM+ BAFF+ CXCL13+	B cell area	Antigen capture and presentation of immune complexes. Maintaining germinal centers. Facilitating the production of high-affinity antibodies.
T cell zone Reticular Cell (TRC)	gp38+ CD31- ER-TR7+ LTβR+ ICAM-1+ VCAM-1+	T cell area	T cell zone maintenance Constructing conduit networks for small molecule transport Antigen presentation
Marginal Reticular Cell (MRC)	gp38+ CD31- MAdCAM+ RANKL+ ER-TR7+	Subcapsular Sinus	Source of CXCL13 Immunological function still unclear
Integrin α7 pericytes (IAP)	gp38- CD31- ITGA7+	Around HEVs (Cortex and Medulla)	Similarities with TRCs Preventing bleeding from HEVs into LN
Blood Endothelial cell (BEC)	gp38- CD31+ RANK+ VCAM-1+	All LN	Blood flow Cell transport
High Endothelial Venule (HEV)	gp38- CD31+ MECA-79+ (PNAd+)	All LN	Defined as specialized BECs Lymphocyte enter the LN
Lymphatic Endothelial cell (LEC)	gp38- CD31+ LYVE-1+, CLCA1, MAdCAM-1$^{+/-}$	All LN	Lymph flow Transport of cells and molecules

Table 2-3: Stromal cell subsets in LN, their location, features and functions (3, 10, 11, 20, 21).

2.2.1. Double Negative stromal cells (DNs)

Double Negative cells (DNs) are heterogeneous non-hematopoietic cells (CD45-negative) that have been named following the lack of expression of both gp38 and CD31. This stromal subset is not well described in the literature. Some DNs can express the Autoimmune Regulatory Element (AIRE) and the Major Histocompatibility Complex – class I (MHC-I) but not the epithelial cell adhesion molecule (EpCAM) (22, 23). More recently, it has been proposed that DNs are mainly constituted of pericytes since they were mainly found next to LN vessels and have a smooth muscle-like structure (24).

2.2.2. Blood Endothelial Cells (BECs) and High Endothelial Venules (HEVs)

BECs are responsible of cell transport within LN: artery(ies) enter the LN hilum, then serve the medulla till the cortex and sometimes the SCS zone. The branching capillaries become arteriovenous communications which give place to HEVs (high endothelial cells) that plays a crucial role in lymphocyte trafficking through their network (25).

HEV have a cuboidal form compared to flat BECs and are rich with cell organelles implicated in biosynthesis (26). HEVs present discontinuous "spot-welded" junctions between cells, which differ from the characteristic tight junctions between BECs. These junctions facilitate lymphocyte entry through HEVs (27). Among all other stromal subsets, HEVs express PNAd (peripheral node addressin), an L-selectin ligand that permits their interaction with lymphocytes; hence HEV play a regulatory role in lymphocyte entry to the LN (25, 27–30). Nevertheless, HEVs keep some plasticity since they can be reverted to PNAd-negative endothelial cells after ligation of the LN afferent lymphatic vessels (31). HEVs regulatory role on cell migration within the LN concerns both plasmacytoid DCs and DC precursors, and also natural killer (NK); however the molecular mechanisms involved are still not totally clear (32–34).

2.2.3. Lymphatic Endothelial Cells (LECs)

LECs form discontinuous button-like junctions of the lymphatic vessels allowing the entrance of fluids and immune cells to the lymph node, thus they play an important role for the immune response (35–37). In the lymphatic capillaries, LECs form zipper-like junctions surrounded by perivascular smooth muscle cells and continuous basement membrane creating impermeable vessels. Specialized LECs form valve leaflets with a spindle like morphology that ensures unidirectional lymph flow (35).

LECs has been characterized as expressing a certain number of markers: the hyaluronic receptor LYVE1, Chloride Channel Accessory 1 (CLCA1), prospero homeobox 1 (Prox-1), the endothelial marker CD31, the transmembrane glycoprotein podoplanin (gp38), integrins ITGA2B and ITGB3, vascular endothelial growth factor 3 (VEGFR3) and neuropilin 2 (NRP2) that both bind VEGF-C in a similar manner (24, 38–40). Prox-1 is a transcription factor that plays a role in LEC fate determination while CLCA1 is involved in Calcium-dependent chloride ion transport (39, 41). In order to attract leukocytes to the LN, LECs express several chemokines like CCL19 and CCL21 that bind CCR7 on the DCs, neutrophils, and recirculating memory T cells (42–46). Their entry is ensured by adhesion molecules expressed on LECs like Podoplanin (gp38) , CLCA1 and MAdCAM-1 (45, 47). However, despite common markers, LECs represent a heterogeneous stromal subset since some markers present a differential expression according to LEC localization (45).

LN LECs express major histocompatibility complex class II (MHC-II) molecules, they also express MHC-I but less than other APCs (*45*, *48*, *49*). LECs do not express costimulatory molecules such as CD80, CD86 or OX40L (*50*). LECs can provide antigen to DCs for MHC-II presentation (*51*). However, Ag presentation by LECs to CD8 T cells is responsible for T cell anergy or deletion following the Ag level (*52*).

During inflammation, LECs enhance immune cell ingress to the LN; thus, the lymph flow is increased thanks to lymphangiogenesis. Lymphangiogenesis is promoted by different ligands VEGFR2 (Vascular endothelial growth factor receptor-2), VEGFR3 and LTβR that are modulated by macrophages (*53–56*).

2.2.4. T cell zone Reticular Cells (TRCs)

TRCs are localized at the T cell zone in close contact with each other as well as with other cells, including lymphocytes, dendritic cells and plasma B cells (*57*). TRCs form a conduit system called reticular fiber network where soluble antigens from afferent lymph can be delivered to antigen-presenting cells, namely DC of the T cell area (Figure 2-2).The reticular fiber network ensures also molecule routing to B cell follicle including different chemokines (*57–60*).

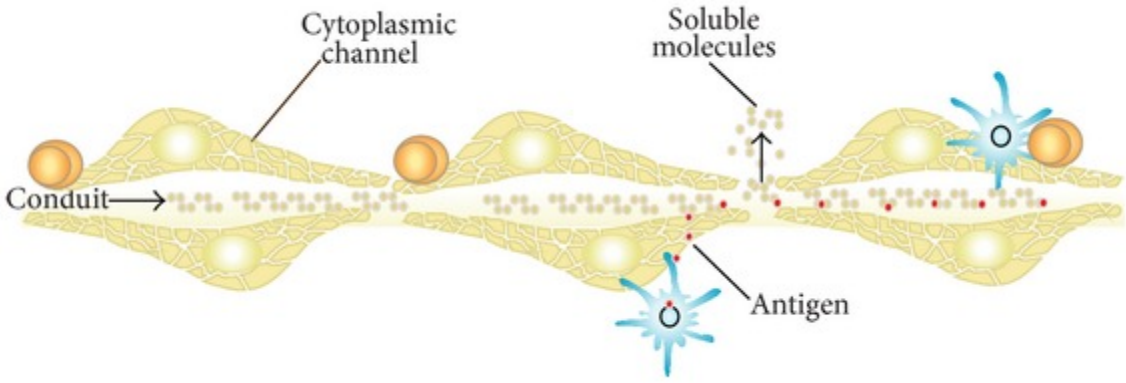

Figure 2-2: TRC network schematic view. *TRC cytoplasm contains intertwined tubules and cisterns that form a cytoplasmic channel where soluble antigens from afferent lymph can be delivered to antigen-presenting cells. The cells are in contact with each other in order to create a conduit system called reticular fiber network* **(58)**.

TRCs play an important role in LN immune response, peripheral tolerance and homeostasis (*61*). Through the homing chemokines CCL19 and CCL21, TRCs regulate not only T cell access and movement in the paracortical area, but also T cell proliferation and

death, and dendritic cells – T cell interaction (62–65). TRCs are also an important source of IL-7, a survival factor for naïve lymphocytes (63, 66). On the cellular level, TRCs actively select antigens entering the SCS: only small molecules (<60 kDa) can enter and are delivered to APCs via the conduits leading to antigen-specific T cell activation (58, 60). Moreover, it has been shown that TRCs play an important function for viral resistance and immunocompetence maintenance (67, 68).

The role of TRCs in peripheral tolerance has been demonstrated in mice. Indeed, TRCs endogenously express peripheral tissue antigens (PTAs) that they present to T cells leading to primary activation and subsequent tolerance among $CD8^+$ T cells. Thus, they participate in self-reactive T cell deletion (23, 69). Furthermore, FRCs can block T cell activation when IFN-γ increases TRC nitrite production, which can interfere with the cell cycle; this mechanism involves programmed cell death protein (PD-1) and its ligand PD-L1 (70, 71).

2.2.5. Marginal Reticular Cells (MRCs)

Marginal Reticular Cells (MRCs) are located at the SCS region just underneath the floor LECs, their presence has been also identified in all secondary lymphoid organs (Figure 2-3) (4). MRCs express CXCL13 and MAdCAM-1 but not CCL21 which differentiate them from TRCs. However, MRCs are the only stromal subset in adult LNs expressing RANKL (5).

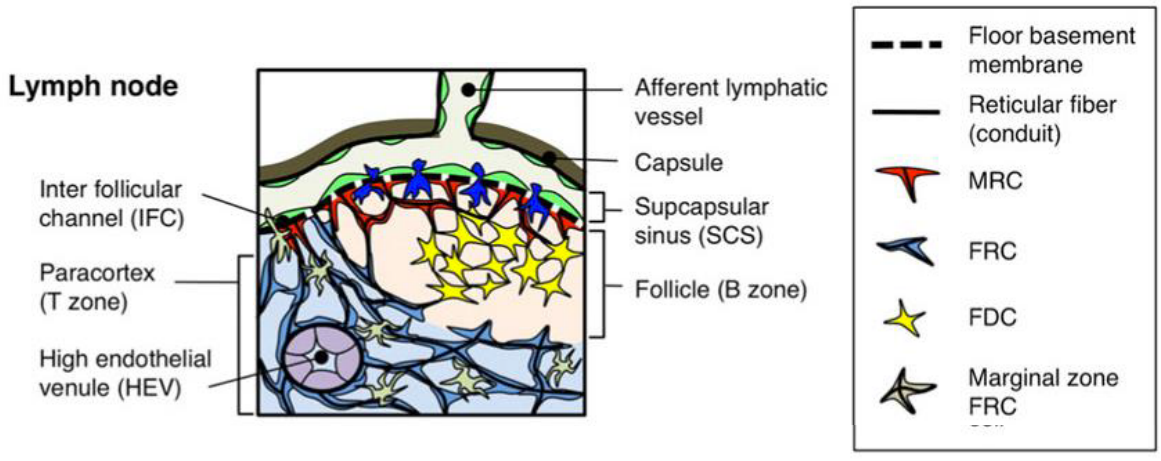

Figure 2-3: MRC localization with the LN. *MRCs are localized underneath floor LECs in contact with B cells. modified after reference* **(4)**.

The involvement of TNF-R1 and/or LTβR for MRC development and differentiation has been raised since in LTα-deficient mice, splenic MRCs are absent (72). As these mice

lack LNs, the incidence of this LTα deficiency for LN MRCs is still not answered (*73*). However, LTβR blockade in normal mice led to disappearance of adhesion molecule MAdCAM-1 and B cell attracting chemokine CXCL13 expressions in the SCS area, but RANKL was still detectable. Thus, LTβR signaling seems necessary for MRC activation and expression of MAdCAM-1 and CXCL13 (*5*, *11*). Besides, T and B cells seems not to be involved in MRC development since SCID (severe combined immunodeficiency) mice present this stromal population. Nevertheless, knowing that LTis express LTαβ and that postnatally they accumulate in the SLO outer cortex where MRCs are localized, the question of LTi involvement could be raised (*5*, *74*).

The involvement of MRCs in antigen transport and presentation, and humoral immune response initiation could be one of their potential functions. Indeed, their localization next to the SCS put them in close contact with lymph-borne antigens and antigen-carrying DCs coming from the periphery (*60*, *75*). Furthermore, MRCs are also in close proximity to SCS macrophages implicated in antigen delivery to B cells. Hence, MRCs may, via the adhesion molecules ICAM-1 and VCAM-1, but also chemokine CXCL13, support the interstitial migration of B cells (*76*, *77*). In addition, MRCs take possibly part in the formation of the conduit network to ensure the transport of small molecules from the SCS into B cell follicles (*60*, *75*).

MRCs are thought to be the LTo adult counterpart, as they share similar markers and a LTβR-dependent expression of ICAM-1, VCAM-1, MAdCAM-1 and CXCL13 (*5*). Indeed, during LN development, LTos localize frequently at the outer sinus where the SCS will form. In addition, LNs have antigen collecting structures that arise during LN organogenesis and that need to maintain postnatally. Hence, MRCs may ensure this stromal organizer of the LN. Furthermore, in adult LN, MRCs share common characteristics with TRCs and FDCs. Taken together, those elements legitimize the question about a possible differentiation of LTos into MRCs after birth, but also the possible MRC-origin of FDCs (*5*, *72*). Nevertheless, many gray areas remain concerning the origin of those mesenchymal stromal subset in the adult.

2.2.6. Follicular Dendritic Cells (FDCs)

FDCs have been first described in the 1960's as non-lymphoid, non-phagocytic dendritic-like cells able to opsonize bacterial antigen at their plasma membrane and to

form networks inside B cell follicles in a "reticular fashion". They have been first baptized Follicular Reticular Cells before being definitely called Follicular Dendritic Cells (*78–81*).

FDC ultrastructure has been described by electronic microscopy: the cell body size is comparable to that of lymphocytes (6-10 µm), then many dendrites can radiate. Their circumference reaches up to 0.3 µm at the proximal level and is reduced to 0.1 µm at the distal part. The FDC cytoplasm is quite poor is cell organelles (Golgi apparatus, mitochondria, endocytosis vesicles, *etc.*), which also explain their non-phagocytic nature. Their external surface can be either smooth or presenting some sprouts (*79*, *80*, *82*, *83*).

FDCs form a tridimensional network that is localized in the center of B cell follicle, they are involved in B cell homing, migration, survival and proliferation. They are also involved in antigen presentation and in T cell-dependent antibody response, and are essential for efficient germinal center (GC) formation. FDC – B cell interaction ensures the functioning of B cell follicles (*8*, *20*). This interaction is important for the maintenance of both cell type. Indeed, it has been shown that chronic B cell depletion in mice leads to the decrease of FDC network formation (*84*). Moreover, in transgenic µMT mice in which B cell development is stopped, FDCs are lacking (*85*).

Even though the mesenchymal origin of FDCs is well established, the exact identity of their precursor(s) is still not totally clear. Genetic studies and fate mapping approaches showed in the spleen that FDCs arise from ubiquitous perivascular precursors (preFDC) expressing platelet-derived growth factor receptor β (PDGFRβ)) and SMA (alpha smooth muscle actin), molecules associated with vascular mural cells. The engagement of these precursors in a FDC pathway is LTβR-dependent (*6*, *86*). Moreover, it has been shown that the white adipose stromal vascular fraction contains, and these precursors were identified as gp38+ CD31- cells (*87*, *88*). Another lineage-tracing approach that uses reporter genes in the spleen showed that FDCs, TRCs and MRCs originate from precursors which express NK2 homeobox 5 protein (NKX2.5) and insulin gene enhancer protein (ISL1). These precursor cells were implanted under the kidney capsule and gave rise to lymphoid structures (*89*). A multicolor fate mapping study using the UBOW system suggested that FDC network development and remodeling proceed in two steps: proliferation then differentiation of the MRCs. This process starts at the LN subcapsular sinus where MRCs are localized, then

the phenotypic transition occurs before acquiring the final FDC characteristics. LN FDCs are then localized in the center of B cell follicle and not at the SCS level anymore (*90*).

In addition to the stromal maker podoplanin (gp38), FDCs are the only stromal subset that express CD21/35 Complement receptors CD21/35; FcγRIIb (CD32) and FcγRIIb (CD23) are mainly expressed by light zone FDCs (*17*). Furthermore, FDCs are major source of CXCL13, a chemokine that binds CXCR5 of B cells and then attracts them to the LN (*91*). The function of these cells is detailed in the next chapter.

2.3. Bibliography

1. C. L. Willard-Mack, Normal structure, function, and histology of lymph nodes. *Toxicol. Pathol.* **34**, 409–424 (2006).

2. T. Junt, E. Scandella, B. Ludewig, Form follows function: lymphoid tissue microarchitecture in antimicrobial immune defence. *Nat. Rev. Immunol.* **8**, 764–775 (2008).

3. S. N. Mueller, R. N. Germain, Stromal cell contributions to the homeostasis and functionality of the immune system. *Nat. Rev. Immunol.* **9**, 618–629 (2009).

4. T. Katakai, Marginal reticular cells: a stromal subset directly descended from the lymphoid tissue organizer. *Front. Immunol.* **3**, 200 (2012).

5. T. Katakai *et al.*, Organizer-like reticular stromal cell layer common to adult secondary lymphoid organs. *J. Immunol. Baltim. Md 1950*. **181**, 6189–6200 (2008).

6. N. J. Krautler *et al.*, Follicular dendritic cells emerge from ubiquitous perivascular precursors. *Cell*. **150**, 194–206 (2012).

7. J. G. Cyster *et al.*, Follicular stromal cells and lymphocyte homing to follicles. *Immunol. Rev.* **176**, 181–193 (2000).

8. R. Roozendaal, R. E. Mebius, Stromal cell-immune cell interactions. *Annu. Rev. Immunol.* **29**, 23–43 (2011).

9. A. Y. Collier, J.-W. Lee, S. J. Turley, Self-encounters of the third kind: lymph node stroma promotes tolerance to peripheral tissue antigens. *Mucosal Immunol.* **1**, 248–251 (2008).

10. J. E. Chang, S. J. Turley, Stromal infrastructure of the lymph node and coordination of immunity. *Trends Immunol.* **36**, 30–39 (2015).

11. J. J. Koning, R. E. Mebius, Interdependence of stromal and immune cells for lymph node function. *Trends Immunol.* **33**, 264–270 (2012).

12. T. Lämmermann, M. Sixt, The microanatomy of T cell responses. *Immunol. Rev.* **221**, 26–43 (2008).

13. A. Link *et al.*, Fibroblastic reticular cells in lymph nodes regulate the homeostasis of naive T cells. *Nat. Immunol.* **8**, 1255–1265 (2007).

14. L. Liu, G.-P. Shi, CD31: beyond a marker for endothelial cells. *Cardiovasc. Res.* **94**, 3–5 (2012).

15. J. L. Astarita, S. E. Acton, S. J. Turley, Podoplanin: emerging functions in development, the immune system, and cancer. *Front. Immunol.* **3**, 283 (2012).

16. S. E. Acton *et al.*, Podoplanin-rich stromal networks induce dendritic cell motility via activation of the C-type lectin receptor CLEC-2. *Immunity*. **37**, 276–289 (2012).

17. C. D. C. Allen, J. G. Cyster, Follicular dendritic cell networks of primary follicles and germinal centers: phenotype and function. *Semin. Immunol.* **20**, 14–25 (2008).

18. C. Mionnet *et al.*, Identification of a new stromal cell type involved in the regulation of inflamed B cell follicles. *PLoS Biol.* **11**, e1001672 (2013).

19. V. Cremasco *et al.*, B cell homeostasis and follicle confines are governed by fibroblastic reticular cells. *Nat. Immunol.* **15**, 973–981 (2014).

20. A. L. Fletcher, S. E. Acton, K. Knoblich, Lymph node fibroblastic reticular cells in health and disease. *Nat. Rev. Immunol.* **15**, 350–361 (2015).

21. M. Buettner, R. Pabst, U. Bode, Stromal cell heterogeneity in lymphoid organs. *Trends Immunol.* **31**, 80–86 (2010).

22. A. L. Fletcher *et al.*, Lymph node fibroblastic reticular cells directly present peripheral tissue antigen under steady-state and inflammatory conditions. *J. Exp. Med.* **207**, 689–697 (2010).

23. J. M. Gardner *et al.*, Deletional tolerance mediated by extrathymic Aire-expressing cells. *Science*. **321**, 843–847 (2008).

24. D. Malhotra *et al.*, Transcriptional profiling of stroma from inflamed and resting lymph nodes defines immunological hallmarks. *Nat. Immunol.* **13**, 499–510 (2012).

25. W. E. Paul, Ed., *Fundamental immunology* (Wolters Kluwer Health/Lippincott Williams & Wilkins, Philadelphia, 7th ed., 2013).

26. P. R. Streeter, B. T. Rouse, E. C. Butcher, Immunohistologic and functional characterization of a vascular addressin involved in lymphocyte homing into peripheral lymph nodes. *J. Cell Biol.* **107**, 1853–1862 (1988).

27. H. Kawashima *et al.*, N-acetylglucosamine-6-O-sulfotransferases 1 and 2 cooperatively control lymphocyte homing through L-selectin ligand biosynthesis in high endothelial venules. *Nat. Immunol.* **6**, 1096–1104 (2005).

28. J.-P. Girard, C. Moussion, R. Förster, HEVs, lymphatics and homeostatic immune cell trafficking in lymph nodes. *Nat. Rev. Immunol.* **12**, 762–773 (2012).

29. S. Miyawaki *et al.*, A new mutation, aly, that induces a generalized lack of lymph nodes accompanied by immunodeficiency in mice. *Eur. J. Immunol.* **24**, 429–434 (1994).

30. E. Umemoto *et al.*, Novel regulators of lymphocyte trafficking across high endothelial venules. *Crit. Rev. Immunol.* **31**, 147–169 (2011).

31. R. E. Mebius, P. R. Streeter, J. Brevé, A. M. Duijvestijn, G. Kraal, The influence of afferent lymphatic vessel interruption on vascular addressin expression. *J. Cell Biol.* **115**, 85–95 (1991).

32. S. Chen, H. Kawashima, J. B. Lowe, L. L. Lanier, M. Fukuda, Suppression of tumor formation in lymph nodes by L-selectin-mediated natural killer cell recruitment. *J. Exp. Med.* **202**, 1679–1689 (2005).

33. K. Liu *et al.*, In vivo analysis of dendritic cell development and homeostasis. *Science*. **324**, 392–397 (2009).

34. S. Seth *et al.*, CCR7 essentially contributes to the homing of plasmacytoid dendritic cells to lymph nodes under steady-state as well as inflammatory conditions. *J. Immunol. Baltim. Md 1950*. **186**, 3364–3372 (2011).

35. P. Baluk *et al.*, Functionally specialized junctions between endothelial cells of lymphatic vessels. *J. Exp. Med.* **204**, 2349–2362 (2007).

36. G. Jurisic, M. Detmar, Lymphatic endothelium in health and disease. *Cell Tissue Res.* **335**, 97–108 (2009).

37. G. Oliver, Lymphatic vasculature development. *Nat. Rev. Immunol.* **4**, 35–45 (2004).

38. M. H. Ulvmar, T. Mäkinen, Heterogeneity in the lymphatic vascular system and its origin. *Cardiovasc. Res.* **111**, 310–321 (2016).

39. M. Furuya *et al.*, Lymphatic endothelial murine chloride channel calcium-activated 1 is a ligand for leukocyte LFA-1 and Mac-1. *J. Immunol. Baltim. Md 1950*. **185**, 5769–5777 (2010).

40. S. Banerji *et al.*, LYVE-1, a new homologue of the CD44 glycoprotein, is a lymph-specific receptor for hyaluronan. *J. Cell Biol.* **144**, 789–801 (1999).

41. J. T. Wigle, G. Oliver, Prox1 function is required for the development of the murine lymphatic system. *Cell*. **98**, 769–778 (1999).

42. M. Weber *et al.*, Interstitial dendritic cell guidance by haptotactic chemokine gradients. *Science*. **339**, 328–332 (2013).

43. C. Beauvillain *et al.*, CCR7 is involved in the migration of neutrophils to lymph nodes. *Blood*. **117**, 1196–1204 (2011).

44. S. K. Bromley, S. Yan, M. Tomura, O. Kanagawa, A. D. Luster, Recirculating memory T cells are a unique subset of CD4+ T cells with a distinct phenotype and migratory pattern. *J. Immunol. Baltim. Md 1950*. **190**, 970–976 (2013).

45. N. Kanemitsu *et al.*, CXCL13 is an arrest chemokine for B cells in high endothelial venules. *Blood*. **106**, 2613–2618 (2005).

46. L. Onder *et al.*, Endothelial cell-specific lymphotoxin-β receptor signaling is critical for lymph node and high endothelial venule formation. *J. Exp. Med.* **210**, 465–473 (2013).

47. L. A. Johnson, D. G. Jackson, Inflammation-induced secretion of CCL21 in lymphatic endothelium is a key regulator of integrin-mediated dendritic cell transmigration. *Int. Immunol.* **22**, 839–849 (2010).

48. R. Förster *et al.*, A putative chemokine receptor, BLR1, directs B cell migration to defined lymphoid organs and specific anatomic compartments of the spleen. *Cell*. **87**, 1037–1047 (1996).

49. D. F. Legler *et al.*, B cell-attracting chemokine 1, a human CXC chemokine expressed in lymphoid tissues, selectively attracts B lymphocytes via BLR1/CXCR5. *J. Exp. Med.* **187**, 655–660 (1998).

50. R. Förster *et al.*, CCR7 coordinates the primary immune response by establishing functional microenvironments in secondary lymphoid organs. *Cell*. **99**, 23–33 (1999).

51. S. Mori *et al.*, Mice lacking expression of the chemokines CCL21-ser and CCL19 (plt mice) demonstrate delayed but enhanced T cell immune responses. *J. Exp. Med.* **193**, 207–218 (2001).

52. W. L. Redmond, B. C. Marincek, L. A. Sherman, Distinct requirements for deletion versus anergy during CD8 T cell peripheral tolerance in vivo. *J. Immunol. Baltim. Md 1950*. **174**, 2046–2053 (2005).

53. A. A. Kyriazis, J. R. Esterly, Development of lymphoid tissues in the human embryo and early fetus. *Arch. Pathol.* **90**, 348–353 (1970).

54. M. Salmi *et al.*, Immune cell trafficking in uterus and early life is dominated by the mucosal addressin MAdCAM-1 in humans. *Gastroenterology*. **121**, 853–864 (2001).

55. C. Cunningham-Rundles, P. P. Ponda, Molecular defects in T- and B cell primary immunodeficiency diseases. *Nat. Rev. Immunol.* **5**, 880–892 (2005).

56. C. M. Roifman, J. Zhang, D. Chitayat, N. Sharfe, A partial deficiency of interleukin-7R alpha is sufficient to abrogate T cell development and cause severe combined immunodeficiency. *Blood*. **96**, 2803–2807 (2000).

57. E. Crivellato, F. Mallardi, Stromal cell organisation in the mouse lymph node. A light and electron microscopic investigation using the zinc iodide-osmium technique. *J. Anat.* **190 (Pt 1)**, 85–92 (1997).

58. H. G. Alvarenga, L. Marti, Multifunctional roles of reticular fibroblastic cells: more than meets the eye? *J. Immunol. Res.* **2014**, 402038 (2014).

59. M. Sixt *et al.*, The conduit system transports soluble antigens from the afferent lymph to resident dendritic cells in the T cell area of the lymph node. *Immunity*. **22**, 19–29 (2005).

60. R. Roozendaal *et al.*, Conduits mediate transport of low-molecular-weight antigen to lymph node follicles. *Immunity*. **30**, 264–276 (2009).

61. A. L. Fletcher, D. Malhotra, S. J. Turley, Lymph node stroma broaden the peripheral tolerance paradigm. *Trends Immunol.* **32**, 12–18 (2011).

62. M. Bajénoff *et al.*, Stromal cell networks regulate lymphocyte entry, migration, and territoriality in lymph nodes. *Immunity*. **25**, 989–1001 (2006).

63. S. A. Luther, T. K. Vogt, S. Siegert, Guiding blind T cells and dendritic cells: A closer look at fibroblastic reticular cells found within lymph node T zones. *Immunol. Lett.* **138**, 9–11 (2011).

64. F. Graw, R. R. Regoes, Influence of the fibroblastic reticular network on cell-cell interactions in lymphoid organs. *PLoS Comput. Biol.* **8**, e1002436 (2012).

65. S. N. Mueller, R. Ahmed, Lymphoid stroma in the initiation and control of immune responses. *Immunol. Rev.* **224**, 284–294 (2008).

66. L. Onder *et al.*, IL-7-producing stromal cells are critical for lymph node remodeling. *Blood*. **120**, 4675–4683 (2012).

67. C.-Y. Yang *et al.*, Trapping of naive lymphocytes triggers rapid growth and remodeling of the fibroblast network in reactive murine lymph nodes. *Proc. Natl. Acad. Sci. U. S. A.* **111**, E109-118 (2014).

68. Q. Chai *et al.*, Maturation of Lymph Node Fibroblastic Reticular Cells from Myofibroblastic Precursors Is Critical for Antiviral Immunity. *Immunity*. **38**, 1013–1024 (2013).

69. J.-W. Lee *et al.*, Peripheral antigen display by lymph node stroma promotes T cell tolerance to intestinal self. *Nat. Immunol.* **8**, 181–190 (2007).

70. S. Siegert, S. A. Luther, Positive and negative regulation of T cell responses by fibroblastic reticular cells within paracortical regions of lymph nodes. *Front. Immunol.* **3**, 285 (2012).

71. E. D. Reynoso, J.-W. Lee, S. J. Turley, Peripheral tolerance induction by lymph node stroma. *Adv. Exp. Med. Biol.* **633**, 113–127 (2009).

72. R. E. Mebius, G. Kraal, Structure and function of the spleen. *Nat. Rev. Immunol.* **5**, 606–616 (2005).

73. P. De Togni *et al.*, Abnormal development of peripheral lymphoid organs in mice deficient in lymphotoxin. *Science*. **264**, 703–707 (1994).

74. T. Cupedo *et al.*, Presumptive lymph node organizers are differentially represented in developing mesenteric and peripheral nodes. *J. Immunol. Baltim. Md 1950*. **173**, 2968–2975 (2004).

75. M. Bajénoff, R. N. Germain, B cell follicle development remodels the conduit system and allows soluble antigen delivery to follicular dendritic cells. *Blood*. **114**, 4989–4997 (2009).

76. Y. R. Carrasco, F. D. Batista, B cells acquire particulate antigen in a macrophage-rich area at the boundary between the follicle and the subcapsular sinus of the lymph node. *Immunity*. **27**, 160–171 (2007).

77. T. G. Phan, J. A. Green, E. E. Gray, Y. Xu, J. G. Cyster, Immune complex relay by subcapsular sinus macrophages and noncognate B cells drives antibody affinity maturation. *Nat. Immunol.* **10**, 786–793 (2009).

78. J. J. Miller, G. J. Nossal, ANTIGENS IN IMMUNITY. VI. THE PHAGOCYTIC RETICULUM OF LYMPH NODE FOLLICLES. *J. Exp. Med.* **120**, 1075–1086 (1964).

79. G. J. Nossal, A. Abbot, J. Mitchell, Z. Lummus, Antigens in immunity. XV. Ultrastructural features of antigen capture in primary and secondary lymphoid follicles. *J. Exp. Med.* **127**, 277–290 (1968).

80. T. E. Mandel, R. P. Phipps, A. P. Abbot, J. G. Tew, Long-term antigen retention by dendritic cells in the popliteal lymph node of immunized mice. *Immunology*. **43**, 353–362 (1981).

81. J. Mitchell, A. Abbot, Ultrastructure of the antigen-retaining reticulum of lymph node follicles as shown by high-resolution autoradiography. *Nature*. **208**, 500–502 (1965).

82. S. Sukumar, M. E. El Shikh, J. G. Tew, A. K. Szakal, Ultrastructural study of highly enriched follicular dendritic cells reveals their morphology and the periodicity of immune complex binding. *Cell Tissue Res.* **332**, 89–99 (2008).

83. A. K. Szakal, R. L. Gieringer, M. H. Kosco, J. G. Tew, Isolated follicular dendritic cells: cytochemical antigen localization, Nomarski, SEM, and TEM morphology. *J. Immunol. Baltim. Md 1950*. **134**, 1349–1359 (1985).

84. A. Cerny, R. M. Zinkernagel, P. Groscurth, Development of follicular dendritic cells in lymph nodes of B cell-depleted mice. *Cell Tissue Res.* **254**, 449–454 (1988).

85. D. Kitamura, J. Roes, R. Kühn, K. Rajewsky, A B cell-deficient mouse by targeted disruption of the membrane exon of the immunoglobulin mu chain gene. *Nature*. **350**, 423–426 (1991).

86. A. Aguzzi, J. Kranich, N. J. Krautler, Follicular dendritic cells: origin, phenotype, and function in health and disease. *Trends Immunol.* **35**, 105–113 (2014).

87. C. Bénézech *et al.*, Lymphotoxin-β receptor signaling through NF-κB2-RelB pathway reprograms adipocyte precursors as lymph node stromal cells. *Immunity*. **37**, 721–734 (2012).

88. W. Tang *et al.*, White fat progenitor cells reside in the adipose vasculature. *Science*. **322**, 583–586 (2008).

89. L. Castagnaro *et al.*, Nkx2-5(+)islet1(+) mesenchymal precursors generate distinct spleen stromal cell subsets and participate in restoring stromal network integrity. *Immunity*. **38**, 782–791 (2013).

90. M. Jarjour *et al.*, Fate mapping reveals origin and dynamics of lymph node follicular dendritic cells. *J. Exp. Med.* **211**, 1109–1122 (2014).

91. K. M. Ansel *et al.*, A chemokine-driven positive feedback loop organizes lymphoid follicles. *Nature*. **406**, 309–314 (2000).

*****

3. B cell follicle structure and function in adult LN

3.1. Cellular Organization

B cell follicles are localized at the cortical zone of the LN. Two types of follicles can be observed: primary follicles found in steady state and composed basically of naïve µ+ ∂+B cells, and secondary follicles formed after immune activation and composed of germinal B and T cells and some macrophages (*1*). Hereafter, the organization of these follicles, their structure and functioning are detailed.

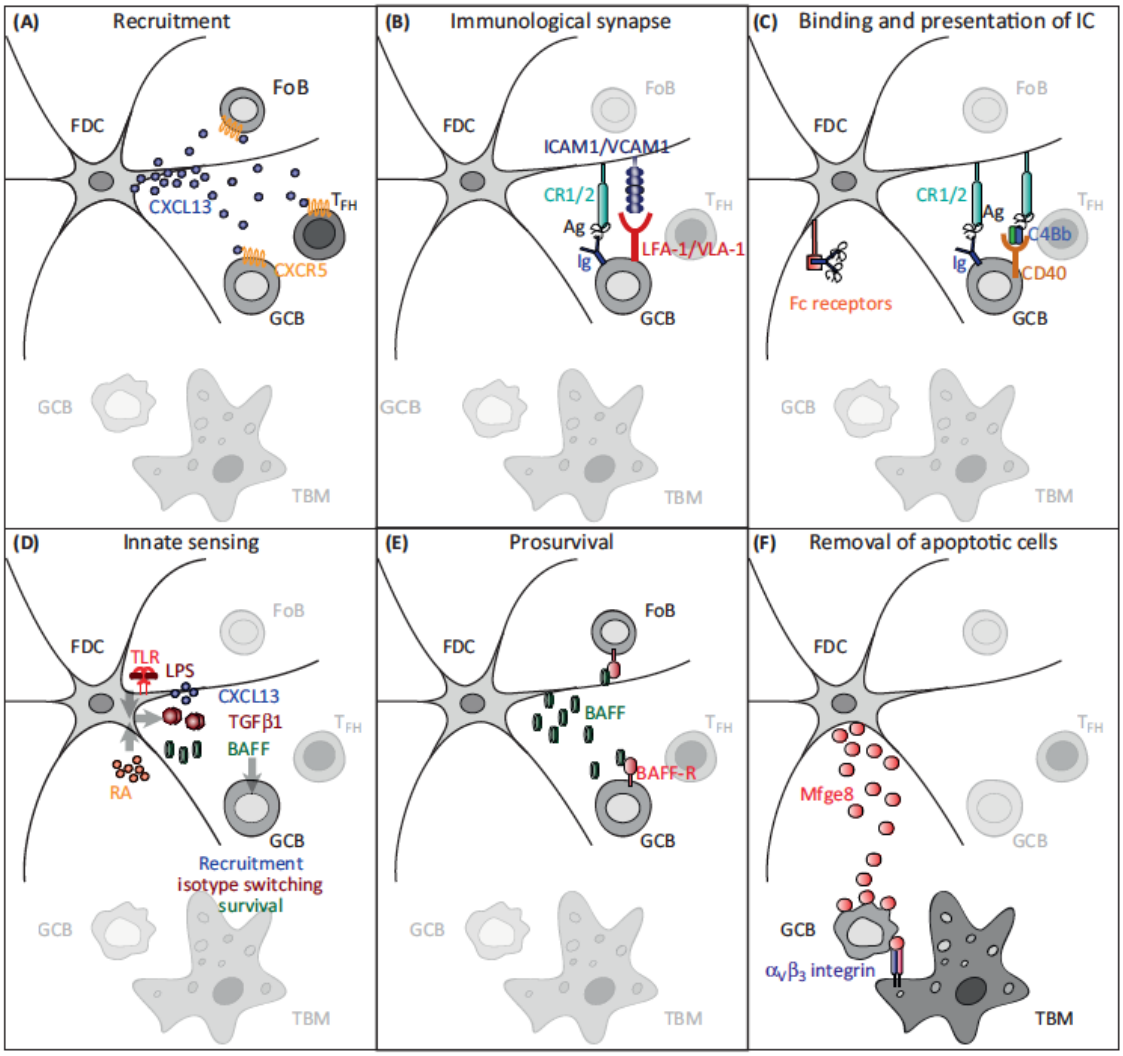

Figure 3-1: Immunological functions of FDCs. *(A) FDCs, major source of CXCL13 in SLOs, recruit CXCR5 expressing FoB cells, GC B cells, and T_{FH} cells into B cell follicles. (B) Immunological synapse involving FDCs and B cells ensured by integrins and adhesion molecules, and leading to BCR signaling. (C) FDCs bind antigen in the form of ICs via Fc and complement receptors (CR1 and CR2); this leads to antigen-specific signaling in GC B cells bearing cognate BCR (Ig). (D) FDC express TLR4 that is upregulated after immune challenge by LPS leading to molecular upregulation of some proliferative factors in favor of GC B cell proliferation and maintenance. (E) B*

cell survival in the follicle is ensured by FDC-BAFF signaling. (F) FDCs induce low affinity GC B cells apoptosis though Mfge8 secretion. Apoptotic cells are then recognized and cleared by TBMs in an $a_v b3$ integrin-dependent manner. Abbreviations: *BCR: B cell receptor; CXCL13: chemokine (C–X–C) motif ligand 13; CXCR5: chemokine (C–X–C motif) receptor 5; FDCs: follicular dendritic cells; FoB cells: follicular B cells; GC: germinal center; ICAM1: intercellular adhesion molecule 1; ICs: immune complexes; LFA-1, lymphocyte function associated antigen 1; LPS: lipopolysaccharide; Mfge8, milk fat EGF-factor 8; PS: phosphatidylserine; TBM: tingible-body macrophage; TFH cells: follicular helper T cells; TGFb: transforming growth factor b1; TLR: toll-like receptor; VCAM1: vascular cell adhesion molecule 1; VLA-4, very late antigen 4. After reference* **(26)**.

3.1.1. B cell homing and migration

During the first days after birth, the LN anlagen is still not well developed. It is mainly constituted of stromal cells and very few hematopoietic cells, since B cells are not circulating yet. Indeed, the first B cells leave the bone marrow at P3 and are firstly found underneath the subcapsular sinus of the LN while FDCs are not present at this stage in LN. Only after P7, the newly formed FDC networks enhance B cell aggregation at the cortical zone. The FDC network is fully formed by the end of the third week after birth (2–4).

FDCs produce CXCL13 which signals through CXCR5 and attracts B cells and specific T cell subsets into the follicles, this cell ingress depends on the CXCL13 gradient (Figure 3-1-A) (4, 5). Nevertheless, B cell responsiveness to the CXCL13 gradient can be overruled by other factors (6). Indeed, HEVs can also express CXCL13 that increases B cell adhesion and ingress involving integrin α4 and αLβ2 and adhesion molecules ICAM and VCAM (7).

The importance of FDCs for B cell follicle structure formation has been shown in transgenic mice where ablation of CD21+ cells (FDCs) led to the loss of the follicular structure but not B cells; still, B cell organization is affected and their displacement is reduced (8). B cells in turn are also indispensable for FDC development and maintenance, they provide FDC with TNF and Lymphotoxin signals (6, 9). Indeed, it has been shown in TNFα and TNFR1 deficient mice that, even though B cells are able to home normally in the cortical zone of LNs, the organized follicular structure and the FDC network fail to form (10). Moreover, when normal adult mice are treated with anti-TNFR1 blocking antibody, the follicular structure is disrupted and so, FDC network is ablated (11). Surprisingly, anti-LTβR blocking antibody does not affect B cell follicle architecture at the adult age in LNs compared to spleen where this structure is altered and the FDC network is disrupted (11, 12). Taken together, these data show that continuous TNFα/TNFR1 signaling is required for B cell follicle formation and maintenance in LNs.

In summary, FDC attraction of B cells to the follicular structure through HEVs is CXCL13-dependent, and involves TNF and LT signaling. This B cell migration could be of a great interest for Ag survey by B cells (Figure 3-2).

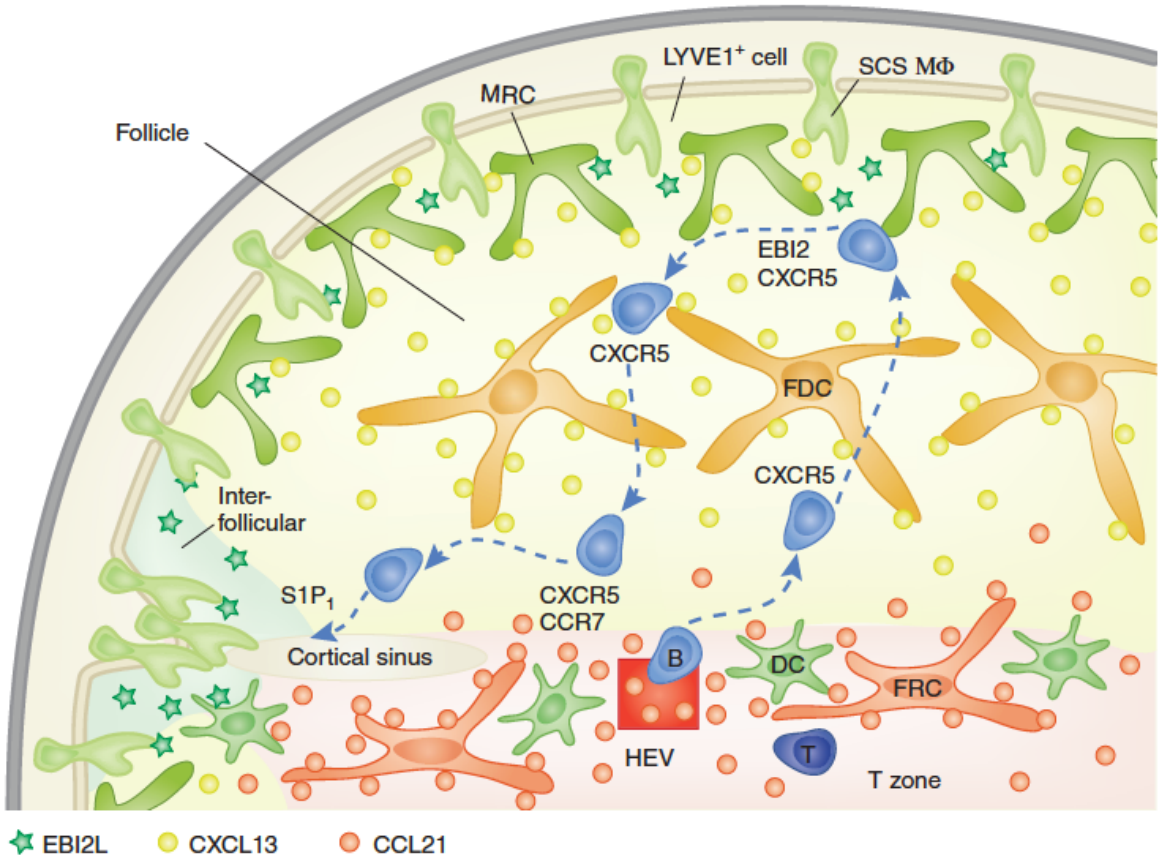

Figure 3-2: B cell dynamics within LN follicles. *HEVs conduct B cells to the LN in a CXCR5-CXCL13-dependent way. Then Both CXCL13 and EBI2L (Epstein Barr virus induced molecule ligand 2), the source of EBI2L is not yet determined. Backward migration through FDC network till T cell zone is enhanced by CCR7 expression. This cell trafficking enhances B cell survey and increase the probability for B cells to encounter antigens presented by subcapsular sinus macrophages MΦ. B cells exist the LN through the cortical sinus. After reference* **(13)**.

After antigen-driven immune activation, B cells migrate to the primary follicle (described above) and proliferate to form GCs: we talk then about secondary follicles. The GCs take a minimum of one week to form but remain for several weeks. They are the place where immunoglobulin (Ig) class switch, somatic mutations and selection of high-affinity B cells occur (*1*, *14*). GCs architecture comprises two histological regions: the dark and the light zone. The dark zone (DZ) is localized close to T cell zone; it contains large proliferating B cells called centroblasts, they markedly reduce their expression of Ig, particularly IgD.

The light zone (LZ) is less dense in cells, B cells are smaller, non-mitotic and they do express surface Ag; they are called centrocytes. LZ contains some Follicular Helper T cells (T_{FH}) that are required for the engagement of humoral immune response. The resting B cells are displaced toward the periphery of the follicle to form the mantle zone (*1*, *6*, *14*). While in primary follicles FDCs are localized in the center of the follicle, in GCs a polarization in their distribution is observed: FDC density is higher in the LZ than in the DZ (*6*). FDCs can retain immune complexes for a long time, which is crucial for GC maintenance, B cell somatic hypermutation (SHM) and immune memory (*15*). New molecular markers are identified in the secondary follicle compared to the primary follicle (Figure 3-3).

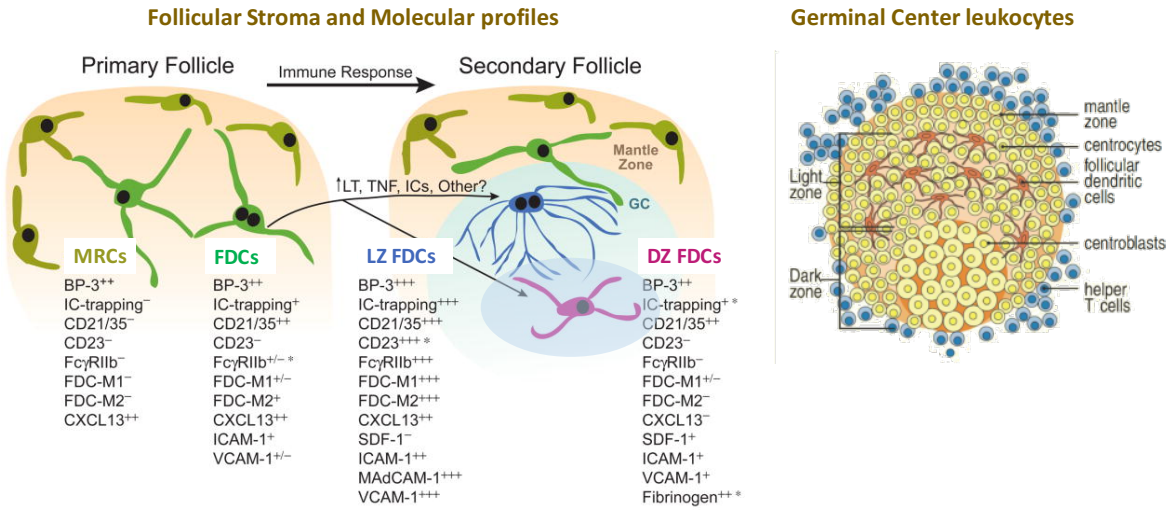

Figure 3-3: B cell area organization in steady state and in the immune context. *Primary follicles are constituted of naïve B cells and FDCs in the center of the follicle. Under immune response, germinal centers arise, they are compartmentalized into two zones: a light zone (LZ) and a dark zone (DZ). DZ is denser in both immune and stromal cells than the LZ. Antigen-specific B cell blasts called centroblasts are localized at the DZ, they give rise to the centrocytes of the LZ. FDCs of the primary follicle are thought to differentiate into a more mature form under LT and TNF signals. Their localization in the GCs is more polarized: they are denser at the DZ than at the LZ. Modified after* **(6, 16–19)**.

The polarization of FDCs is coupled to differential expression of chemokines: while LZ FDCs express CXCL13 to attract B cells, DZ FDCs express CXCL12, a chemokine that binds CXCR4 of centroblasts. Moreover, LZ FDCs express high levels of ICAM-1 and MAdCAM-1 suggesting a role of these adhesion molecules in B cell retention (6). It has been shown that B cell attachment is more static in the DZ compared to LZ where they are more mobile

(20). GC B cells express high levels of LTα1β2 compared to naïve B cells, in vitro experiments suggest that these high levels may be responsible of LZ FDC expression profiles of adhesion molecules (21). Hence, GC FDCs are seen as a mature form of FDCs.

3.1.2. B cell survival and proliferation

B cell Activating Factor (BAFF), a member of the TNFSF, is expressed by stromal cells i.e. FDCs; a minor expression level is also observable in hematopoietic cells. BAFF has been shown to interact with BAFF receptor on B cell enhancing survival, growth and proliferation (22, 23). Moreover, genetic studies conducted in BAFF deficient mice show that even though BAFF is not required for the GC response, the sustainability of such response relies on BAFF (Figure 3-1-E) (24–26). In this case, BAFF signals through BCMA (B cell maturation antigen) and TACI (transmembrane activator and calcium modulator and cyclophilin-ligand interactor), two molecules expressed by GC B cells (27, 28).

Besides, FDCs provide GC with the pro-inflammatory interleukin-6 (IL-6). The lack of this cytokine leads to GC size reduction and defective upregulation of complement factor 3 leading to a defective complement-signaling (29, 30). A role of FDC – Interleukin 15 has been also shown in human GC B cell proliferation (31). Another molecule, CD320, discovered in human tonsil seems also necessary for GC B cell proliferation and plasma cell differentiation (32, 33). The GC B cell survival relies also on other FDC-expressed molecules : Notch ligands Delta-like 1 (Dll1) and Jagged 1 (Jg1) that interact with Notch 1 and 2 on GC B cells (34). Hence, through different trophic factors, FDCs enhance B cell survival, proliferation and growth (26).

3.1.3. The Germinal Center reaction: a crucial role for FDCs

3.1.3.1. IC delivery to FDCs

The localization of FDCs at the center of the primary follicle keeps opsonized Ag away from DC or macrophage seizure (13). However, it raises the question about IC delivery to FDCs. Different hypotheses have been proposed to answer this question evoking either a SCS macrophage/naïve B cell axis at the distal follicle or a DC/B cell axis at the proximal follicle or the conduit system (Figure 3-4) (35–38). Indeed, In vivo imaging showed that afferent lymphatic vessels deliver soluble ICs to LN SCS where macrophages possibly capture it via FcγR and complement CR3, then non-cognate follicular B cells uptake IC in a

CR2-dependent manner Figure 3-4). Another mechanism may involve the C-type lectin SIGNR1 of the SCS macrophages and probably DCs that then activate the classical complement pathway (C3d). ICs are then transmitted to FDCs via their complement receptors (CRs) (*13*, *39–42*). Complement receptors CD21/35 are found on all FDC subtypes and are required for antibody response to several antigens (*43*). Moreover, deficiency in those complement receptors on FDCs has been shown to disrupt both primary and secondary immune responses (*44*).

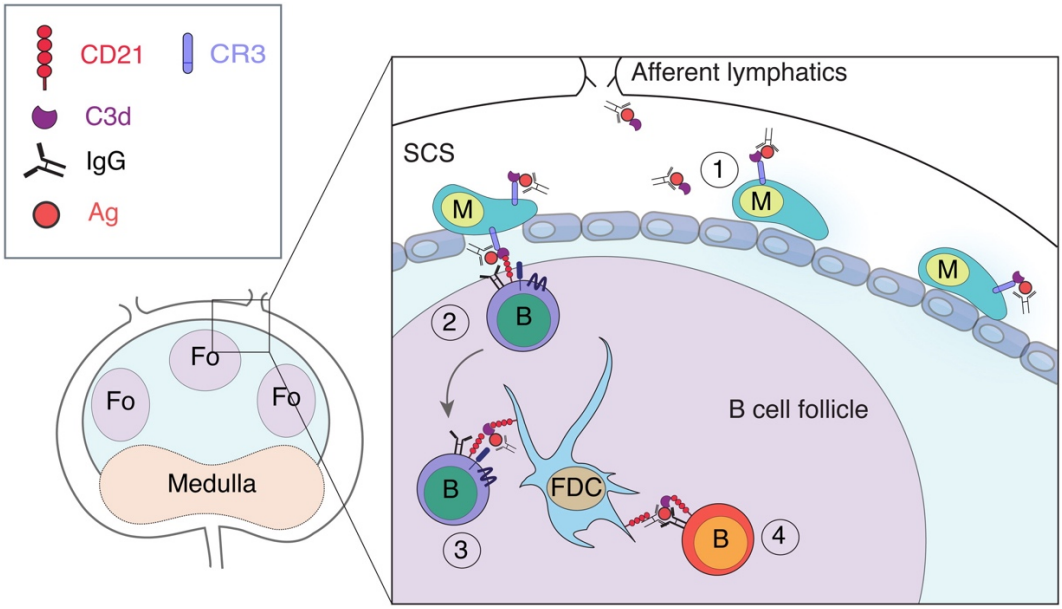

Figure 3-4: Recognition of B cell antigen in the LN. *(1) Immune complexes (ICs) are driven to the subcapsular sinus through the afferent lymphatic vessels and captured by the Complement Receptor 3 (CR3) of the macrophages. (2) Naïve B cells transport the opsonized ICs to the FDCs that (3) trap it via their Complement Receptors 2 (CR2). (4) Cognate B cells capture the antigen directly from the surface of FDCs. Adapted after* **(40, 41)**

3.1.3.2. Ag presentation by FDCs

FDCs have first been identified thanks to their capacity of retaining antigens (*45*). Contrary to DCs, FDCs do not phagocyte the antigen but present it on their membranes in its natural conformation since they do not involve protein cleavage but multimerization by arranging surface bound antigen with certain periodicity (200-500 Angstrom) in order to optimize the cross-linkage with BCRs (*46–49*). Immune Complexes (ICs) are presented on the surface of FDCs in immune complex coated bodies called "Iccosomes". Those beaded structures are transmitted to B cells in the few days following the Ag capture and are then

presented to T cells (Figure 3-1-B and C) (26, 50–52). The retention of Ag by FDCs requires the expression of membrane receptors of the fragment crystallizable region (Fc) of the antibodies (53). FcγRIIb (CD32) and FcεRIIb (CD23) show high expression levels in LZ FDCs compared to DZ and primary follicle (Figure 3-1-C) (6). Indeed, after opsonized IC capture via CRs, FcR expression is upregulated (41). FcγRIIb is implicated in GC enhancement. Few days after the beginning of humoral response, FcγRIIb levels increase considerably on the FDC surface. A positive loop is enhanced late after, and FDCs overexpress adhesion molecules and cytokines (52). IC presentation to B cells show similarities with T cell activation by APCs; however, while it is an early event for T cells, it occurs after a first encounter with the Ag for FDCs (Figure 3-5-B) (49).

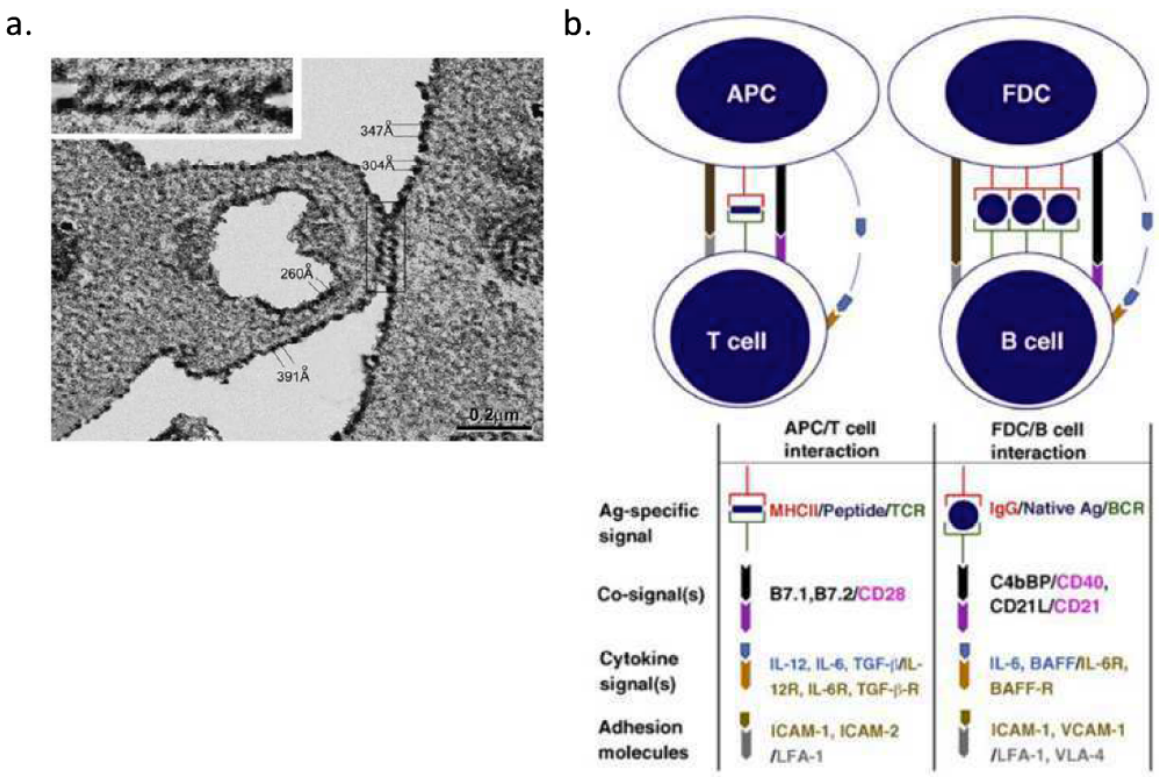

Figure 3-5: Antigen presentation by FDCs: B and T cells activation. *(a) Electronic Microscopy image showing the periodicity of immune complexes (horseradish peroxidase) on FDCs. The zippering of the membrane may explain the long term retention. (b) Antigen presentation on B and T cells showing the difference in engagement of Ags between each model. After reference* **(49)**

3.1.3.3. *Importance of Ag presentation by FDCs*

Ag presentation by the FDCs is necessary for the antibody affinity maturation process of B cells (*1*). ICs are presented in different ways leading to B cell selection in GCs and then to either B cell stimulations through CD21 and BCR (B cell receptors) clustering or inhibition by binding FcγRIIb and this in a BAFF-dependent way (*15*, *54–56*).

Under steady state, FcγRIIb trap the IgG at the surface of both FDCs and B cells, and so participate in the regulation of the humoral response. On the B cell surface, once BCR recognize the Ag of the IC, the adjacent FcγRIIb binds the IgG of the same IC leading to the inhibition of B cell activation via the tyrosine-based inhibitory motif (ITIM). Under immune challenge and after IC capture by the FDC, the FcγRIIb expression is strongly upregulated on FDCs leading to a cross-linking between BCR from B cell and FcγRIIb-IgG-Ag from FDC and then the dissociation of the BCR-FcγRIIb complex of the B cell. Thus, the inhibitory signal is stopped and B cell are activated (*49*, *52*, *57–60*).

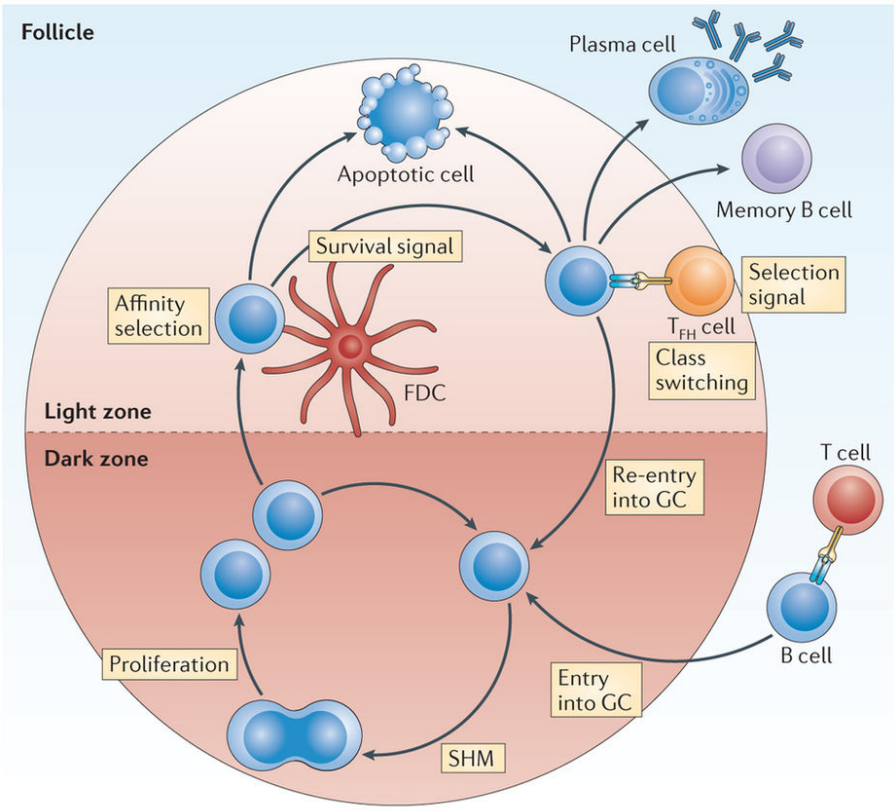

Figure 3-6: The germinal center reaction. *While somatic hypermutation and proliferation of B cells occurs in the dark zone, affinity selection of B cells by FDCs take place in the light zone. Selected B cells receive the selection signal from follicular helper T cells and perform class switching to differentiate into antibody secreting cells (Plasma Cells) and memory B cells. Other cells enter apoptotic cycle and are eliminated. After* (57).

During the GC reaction, B cells enter the DZ after presenting Ag to T helper cells. At DZ, they undergo somatic hypermutation (SHM) and proliferate then go back to the LZ where they are screened by FDC presenting the IC. Only B cells with high-affinity BCRs receive proliferative signals, the others follow apoptosis. Then B cells compete for Follicular Helper T cell (T_{FH}) that keep the highest affinity B cell. This one re-enter the DZ and go through a new SHM and proliferation cycle, then can exit as either plasma or memory cells. FDCs can control the number of Ags on their surface and so might influence affinity maturation (Figure 3-6) (*6*, *26*, *57*). Besides, T_{FH} migration to the GC is also mediated by FDCs in a CXCL13/CXCR5 way (*58*).

3.1.3.4. FDC role in innate immunity

Finally, it has been shown that FDCs express Toll-Like Receptor 4 (TLR4), known for its implication in bacterial lipopolysaccharide (LPS) detection. Moreover, TLR4 is upregulated in FDCs during the GC response. Indeed, FDC-TLR4 acts as an innate immune sensor, and its importance for affinity maturation has been demonstrated. In addition, TLRs seem also to control FDC maintenance, and then GC development and also IgA secretion (Figure 3-1-D) (*26*).

3.1.4.FDC in peripheral tolerance and autoimmunity prevention

B cell lymphopoiesis takes place in the bone marrow (BM), then immature B cells migrate to the spleen to achieve the maturation process (*63*). In order to control auto-reactivity of B cells, immature B cells that recognize self-antigens presented by splenic FDCs are eliminated (*64*, *65*). Since somatic mutations of B cells during the humoral immune response can generate auto-immune B cells, it has been suggested that FDCs may also play a regulatory role in other SLOs to maintain peripheral tolerance (*26*, *66*).

It has even been suggested that FDCs play a role in tolerizing T cells: LN resident DCs survey the antigen retained by FDCs in order to present the Ag to CD8+ T cells. Indeed, when FDCs were loaded by purified antigen associated with placental micro-particles after pregnancy, a T cell deletion has been induced under inflammatory conditions (*67*). These studies support the role of FDCs in auto-immunity through either IC presentation or T_{FH} recruitment. Hence, the FDC tolerogenic action includes the enhancement of tingible-body

macrophages (TBM) activity in the removal of apoptotic and auto-reactive B cell, and also inducing the generation of tolerogenic DCs unable to stimulate T cells (26).

Another implication of FDCs in autoimmunity prevention in GCs concerns the clearance of apoptotic cells. Since a lot of B cells in GCs do not show a high affinity for the Ag and some of them are even auto-reactive, those cells are programmed to die and are cleared by Tingible-Body Macrophages (TBM). It has been demonstrated that FDCs play a licensing role in this process through Milk fat globule-EGF-factor 8 (MFGE8), a molecule identical to FDC-M1, that interacts with integrins on TBMs and then permits a highly efficient opsonization of dying B cells (Figure 3-1-F) (26, 68, 69).

3.2. TNF and TNF-R super family signaling

As previously described, TNF and TNFR super family members play a crucial role during LN development; their role in adult LN has also been studied. Here, we will focus on TNF(R)SF and some other chemokines in their role in B cell follicle structure and function.

3.2.1. LTβR signaling

Different studies show that LTβR is expressed by the stromal compartment while its ligands are expressed by hematopoietic cells in adult LN (70). LTβR blockade experiments in adult mice showed that multiple FDC markers (FDC-M1, FDC-M2, and MAdCAM-1) disappear upon LTβR blockade (71). Moreover, CXCL13 and CCL19 expression is diminished, and thus adhesion molecules on HEVs (PNAd and MAdCMA-1) leading to the reduction of lymphocyte ingress to LNs. Consequently, newly formed IC capture was prevented and the trapped ICs were released after LT blockade (72–74). The role of LT signaling has also been studied during viral infection. LTβ-deficient mice show a conserved B cell response, nevertheless, the response against non-replicating Ag was impaired (75, 76), however a LTβR blockade showed a more severe consequence since antibody maturation was impaired, and the $CD4_+$ and $CD8_+$ T cell responses were deregulated (77). Beyond the lymphocyte impairment, LT deficiency affects lymphangiogenesis and lymph velocity (78, 79). During an immune reaction the medullary region swells and is filled with lymphocytes, it was demonstrated that LTβR is also involved in this process, since its blockade reduces the medullary remodeling and the plasma cell niche in the LN (80).

3.2.2. TNFα/TNFR signaling

The role of TNF signaling in SLO development and organization has been shown in different studies. In TNFα deficient mice, SLOs are still formed but the FDC network and the B cell follicles are missing in the spleen. This phenotype can be recovered by the administration of TNFα (*81*, *82*). Very interestingly, in LTα deficient mice, the complementation with the TNFα transgene restores the B/T cell segregation and preserves partially the B cell follicle, FDC network and GCs in a TNFR1-dependent way (*83*).

In LNs, TNFα or TNFR1 deficiency does not affect B cell homing at the cortical zone but the follicular structure is impaired and so the FDC network but not the SCS macrophages (*10*, *84*). Furthermore, another genetic study showed that the major source of TNFα, required for the B cell follicle formation, are B cells with a distinct contribution of T cells. In mice whose B and T cells are deficient for TNFα, LN FDC networks are completely missing. Moreover, the mice failed to develop B cell follicles and GCs, and the B cell/T cell compartmentalization is disturbed (*74*).

Continuous TNFR1 signaling is also essential for B cell follicle maintenance in SLOs. The blockade of TNFR1 signaling in adult wt mice led to the disruption of LN B cell follicular localization and the reduction of the FDC network leading to a defect in the IC maintenance but not IC delivery (*11*, *71*). These data support a role of TNFα signaling in humoral immune response in the LN. Indeed, in TNFα deficient mice, after an immune challenge, high affinity IgG secretion is highly reduced. The same result was obtained with or without splenectomy, showing that TNFα signaling is essential for Ig class switch in LNs (*74*).

Besides, TNFR1 signaling has been shown to play a pro-apoptotic role for CD4 and CD8 T cells during systemic infections in mLNs; on the other hand, CD95, another TNFSF, ensures B cell apoptosis (*85*).

3.2.3. RANK/RANKL signaling

The role of RANKL as enhancer of SLO growth has been shown in different studies using RANKL-blockade or overexpression experiments (*86–90*). This role may be fulfilled through lymphocyte recruitment to LN by different chemokines and adhesion molecules (*91–96*). Indeed, studies support that RANKL activates endothelial cells and thus prevents their apoptosis and enhances angiogenesis (*97*, *98*)

However, RANK/RANKL signaling in B cell follicle formation in LNs has not been well addressed. A genetic study using RANKL-KO mice showed the impairment of the follicular structure in the spleen and a failure of B cell homing at the cortical zone in the cervical LN miniatures. However, in this mouse model, splenic GCs were formed upon T cell dependent antigen immunization suggesting a dispensable contribution of RANKL to GC formation and maintenance. The rescue of RANKL deficiency in those mice through transgenic expression of RANKL in B and T cells restored LN formation but not the follicular structure (*99*). Those findings are concomitant with another conducted on mouse embryos showing a deficiency in a RANKL signal transducer TRAF-6. The administration of IL-7 rescued mLN formation but not B cell follicles (*88*). A study of RANKL blockade during the different stages of embryonic development demonstrated that B cell follicle formation was impaired after birth, accompanied by misplaced FDCs, and reduced VCAM-1 staining (*89*). Our lab showed that postnatal overexpression of RANK leads to an upregulation of some lymphocytes attracting chemokines CXCL13, CCL19, and adhesion molecules VCAM-1 and MAdCAM-1. Moreover, RANK overexpression leads to an increase in LN size and an increase in smaller but clearly defined B cell follicles, all comprising FDCs (*87*). Taken together, these studies suggest a possible implication of RANKL in B cell follicle formation. Very interestingly, MRCs, a reticular stromal subset that has been discovered recently, is shown to express RANKL in adult LN (*100*). The localization of these cell between the subcapsular sinus and the B cell follicles raises their role in B cell follicle homeostasis, organization and maintenance (*100*).

RANK/RANKL signaling also plays a role in adaptive immune responses. Activated CD4 and CD8 T cells express both surface and soluble RANKL (*101*, *102*). DCs express RANK, and it was shown, in vitro, that RANKL confers a better survival to DCs (*101*, *103–105*). RANKL stimulated DCs produce pro-inflammatory cytokines and T cell differentiation factors (*101*). Conversely, RANKL activation of DCs, in an oral tolerance model, was associated with tolerance (*105*). Moreover, RANKL stimulation on Langerhans cells and macrophages triggered anti-inflammatory effects (*106*, *107*). In addition, a role of RANKL in immune tolerance and autoimmunity suppression through Treg cells has been highlighted (*108*, *109*).

3.3. Bibliography

1. I. C. MacLennan, Germinal centers. *Annu. Rev. Immunol.* **12**, 117–139 (1994).

2. T. Cupedo, W. Jansen, G. Kraal, R. E. Mebius, Induction of secondary and tertiary lymphoid structures in the skin. *Immunity*. **21**, 655–667 (2004).

3. M. C. Coles *et al.*, Role of T and NK cells and IL7/IL7r interactions during neonatal maturation of lymph nodes. *Proc. Natl. Acad. Sci. U. S. A.* **103**, 13457–13462 (2006).

4. T. Cupedo *et al.*, Initiation of cellular organization in lymph nodes is regulated by non-B cell-derived signals and is not dependent on CXC chemokine ligand 13. *J. Immunol. Baltim. Md 1950*. **173**, 4889–4896 (2004).

5. K. M. Ansel *et al.*, A chemokine-driven positive feedback loop organizes lymphoid follicles. *Nature*. **406**, 309–314 (2000).

6. C. D. C. Allen, J. G. Cyster, Follicular dendritic cell networks of primary follicles and germinal centers: phenotype and function. *Semin. Immunol.* **20**, 14–25 (2008).

7. N. Kanemitsu *et al.*, CXCL13 is an arrest chemokine for B cells in high endothelial venules. *Blood*. **106**, 2613–2618 (2005).

8. X. Wang *et al.*, Follicular dendritic cells help establish follicle identity and promote B cell retention in germinal centers. *J. Exp. Med.* **208**, 2497–2510 (2011).

9. C. F. Ware, Network communications: lymphotoxins, LIGHT, and TNF. *Annu. Rev. Immunol.* **23**, 787–819 (2005).

10. M. Pasparakis *et al.*, Peyer's patch organogenesis is intact yet formation of B lymphocyte follicles is defective in peripheral lymphoid organs of mice deficient for tumor necrosis factor and its 55-kDa receptor. *Proc. Natl. Acad. Sci. U. S. A.* **94**, 6319–6323 (1997).

11. P. D. Rennert, D. James, F. Mackay, J. L. Browning, P. S. Hochman, Lymph node genesis is induced by signaling through the lymphotoxin beta receptor. *Immunity*. **9**, 71–79 (1998).

12. J. L. Gommerman *et al.*, Manipulation of lymphoid microenvironments in nonhuman primates by an inhibitor of the lymphotoxin pathway. *J. Clin. Invest.* **110**, 1359–1369 (2002).

13. J. G. Cyster, B cell follicles and antigen encounters of the third kind. *Nat. Immunol.* **11**, 989–996 (2010).

14. S. N. Mueller, R. N. Germain, Stromal cell contributions to the homeostasis and functionality of the immune system. *Nat. Rev. Immunol.* **9**, 618–629 (2009).

15. T. E. Mandel, R. P. Phipps, A. Abbot, J. G. Tew, The follicular dendritic cell: long term antigen retention during immunity. *Immunol. Rev.* **53**, 29–59 (1980).

16. T. Katakai, Marginal reticular cells: a stromal subset directly descended from the lymphoid tissue organizer. *Front. Immunol.* **3**, 200 (2012).

17. Janeway's immunobiology - NLM Catalog - NCBI, (available at https://www.ncbi.nlm.nih.gov/nlmcatalog/101568727).

18. C. D. C. Allen, T. Okada, J. G. Cyster, Germinal-center organization and cellular dynamics. *Immunity*. **27**, 190–202 (2007).

19. J. B. Beltman, C. D. C. Allen, J. G. Cyster, R. J. de Boer, B cells within germinal centers migrate preferentially from dark to light zone. *Proc. Natl. Acad. Sci. U. S. A.* **108**, 8755–8760 (2011).

20. T. A. Schwickert *et al.*, In vivo imaging of germinal centres reveals a dynamic open structure. *Nature*. **446**, 83–87 (2007).

21. H. Husson *et al.*, Functional effects of TNF and lymphotoxin alpha1beta2 on FDC-like cells. *Cell. Immunol.* **203**, 134–143 (2000).

22. P. Schneider *et al.*, BAFF, a novel ligand of the tumor necrosis factor family, stimulates B cell growth. *J. Exp. Med.* **189**, 1747–1756 (1999).

23. K. Suzuki *et al.*, The sensing of environmental stimuli by follicular dendritic cells promotes immunoglobulin A generation in the gut. *Immunity*. **33**, 71–83 (2010).

24. Z. S. M. Rahman, S. P. Rao, S. L. Kalled, T. Manser, Normal induction but attenuated progression of germinal center responses in BAFF and BAFF-R signaling-deficient mice. *J. Exp. Med.* **198**, 1157–1169 (2003).

25. K. A. Vora *et al.*, Cutting edge: germinal centers formed in the absence of B cell-activating factor belonging to the TNF family exhibit impaired maturation and function. *J. Immunol. Baltim. Md 1950*. **171**, 547–551 (2003).

26. A. Aguzzi, J. Kranich, N. J. Krautler, Follicular dendritic cells: origin, phenotype, and function in health and disease. *Trends Immunol.* **35**, 105–113 (2014).

27. J. R. Darce, B. K. Arendt, S. K. Chang, D. F. Jelinek, Divergent effects of BAFF on human memory B cell differentiation into Ig-secreting cells. *J. Immunol. Baltim. Md 1950*. **178**, 5612–5622 (2007).

28. C.-S. Park, Y. S. Choi, How do follicular dendritic cells interact intimately with B cells in the germinal centre? *Immunology*. **114**, 2–10 (2005).

29. C. Deng, E. Goluszko, E. Tüzün, H. Yang, P. Christadoss, Resistance to experimental autoimmune myasthenia gravis in IL-6-deficient mice is associated with reduced germinal center formation and C3 production. *J. Immunol. Baltim. Md 1950*. **169**, 1077–1083 (2002).

30. M. Kopf, S. Herren, M. V. Wiles, M. B. Pepys, M. H. Kosco-Vilbois, Interleukin 6 influences germinal center development and antibody production via a contribution of C3 complement component. *J. Exp. Med.* **188**, 1895–1906 (1998).

31. C.-S. Park, S.-O. Yoon, R. J. Armitage, Y. S. Choi, Follicular dendritic cells produce IL-15 that enhances germinal center B cell proliferation in membrane-bound form. *J. Immunol. Baltim. Md 1950*. **173**, 6676–6683 (2004).

32. X. Zhang *et al.*, The distinct roles of T cell-derived cytokines and a novel follicular dendritic cell-signaling molecule 8D6 in germinal center-B cell differentiation. *J. Immunol. Baltim. Md 1950*. **167**, 49–56 (2001).

33. L. Li *et al.*, Identification of a human follicular dendritic cell molecule that stimulates germinal center B cell growth. *J. Exp. Med.* **191**, 1077–1084 (2000).

34. S.-O. Yoon, X. Zhang, P. Berner, B. Blom, Y. S. Choi, Notch ligands expressed by follicular dendritic cells protect germinal center B cells from apoptosis. *J. Immunol. Baltim. Md 1950*. **183**, 352–358 (2009).

35. T. G. Phan, I. Grigorova, T. Okada, J. G. Cyster, Subcapsular encounter and complement-dependent transport of immune complexes by lymph node B cells. *Nat. Immunol.* **8**, 992–1000 (2007).

36. M. Bajénoff, R. N. Germain, B cell follicle development remodels the conduit system and allows soluble antigen delivery to follicular dendritic cells. *Blood*. **114**, 4989–4997 (2009).

37. E. Heinen *et al.*, Transfer of immune complexes from lymphocytes to follicular dendritic cells. *Eur. J. Immunol.* **16**, 167–172 (1986).

38. L. Martínez-Pomares *et al.*, Fc chimeric protein containing the cysteine-rich domain of the murine mannose receptor binds to macrophages from splenic marginal zone and lymph node subcapsular sinus and to germinal centers. *J. Exp. Med.* **184**, 1927–1937 (1996).

39. T. I. Arnon, R. M. Horton, I. L. Grigorova, J. G. Cyster, Visualization of splenic marginal zone B cell shuttling and follicular B cell egress. *Nature*. **493**, 684–688 (2013).

40. S. F. Gonzalez *et al.*, Trafficking of B cell antigen in lymph nodes. *Annu. Rev. Immunol.* **29**, 215–233 (2011).

41. M. C. Carroll, D. E. Isenman, Regulation of humoral immunity by complement. *Immunity*. **37**, 199–207 (2012).

42. Y.-S. Kang *et al.*, A dominant complement fixation pathway for pneumococcal polysaccharides initiated by SIGN-R1 interacting with C1q. *Cell*. **125**, 47–58 (2006).

43. M. C. Carroll, The role of complement and complement receptors in induction and regulation of immunity. *Annu. Rev. Immunol.* **16**, 545–568 (1998).

44. Y. Fang, C. Xu, Y. X. Fu, V. M. Holers, H. Molina, Expression of complement receptors 1 and 2 on follicular dendritic cells is necessary for the generation of a strong antigen-specific IgG response. *J. Immunol. Baltim. Md 1950*. **160**, 5273–5279 (1998).

45. J. Mitchell, A. Abbot, Ultrastructure of the antigen-retaining reticulum of lymph node follicles as shown by high-resolution autoradiography. *Nature*. **208**, 500–502 (1965).

46. J. M. Vyas, A. G. Van der Veen, H. L. Ploegh, The known unknowns of antigen processing and presentation. *Nat. Rev. Immunol.* **8**, 607–618 (2008).

47. S. Sukumar, M. E. El Shikh, J. G. Tew, A. K. Szakal, Ultrastructural study of highly enriched follicular dendritic cells reveals their morphology and the periodicity of immune complex binding. *Cell Tissue Res.* **332**, 89–99 (2008).

48. Y. Wu *et al.*, Immune complex-bearing follicular dendritic cells deliver a late antigenic signal that promotes somatic hypermutation. *J. Immunol. Baltim. Md 1950*. **180**, 281–290 (2008).

49. M. E. M. El Shikh, R. M. El Sayed, S. Sukumar, A. K. Szakal, J. G. Tew, Activation of B cells by antigens on follicular dendritic cells. *Trends Immunol.* **31**, 205–211 (2010).

50. A. K. Szakal, R. L. Gieringer, M. H. Kosco, J. G. Tew, Isolated follicular dendritic cells: cytochemical antigen localization, Nomarski, SEM, and TEM morphology. *J. Immunol. Baltim. Md 1950*. **134**, 1349–1359 (1985).

51. A. K. Szakal, M. H. Kosco, J. G. Tew, FDC-iccosome mediated antigen delivery to germinal center B cells, antigen processing and presentation to T cells. *Adv. Exp. Med. Biol.* **237**, 197–202 (1988).

52. M. E. El Shikh, R. El Sayed, A. K. Szakal, J. G. Tew, Follicular dendritic cell (FDC)-FcgammaRIIB engagement via immune complexes induces the activated FDC phenotype associated with secondary follicle development. *Eur. J. Immunol.* **36**, 2715–2724 (2006).

53. C. T. Schnizlein, M. H. Kosco, A. K. Szakal, J. G. Tew, Follicular dendritic cells in suspension: identification, enrichment, and initial characterization indicating immune complex trapping and lack of adherence and phagocytic activity. *J. Immunol. Baltim. Md 1950*. **134**, 1360–1368 (1985).

54. J. V. Ravetch, L. L. Lanier, Immune inhibitory receptors. *Science*. **290**, 84–89 (2000).

55. L. Gorelik *et al.*, Cutting edge: BAFF regulates CD21/35 and CD23 expression independent of its B cell survival function. *J. Immunol. Baltim. Md 1950*. **172**, 762–766 (2004).

56. H. Hase *et al.*, BAFF/BLyS can potentiate B cell selection with the B cell coreceptor complex. *Blood*. **103**, 2257–2265 (2004).

57. B. A. Heesters, R. C. Myers, M. C. Carroll, Follicular dendritic cells: dynamic antigen libraries. *Nat. Rev. Immunol.* **14**, 495–504 (2014).

58. S. Hardtke, L. Ohl, R. Förster, Balanced expression of CXCR5 and CCR7 on follicular T helper cells determines their transient positioning to lymph node follicles and is essential for efficient B cell help. *Blood*. **106**, 1924–1931 (2005).

59. J. G. Tew, J. Wu, M. Fakher, A. K. Szakal, D. Qin, Follicular dendritic cells: beyond the necessity of T cell help. *Trends Immunol.* **22**, 361–367 (2001).

60. Y. Aydar, P. Balogh, J. G. Tew, A. K. Szakal, Altered regulation of Fc gamma RII on aged follicular dendritic cells correlates with immunoreceptor tyrosine-based inhibition motif signaling in B cells and reduced germinal center formation. *J. Immunol. Baltim. Md 1950*. **171**, 5975–5987 (2003).

61. Y. Aydar, J. Wu, J. Song, A. K. Szakal, J. G. Tew, FcgammaRII expression on follicular dendritic cells and immunoreceptor tyrosine-based inhibition motif signaling in B cells. *Eur. J. Immunol.* **34**, 98–107 (2004).

62. D. Qin *et al.*, Fc gamma receptor IIB on follicular dendritic cells regulates the B cell recall response. *J. Immunol. Baltim. Md 1950*. **164**, 6268–6275 (2000).

63. R. R. Hardy, S. A. Shinton, Characterization of B lymphopoiesis in mouse bone marrow and spleen. *Methods Mol. Biol. Clifton NJ.* **271**, 1–24 (2004).

64. I. W. Yau *et al.*, Censoring of self-reactive B cells by follicular dendritic cell-displayed self-antigen. *J. Immunol. Baltim. Md 1950.* **191**, 1082–1090 (2013).

65. D. Y. Hur *et al.*, Role of follicular dendritic cells in the apoptosis of germinal center B cells. *Immunol. Lett.* **72**, 107–111 (2000).

66. R. Brink, The imperfect control of self-reactive germinal center B cells. *Curr. Opin. Immunol.* **28**, 97–101 (2014).

67. M. L. McCloskey, M. A. Curotto de Lafaille, M. C. Carroll, A. Erlebacher, Acquisition and presentation of follicular dendritic cell-bound antigen by lymph node-resident dendritic cells. *J. Exp. Med.* **208**, 135–148 (2011).

68. J. Kranich *et al.*, Follicular dendritic cells control engulfment of apoptotic bodies by secreting Mfge8. *J. Exp. Med.* **205**, 1293–1302 (2008).

69. R. Hanayama *et al.*, Autoimmune disease and impaired uptake of apoptotic cells in MFG-E8-deficient mice. *Science.* **304**, 1147–1150 (2004).

70. D. Malhotra *et al.*, Transcriptional profiling of stroma from inflamed and resting lymph nodes defines immunological hallmarks. *Nat. Immunol.* **13**, 499–510 (2012).

71. F. Mackay, J. L. Browning, Turning off follicular dendritic cells. *Nature.* **395**, 26–27 (1998).

72. J. L. Browning *et al.*, Lymphotoxin-beta receptor signaling is required for the homeostatic control of HEV differentiation and function. *Immunity.* **23**, 539–550 (2005).

73. J.-P. Girard, C. Moussion, R. Förster, HEVs, lymphatics and homeostatic immune cell trafficking in lymph nodes. *Nat. Rev. Immunol.* **12**, 762–773 (2012).

74. A. V. Tumanov *et al.*, Cellular source and molecular form of TNF specify its distinct functions in organization of secondary lymphoid organs. *Blood.* **116**, 3456–3464 (2010).

75. V. Kumar *et al.*, Global lymphoid tissue remodeling during a viral infection is orchestrated by a B cell-lymphotoxin-dependent pathway. *Blood.* **115**, 4725–4733 (2010).

76. T. Junt *et al.*, Expression of lymphotoxin beta governs immunity at two distinct levels. *Eur. J. Immunol.* **36**, 2061–2075 (2006).

77. D. D. McCarthy *et al.*, The lymphotoxin pathway: beyond lymph node development. *Immunol. Res.* **35**, 41–54 (2006).

78. R. H. Mounzer *et al.*, Lymphotoxin-alpha contributes to lymphangiogenesis. *Blood.* **116**, 2173–2182 (2010).

79. S. Chyou *et al.*, Fibroblast-type reticular stromal cells regulate the lymph node vasculature. *J. Immunol. Baltim. Md 1950.* **181**, 3887–3896 (2008).

80. J. Abe *et al.*, B cells regulate antibody responses through the medullary remodeling of inflamed lymph nodes. *Int. Immunol.* **24**, 17–27 (2012).

81. M. Pasparakis, L. Alexopoulou, V. Episkopou, G. Kollias, Immune and inflammatory responses in TNF alpha-deficient mice: a critical requirement for TNF alpha in the formation of primary B cell follicles, follicular dendritic cell networks and germinal centers, and in the maturation of the humoral immune response. *J. Exp. Med.* **184**, 1397–1411 (1996).

82. M. Pasparakis, L. Alexopoulou, E. Douni, G. Kollias, Tumour necrosis factors in immune regulation: everything that's interesting is...new! *Cytokine Growth Factor Rev.* **7**, 223–229 (1996).

83. L. Alexopoulou, M. Pasparakis, G. Kollias, Complementation of lymphotoxin alpha knockout mice with tumor necrosis factor-expressing transgenes rectifies defective splenic structure and function. *J. Exp. Med.* **188**, 745–754 (1998).

84. M. Pasparakis, S. Kousteni, J. Peschon, G. Kollias, Tumor necrosis factor and the p55TNF receptor are

required for optimal development of the marginal sinus and for migration of follicular dendritic cell precursors into splenic follicles. *Cell. Immunol.* **201**, 33–41 (2000).

85. J. de Meis *et al.*, Atrophy of mesenteric lymph nodes in experimental Chagas' disease: differential role of Fas/Fas-L and TNFRI/TNF pathways. *Microbes Infect.* **8**, 221–231 (2006).

86. C. G. Mueller, E. Hess, Emerging Functions of RANKL in Lymphoid Tissues. *Front. Immunol.* **3**, 261 (2012).

87. E. Hess *et al.*, RANKL induces organized lymph node growth by stromal cell proliferation. *J. Immunol. Baltim. Md 1950*. **188**, 1245–1254 (2012).

88. K. A. Knoop, B. R. Butler, N. Kumar, R. D. Newberry, I. R. Williams, Distinct developmental requirements for isolated lymphoid follicle formation in the small and large intestine: RANKL is essential only in the small intestine. *Am. J. Pathol.* **179**, 1861–1871 (2011).

89. M. Sugiyama *et al.*, Expression pattern changes and function of RANKL during mouse lymph node microarchitecture development. *Int. Immunol.* **24**, 369–378 (2012).

90. G. Eberl *et al.*, An essential function for the nuclear receptor RORgamma(t) in the generation of fetal lymphoid tissue inducer cells. *Nat. Immunol.* **5**, 64–73 (2004).

91. T. Cupedo *et al.*, Presumptive lymph node organizers are differentially represented in developing mesenteric and peripheral nodes. *J. Immunol. Baltim. Md 1950*. **173**, 2968–2975 (2004).

92. C. Bénézech *et al.*, Ontogeny of stromal organizer cells during lymph node development. *J. Immunol. Baltim. Md 1950*. **184**, 4521–4530 (2010).

93. K. Honda *et al.*, Molecular basis for hematopoietic/mesenchymal interaction during initiation of Peyer's patch organogenesis. *J. Exp. Med.* **193**, 621–630 (2001).

94. S. A. Luther, K. M. Ansel, J. G. Cyster, Overlapping roles of CXCL13, interleukin 7 receptor alpha, and CCR7 ligands in lymph node development. *J. Exp. Med.* **197**, 1191–1198 (2003).

95. D. Finke, H. Acha-Orbea, A. Mattis, M. Lipp, J. Kraehenbuhl, CD4+CD3- cells induce Peyer's patch development: role of alpha4beta1 integrin activation by CXCR5. *Immunity*. **17**, 363–373 (2002).

96. A. White *et al.*, Lymphotoxin a-dependent and -independent signals regulate stromal organizer cell homeostasis during lymph node organogenesis. *Blood*. **110**, 1950–1959 (2007).

97. H.-H. Kim *et al.*, RANKL regulates endothelial cell survival through the phosphatidylinositol 3'-kinase/Akt signal transduction pathway. *FASEB J. Off. Publ. Fed. Am. Soc. Exp. Biol.* **17**, 2163–2165 (2003).

98. J.-K. Min *et al.*, TNF-related activation-induced cytokine enhances leukocyte adhesiveness: induction of ICAM-1 and VCAM-1 via TNF receptor-associated factor and protein kinase C-dependent NF-kappaB activation in endothelial cells. *J. Immunol. Baltim. Md 1950*. **175**, 531–540 (2005).

99. D. Kim *et al.*, Regulation of peripheral lymph node genesis by the tumor necrosis factor family member TRANCE. *J. Exp. Med.* **192**, 1467–1478 (2000).

100. T. Katakai *et al.*, Organizer-like reticular stromal cell layer common to adult secondary lymphoid organs. *J. Immunol. Baltim. Md 1950*. **181**, 6189–6200 (2008).

101. R. Josien, B. R. Wong, H. L. Li, R. M. Steinman, Y. Choi, TRANCE, a TNF family member, is differentially expressed on T cell subsets and induces cytokine production in dendritic cells. *J. Immunol. Baltim. Md 1950*. **162**, 2562–2568 (1999).

102. R. Wang *et al.*, Regulation of activation-induced receptor activator of NF-kappaB ligand (RANKL) expression in T cells. *Eur. J. Immunol.* **32**, 1090–1098 (2002).

103. B. R. Wong *et al.*, TRANCE (tumor necrosis factor [TNF]-related activation-induced cytokine), a new TNF family member predominantly expressed in T cells, is a dendritic cell-specific survival factor. *J. Exp. Med.* **186**, 2075–2080 (1997).

104. W. C. Dougall *et al.*, RANK is essential for osteoclast and lymph node development. *Genes Dev.* **13**, 2412–2424 (1999).

105. E. Williamson, J. M. Bilsborough, J. L. Viney, Regulation of mucosal dendritic cell function by receptor activator of NF-kappa B (RANK)/RANK ligand interactions: impact on tolerance induction. *J. Immunol. Baltim. Md 1950*. **169**, 3606–3612 (2002).

106. K. Maruyama *et al.*, Receptor activator of NF-kappa B ligand and osteoprotegerin regulate proinflammatory cytokine production in mice. *J. Immunol. Baltim. Md 1950*. **177**, 3799–3805 (2006).

107. R. Yoshiki *et al.*, IL-10-producing Langerhans cells and regulatory T cells are responsible for depressed contact hypersensitivity in grafted skin. *J. Invest. Dermatol.* **129**, 705–713 (2009).

108. T. Totsuka *et al.*, RANK-RANKL signaling pathway is critically involved in the function of CD4+CD25+ regulatory T cells in chronic colitis. *J. Immunol. Baltim. Md 1950*. **182**, 6079–6087 (2009).

109. E. A. Green, Y. Choi, R. A. Flavell, Pancreatic lymph node-derived CD4(+)CD25(+) Treg cells: highly potent regulators of diabetes that require TRANCE-RANK signals. *Immunity*. **16**, 183–191 (2002).

*****

4. Scientific Question and Hypothesis

Our laboratory studies the role of stromal cells in the function of the immune system. Not only does stroma provide structural cues for cell mobility and position but also delivers regulatory signals for cell viability, proliferation and differentiation. Thus, in secondary lymphoid organs, i.e. LNs and spleen, the fibroblastic follicular dendritic cells (FDCs) organize B cells into primary follicles and GCs, provide intact antigen for B cell receptor activation and survival signals and thus support B cell differentiation and affinity maturation (*1*). The recently discovered marginal reticular cells (MRCs), also fibroblastic cells, are localized in the marginal zone situated on the outer border of B cell follicles. They express RANKL and the chemokine CXCL13 (*2*). An MRC-like cell line supports B cell migration (*2*), suggesting that MRCs could play an important role in B cell biology, but so far their function *in vivo* remains unknown. Recently, it has been suggested that MRCs are precursor cells for FDCs (*3*).

RANKL (receptor activator of NF-κB ligand) is member of the Tumor necrosis factor (TNF) super-family (SF) and signals via RANK. It plays an important role for immune cells by promoting bone marrow hematopoiesis (by inducing the differentiation of the bone matrix degrading osteoclasts), mobilization of hematopoietic stem cells and by LN development (*4*). In the adult, RANKL is constitutively expressed by MRCs, while, under conditions of inflammation, keratinocytes and T cells also express RANKL. The receptor RANK is expressed by macrophages and dendritic cells, but also by epithelial cells and endothelial cells. The function of RANKL expressed by MRCs had not been investigated.

The **objectives of the thesis** are to better understand the role of RANKL expressed by MRCs in the regulation of B cell activity. Because MRCs are positioned in close vicinity to B cells and may be precursors of FDCs, it is likely that MRCs play a role in B cell recruitment and B cell activation (Figure 4-1).

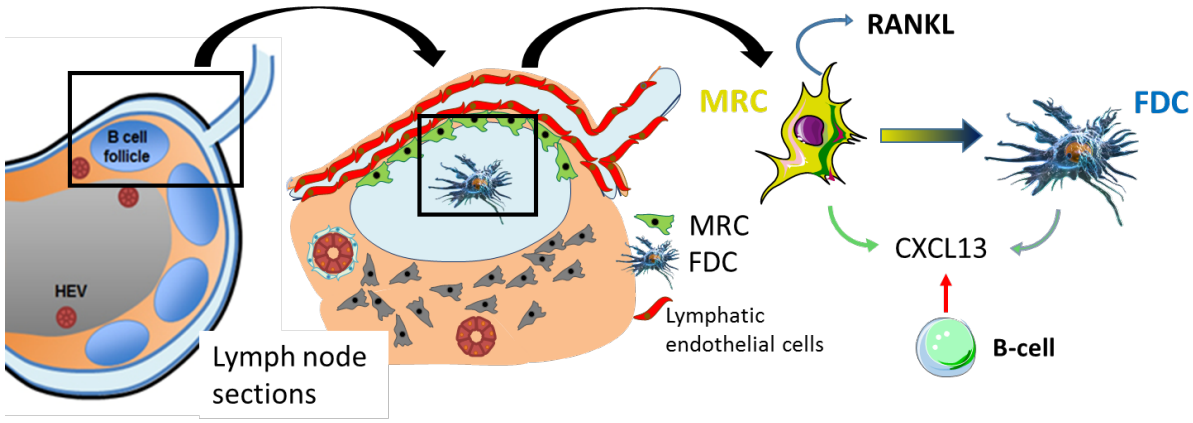

Figure 4-1: Working Hypothesis. *Left: Secondary lymphoid organs such as lymph nodes comprise B cells assembled in follicles. Center: FDCs reside within follicles while the MRCs line the border next to lymphatic endothelial cells. Right: MRCs express RANKL and may be precursors for FDC. MRCs and FDCs produce CXCL13, a chemokine that attracts B cells.*

References:

1. M. E. M. El Shikh, C. Pitzalis, Follicular dendritic cells in health and disease. *Front. Immunol.* **3**, 292 (2012).

2. T. Katakai *et al.*, Organizer-like reticular stromal cell layer common to adult secondary lymphoid organs. *J. Immunol. Baltim. Md 1950.* **181**, 6189–6200 (2008).

3. M. Jarjour *et al.*, Fate mapping reveals origin and dynamics of lymph node follicular dendritic cells. *J. Exp. Med.* **211**, 1109–1122 (2014).

4. C. G. Mueller, E. Hess, Emerging Functions of RANKL in Lymphoid Tissues. *Front. Immunol.* **3**, 261 (2012).

*****

RESULTS

Results

In order to address the raised questions, the work presented in the following article has been realized:

Article 1

Stromal cells regulate B cell organization and immune response through RANKL

F. ALLOUSH, O. Cordeiro, C. MUELLER

In preparation

Stromal cells regulate B cell organization and immune response through RANKL

Farouk Alloush[1] Olga Cordeiro[1], Christopher G. Mueller[1, 2]

[1] University of Strasbourg, CNRS UPR 3572, Immunopathology and therapeutic chemistry, 67000 Strasbourg, France

[2] Corresponding author Tel: +33 (0)3 88 41 71 14, Fax. +33 (0)3 88 61 06 80

c.mueller@ibmc-cnrs.unistra.fr

Abstract

RANKL plays an important role in key steps of hematopoiesis and the development of secondary lymphatic organs. Yet, although RANKL is constitutively expressed by stroma of secondary lymphoid organs in the adult, its role in the regulation of the immune response remains incompletely understood. Here, using conditional knock-out mice, we have studied the function of RANKL expressed by the stromal marginal reticular cells (MRCs) of lymph nodes. We found that MRC RANKL is required for expression of CXCL13 and the differentiation of follicular dendritic cells. The stromal cells display reduced transcription of *Tnfr1* while the levels of *Ltbr* and the ligands are unchanged. Immunization restores CXCL13 expression and FDC formation leading to a normal germinal center reaction. However, there is a dysfunctional IgM response, and the *Tnfr1* mRNA expression remains diminished. This shows that stromal RANKL oversees B cell stroma activation by modifying TNFR1 expression.

Introduction

In the embryo, RANKL produced by hematopoietic lymphoid tissue inducing cells (LTis) and by the stromal lymphoid tissue organizers (LTOs) (for review see (Mueller and Hess, 2012)) activates the lymphatic endothelial cells to initiate the development of secondary lymphoid organs (SLOs) (Onder et al., 2017). The engagement of LTβR on LTOs by LTIs then leads to the release of more chemotactic stimuli and adhesion molecules to accelerate the

recruitment of hematopoietic cells (Vondenhoff et al., 2009). Beyond SLO development, stromal cells are increasingly recognized as key regulators of the immune response (Buckley et al., 2015). They release chemotactic cytokines to recruit immune cells through HEVs, to compartmentalize SLOs into B cell follicles and T cell zone and to provide survival and activation cues for immune cells. In the adult lymph node (LN), a subset of stromal cells, the MRCs, express RANKL (Katakai et al., 2008). However the role of MRC RANKL is not known. RANKL regulates a number of important steps in hematopoiesis. In the bone, it is expressed by osteoblasts and osteocytes and activates osteoporosis from myeloid precursor cells to allow the residence of hematopoietic stem cells and thus sustained immune cell output. In the thymus, RANKL activates the differentiation of mTECs and thus plays an important part in central tolerance (for review see (Mueller and Hess, 2012)). In the tissue, it controls epidermal cell renewal and thus Langerhans cell numbers (Barbaroux et al., 2008). Although mature DCs express RANK and respond to RANKL by activation of cell survival programs, RANKL is redundant with CD40L that is also produced by activated T cells and so far no role of RANKL for DC activation in the KO mice has been found (Bachmann et al., 1999). Also mice with conditional deficiency of RANKL in T cells show a normal immune activation in the LNs, as judged by the output and polarization of T cells (Guerrini et al., 2015). Yet, a number of different mouse models suggest a role of RANKL in the differentiation of B cell associated stroma. LNs rescued in mice deficient in the RANK signaling component TRAF6 by administration of IL-7 lacked B cells and FDCs (Yoshida et al., 2002). However, TRAF6 is a signaling component for other TNFRSF members, notably TNFR1, a critical receptor for FDC differentiation (Rennert etal., 1998; Endres etal., 1999). More direct evidence comes from experiments where a RANKL-neutralizing antibody was administrated to embryos. This resulted in reduced LN B cell numbers, misplaced FDCs and reduced VCAM-1 (FDC) staining (Sugiyamaet al., 2012). In addition, Knoop and colleagues noted an absence of B cells in the small intestine cryptopatches of RANKL KO mice and observed that most B cell associated stromal cells lacked VCAM-1 and CXCL13 expression (Knoop et al., 2011). However, in all these models unconditional loss of TRAF6, RANK or RANKL would also negatively affect hematopoiesis resulting in reduced B cell numbers. Because B cells provide key signals for the differentiation of the associated stroma cells, notably LTα and LTβ, the stromal defect could be secondary to reduced B cell numbers.

However, we had shown that the postnatal RANKL overexpression specifically in the skin resulted in an increase in FDCs of the draining LNs concomitant with a greater number of B cell follicles and a larger LN (Hess et al., 2012).

To better address the role of RANKL-expressing stroma we have generated a mouse that lacks stromal RANKL by using a LTO-targeted gene deletion approach. We show that among the stromal cells the MRCs express high amount of RANKL, but the differentiation of MRCs is not affected by the lack of RANKL. However, the expression of CXCL13 by MRCs and the differentiation of FDCs is greatly reduced in vivo. Because LTβR and TNFR1 transduce key signals for CXCL13 production and FDC differentiation, we tested the expression of these receptors and their ligands and found a diminished TNFR1 transcription. CXCL13 expression and FDC and that of of stroma is not negatively ain stromaImportantly, these changes occurred in the absence of inflammation (ref). Therefore, there is supportive evidence for a role of RANKL in the differentiation and activation of B cell associated stroma, however definite proof and underlying mechanisms are lacking.

Material and Methods

Mice

C57BL/6 (Charles River Laboratories France) and other mice were bred and kept in specific pathogen-free conditions. All experiments were carried out in conformity with the animal bioethics legislation and institutional guidelines. To generate mice with conditional RANKL deficiency in MRCs (RANKL$^{\Delta CCL19}$), mice containing a single copy of the *Ccl19-cre* BAC transgene (Chai et al., 2013) were crossed with *Rankl*$^{flox/flox}$ (B6.129-Tnfsf11tm1.1Caob/J) mice (Xiong et al., 2011). Unless otherwise indicated all mice were used when 8 weeks old.

Cell isolation

Skin-draining LNs (inguinal, axillary, brachial, cervical, auricular, and popliteal) for each mouse were taken and cut using a scalpel. Then LNs were digested using 3 ml of enzyme mix prepared in RPMI 1640 Gibco®, 2% fetal calf serum, and following enzymes: 1 mg/ml collagenase D (Roche), 0.1 mg/ml DNase I (Roche), and 1 mg/ml Dispase II (Roche) at 37°C

for 1 hour under agitation. Cells are then gently homogenized by pipetting and the digestion is stopped with 5 mM of EDTA, then cell suspension was filtered through a 100 µm cell strainer. Red blood cells are lyzed in ammonium-chloride-potassium buffer (NH_4CL 0.15 M, $KHCO_3$ 1 mM, and EDTA 0.1 mM) for 1 min, cells were washed and counted. CD45+ and Ter119+ cells were depleted using microbeads (MACS Miltenyi Biotech) before flow cytometry analysis of sorting.

Flow cytometry and immunofluorescence

Primary and secondary antibodies used are listed in Supplemental Table S1. Flow cytometry was performed on a FACS Gallios (Beckman-Coulter) and analyzed with FlowJo software (Treestar). Cell sorting was performed on FACS ARIA (BD Biosciences). For immunofluorescence analysis, LNs were frozen in Tissue-Tek O.C.T. (EMS, Electron Microscopy Science). Eight µm LN sections were cut on a cryostat (Leica), fixed in cold acetone and blocked with TNB Buffer (Cold Spring Harbor). After immunolabelling, sections were mounted in Fluomount (Dako) and images acquired on a spinning disk inverted microscope (Carl Zeiss) with a confocal head (Yokogawa CSU) and the appropriate software (Metamorph). Images were analyzed, and staining areas and intensities were quantified using the open source imageJ software.

Quantitative reverse transcription coupled polymerase chain reaction (qRT-PCR)

RNA was extracted using the RNeasy Mini or Micro kit (Qiagen) and cDNA was synthesized with Maxima First Strand cDNA Synthesis Kit (Thermo Scientific) or Improm-II (Promega) using oligo(dT)15 primers. RT-PCR was performed using Luminaris color HiGreen qPCR Master Mix (Thermo Scientific). Primers are listed in supplementary Table S2. Quantitative RT-PCR was run on a Bio-Rad CFX96 thermal cycler, and threshold values (Ct) of the target genes "X" were normalized to housekeeping genes "HKG" (GAPDH or ACTIN) following the formula : $\Delta Ct = Ct_X - Ct_{HKG}$. The relative quantification was performed as $2^{-\Delta Ct}$.

Immunization and ELISA

Mice were injected in each posterior limb with heat inactivated *Bordetella pertussis* (10^7 bacteria), 250µg $Al(OH)_3$ and 30 µg of chicken ovalbumin. Chicken OVA-reactive serum IgM and IgG were measured by direct ELISA.

Statistical analysis

Unpaired two-tailed Student t-test and Mann Whitney were used on GraphPad Prism version 5 for Mac (GraphPad software). The p values <0.05 were considered statistically significant.

Results

Validation of the MRC conditionnel RANKL knock out model

To understand the function of MRC RANKL, we generated a conditional knock-out under the control of the *Ccl19* promoter, which is active in LTOs that give rise all LN stromal cells including MRCs (Chai et al., 2013). Unlike the unconditional RANKL KO (Kong et al., 1999), LNs were present in $RANKL^{\Delta CCL19}$ mice. Immunolabelling of the E18.5 inguinal LN revealed a strong reduction of RANKL but normal presence of $CD4^+$ LTi cells and lymphatic endothelial cells (**Figure 1A**). In the adult LN there was a complete absence of RANKL (**Figure 1B**). We next sorted MRCs from adult WT and KO animals as MAdCAM-1^+ VCAM-1^+ cells among the gp38^+ CD31^- FRCs (**Figure 1C**) (Katakai et al., 2008) and measured *Rankl* gene transcription by qRT-PCR. MRCs were present at normal proportions demonstrating that loss of RANKL had no negative impact on MRC differentiation (**Figure 1D**). MRCs from WT mice transcribed *Rankl*, whereas the remaining stromal cells (TRCs) were virtually devoid of it (**Figure 1E**). No *Rankl* transcripts were detectable neither in MRCs nor in TRCs of $RANKL^{\Delta CCL19}$ mice. These data validate the MRC-specific RANKL knock out mouse model.

MRC RANKL regulates CXCL13 production and FDC differentiation

Because an MRC-like cell line was shown to interact with B cells (Katakai et al., 2008), we next scrutinized the LNs for B cell numbers and formation of B cell follicles. We saw a tendency for reduction in B cell numbers in $RANKL^{\Delta CCL19}$ mice although this difference was not statistically significant (**Fig. 2A**). Immunostaining of popliteal LN sections showed that B cell follicles were less clearly segregated from the T cell zone (**Fig. 2B**). Because CXCL13 released by MRCs and FDCs plays an important role in B cell ingress and their accumulation in follicles, we stained the LN sections for CXCL13. In WT mice, CXCL13 expression was seen

in the outer (marginal) follicular area and in the center of most follicles (see arrows), in accord with expression by MRCs and FDCs, respectively. However, in RANKL$^{\Delta CCL19}$ mice, CXCL13 expression was almost undetectable (**Fig. 2B**). We therefore measured *Cxcl13* transcription in LNs and in sorted MRCs by qRT-PCR and found significantly reduced levels in RANKL$^{\Delta CCL19}$ mice (**Fig. 2C**). Since the expression of CXCL13 was also reduced within the center of the follicle where FDC normally reside, we also determined the presence of FDC by staining LN sections for CR1/CD35. Only rudimentary FDC networks were detectable in the KO mice (**Fig. 2B**). Because it was not possible to reproducibly identify FDCs by FACS (**Fig. S1**), we quantified CR1/CD35 expression on different LN sections from different mice. These analyses showed a clear reduction, and CR1/CD35 staining intensity was also significantly reduced (**Fig. 2D**). Therefore, MRC RANKL regulates CXCL13 expression by MRCs and the formation of the FDC network.

Stromal TNFR1 expression is RANKL-dependent

It is known that TNFR1 and LTβR co-signaling is required for optimal stromal CXCL13 expression (Grabner et al., 2009) and that TNFR1 is required for FDC formation (Pasparakis et al., 1997). To understand the mechanism underlying the control over CXCL13 expression and FDC formation by RANKL, we measured the expression of *Lt*α, *Lt*β, *Tnf*α and their respective receptors *Lt*β*r* and *Tnfr1* by qRT-PCR in whole LNs (**Fig. 3A**). We found that the expression of all genes was normal except for *Tnfr1* that was significantly reduced. To determine whether this reduction was also seen in stromal cells, we measured its mRNA in sorted MRCs and TRCs. Indeed, there was a significant reduction of *Tnfr1* in both stromal subsets whilst that of *Lt*β*r* was unchanged (**Fig. 4B**). It was not possible to confirm this reduction on the protein levels as stromal TNFR1 could not be detected by FACS (**Fig. S2**). Taken together, MRC RANKL controls CXCL13 expression and FDC differentiation by stimulating stromal TNFR1 expression.

Inflammation overcomes RANKL-restricted CXCL13 expression and FDC formation

Because CXCL13 and FDCs play an important role in the germinal center reaction that leads to the production of high affinity Ab secreting, class-switched B cells, we assessed the impact of RANKL-deficiency on the humoral immune response. RANKL$^{\Delta CCL19}$ and littermate

control mice were i.fp. immunized with ovalbumin in alum and heat-inactivated *B. pertussis*. Blood was drawn after each immunization, and the level of anti-OVA IgG and IgM was measured by ELISA. At the end of the experiment, mice were sacrificed and the draining popliteal LNs analyzed (**Fig. 4A**). IgG production showed no significant difference between the KO and WT control mice at any stage during immunization (**Fig. 4B**). However, surprisingly, no IgM was detected in the KO mice while some WT mice strongly produced this isotype (**Fig. 4B**). The popliteal LNs were analyzed for *Cxcl13* mRNA expression (**Fig. 4C**), or, alternatively, stained for B220, CXCL13 and CD35, and the extent of the $CD35^+$ FDC network and the intensity of CD35 expression was determined (**Fig. 4D,E**). There was no difference in the level of *Cxcl13* and the extent and the intensity of CD35 staining were similar. Finally, the sections were also stained for $GL7^+$ germinal center B cells (**Fig. 4F**). GL7-staining was present in both genotypes. Therefore, inflammation can overcome RANKL-restricted CXCL13 expression and FDC formation to generate a normal germinal center reaction. We next tested whether this relief is accompanied by normalization of *Tnfr1* expression. Although the levels increased in both genotypes compared to the non-immunized LNs, *Tnfr1* expression remained significantly lower in the $RANKL^{\Delta CCL19}$ mice, showing that the reduced TNFR1 expression resists the inflammatory stimulus.

Discussion

The molecular signals that oversee the activation of the B cell-associated stroma are incompletely understood. Here were showed that RANKL produced by MRCs is required for the production of CXCL13 by MRCs and the formation of the FDC network in the steady state. Reduced expression of stromal *Tnfr1* is a likely underlying reason for this defect. Inflammation can overcome this restriction to generate a normal germinal center response, however this occurs without normalizing *Tnfr1* expression.

MRCs have been identified in LNs based on expression of MAdCAM-1 and RANKL. Because MAdCAM-1 is expressed by other cells, such as endothelial cells or FDCs (Pabst et al., 2000), a conditional RANKL MRC KO could not rely on a MAdCAM-1-driven Cre construct. RANKL is produced by osteoblasts and activated T cells (Wong et al., 1997), making also a RANKL promoter-driven Cre strategy was unattractive. MRCs, alike all LN stromal cells, are thought to derive from a common embryonic stromal cell progenitor (LTO), that coexpresses CCL19

and RANKL (Katakai, 2012). We therefore opted for the *Ccl19-Cre* mouse (Chai et al., 2013) to generate a stromal-cell specific RANKL KO. LTOs showed strongly reduced RANKL expression, and the TNFSF was undetectable in adult MRCs. This data supports the idea that MRCs derive from CCL19-expressing LTOs. The non-MRC adult stroma (TRC) showed only little RANKL expression in WT mice suggesting that the MRCs are the major RANKL-producing stromal cells, although we cannot fully rule out the existence of a different RANKL$^+$ stromal subset among the TRCs. Although we have not analyzed osteoclastogenesis in these mice, the output of hematopoietic cells was normal as the number of B and T cells in the spleen and in mesenteric LNs, organs that are not affected by the KO strategy, showed normal B cell and T cell numbers (data not shown). This validates our strategy of a MRC-specific KO without affecting osteoclastogenesis and thus immune cell output.

The MRCs were still present in the RANKL KO mice based on their identification as cells expressing MAdCAM-1 and VCAM-1 (Katakai et al., 2008). Therefore, RANKL is not necessary for MRC differentiation. However RANKL was required for the expression of CXCL13 by MRCs. It was also required for FDC differentiation as evidenced by the absence of the FDC-specific marker CR1/CD35 and CXCL13 within the center of the B cell follicle where FDC reside. However, identification of FDCs as gp38$^+$CR1/CD35$^+$ cells by FACS was too imprecise and the cell numbers too low to reflect the changes observed with CXCL13 and CD35 staining of LN sections. Indeed, it is known that FDCs are very difficult to isolate even when using the conditions that successfully liberate MRCs. The low B cell follicle cell density and its imprecise boundary with the T cell zone is in accord with reduced CXCL13 levels. However, we did not observe the accumulation of B cells in a ring-like structure, as observed in the absence of FDC generated either using a FDC-specific ablation strategy (Wang et al., 2011) or by deletion of TNFR1 (Pasparakis et al., 1997). A low level of FDC CXCL13 expression maybe preserved in the RANKL KO mice to generate a loosely organized B cell follicle; alternatively, because of the equally strong reduction of MRC CXCL13, there is may be little chemotactic cue to attract the B cells into the marginal zone to form this ring-like structure. Because CXCL13 is a key B cell ingress chemokine (Kanemitsu et al., 2005), an additional means to test for loss of CXCL13 would be to adoptively transfer B cells into RANKL KO mice and score for the entry of B cells into the LN.

Based on marker distribution pattern during development and the immune response it was concluded that FDC derive from MRCs (Jarjour et al., 2014). The absence of FDCs together with a lack of CXCL13 expression by MRCs is compatible with this idea. Hence, RANKL would activate a program in MRC that jointly regulates CXCL13 expression and FDC differentiation. However, our data is not in conflict with an alternative scenario that FDC arise from other precursors (Mionnet et al., 2013). To clarify this it may be useful to identify the RANKL-responsive cell type. In the first model, MRCs but not FDCs would express RANK. In the second model, MRCs and a yet unidentified stromal cell express RANK (this stromal cell could be LTOs and in this case FDCs derive from LTOs, at least in the steady state). However, in fact, we have assessed RANK expression on the mRNA level and found that the fibroblastic stromal cell do not transcribe this gene, which is in accord with its absence from other fibroblasts, such as osteoblasts (data not shown). Further, *Ccl19-Cre Rank flox/flox* mice do not show defects in CXCL13 expression or FDC formation (data not shown). Thus, it appears that the RANKL control of FDC differentiation and CXCL13 expression does not occur via a direct activation of a stromal cell type. Further work is required to elucidate the identity of the cellular mediator. It is noteworthy that CD40 activates human FDC-like cells to express the non-signalling receptor OPG, indicative of a retroactive control loop of FDC network formation (ref).

Genetic deletion of *Tnfα* or *Tnfr1* or the neutralization of TNFα leads to the absence of FDCs (Pasparakis et al., 1997), and TNFR1 and LTβR costimulation of stromal cells is required for optimal CXCL13 production (Grabner et al., 2009). Our analysis of LTβR and TNFR1 expression and their ligands pointed to the downregulation of TNFR1 on stromal cells as a likely mechanism for the reduced B cell-stroma activation. The TNFR1 promoter comprises NF-κB, AP-1 and C/EBP binding sites as well as GAS and STAT-1 sites (IFN-γ activation) opening various possibility of regulation by the RANKL-responsive cell (Puimege et al., 2014).

After immunization a germinal center reaction occurred in the KO mice that was indistinguishable from WT mice, indicating that the RANKL restriction on B cell-associated stroma responsible for CXCL13 production and FDC formation can be bypassed by a strong inflammatory response. Although a more detailed analysis of affinity maturation is lacking, we would predict also a normal affinity maturation because of the clear presence of FDCs.

We can see two reasons for this normalization: either the production of RANKL by activated T cells or the increased production of TNFα or LTα to trigger normal TNFR1 signaling in spite of reduced receptor expression. To address the first possibility, RANKL-deficient T cells could be adoptively transferred. To address the second possibility, TNFR1 signaling in response to increasing concentrations of TNFα/LTα could be measured *in vitro*. Intriguingly, *Tnfr1* mRNA expression remained low even after repeated immunization. Moreover, even though IgG production was normal, the RANKL$^{\Delta CCL19}$ mice failed to produce high amounts of IgM after repeated immune immunization. This suggests that some aspects of RANKL restriction on B cell associated stroma is maintained, reflected in the inability of B cells to produce IgM and which would implicate TNFR1 signaling. While we cannot ascertain that B cell stroma is directly implicated, it nevertheless likely as stroma also produces factors such as BAFF and CXCL12 (Hargreaves et al., 2001, Cremasco et al., 2014) that regulate the extrafollicular maturation of B cells and the survival of plasma cells of Ig (Benson et al., 2008, Hargreaves et al., 2001). CXCL12 is induced by TNFα/LTα by different cells including MRC-like stromal cells (Katakai et al., 2008).

These data show that immune stroma plays an important role in the organization of B cell follicles and the humoral immune response. Embryonic RANKL production appears to control B cell stroma reactivity to TNFα/LTα by regulating TNFR1 expression.

Acknowledgements

CGM was supported by l'Agence Nationale pour la Recherche (Program "Investissements d'Avenir", ANR-10-LABX-0034 MEDALIS; ANR-11-EQPX-022). We thank the laboratory for discussion and Vincent Flacher for critical reading of the manuscript. We are grateful to Sophie Guillot (Institut Pasteur, Paris) for the heat-inactivated *B. pertussis*. We acknowledge the Idex-University of Strasbourg for the PhD fellowship and the University of Strasbourg International Doctoral Programme / Eurometropole de Strasbourg for extension.

References

BACHMANN, M. F., WONG, B. R., JOSIEN, R., STEINMAN, R. M., OXENIUS, A. & CHOI, Y. 1999. TRANCE, a tumor necrosis factor family member critical for CD40 ligand-independent T helper cell activation. *J. Exp. Med.,* 189**,** 1025-31.

BARBAROUX, J. B., BELEUT, M., BRISKEN, C., MUELLER, C. G. & GROVES, R. 2008. Epidermal receptor activator of NF-kB ligand controls Langerhans cell numbers and proliferation. *J. Immunol.,* 181**,** 1103-08.

BENSON, M. J., DILLON, S. R., CASTIGLI, E., GEHA, R. S., XU, S., LAM, K. P. & NOELLE, R. J. 2008. Cutting edge: the dependence of plasma cells and independence of memory B cells on BAFF and APRIL. *J Immunol.,* 180**,** 3655-9.

BUCKLEY, C. D., BARONE, F., NAYAR, S., BENEZECH, C. & CAAMANO, J. 2015. Stromal cells in chronic inflammation and tertiary lymphoid organ formation. *Annu Rev Immunol.,* 33:715-45**.,** 10.1146/annurev-immunol-032713-120252.

CHAI, Q., ONDER, L., SCANDELLA, E., GIL-CRUZ, C., PEREZ-SHIBAYAMA, C., CUPOVIC, J., DANUSER, R., SPARWASSER, T., LUTHER, S. A., THIEL, V., RULICKE, T., STEIN, J. V., HEHLGANS, T. & LUDEWIG, B. 2013. Maturation of lymph node fibroblastic reticular cells from myofibroblastic precursors is critical for antiviral immunity. *Immunity.,* 38**,** 1013-24.

CREMASCO, V., WOODRUFF, M. C., ONDER, L., CUPOVIC, J., NIEVES-BONILLA, J. M., SCHILDBERG, F. A., CHANG, J., CREMASCO, F., HARVEY, C. J., WUCHERPFENNIG, K., LUDEWIG, B., CARROLL, M. C. & TURLEY, S. J. 2014. B cell homeostasis and follicle confines are governed by fibroblastic reticular cells. *Nat Immunol,* 24.

GRABNER, R., LOTZER, K., DOPPING, S., HILDNER, M., RADKE, D., BEER, M., SPANBROEK, R., LIPPERT, B., REARDON, C. A., GETZ, G. S., FU, Y. X., HEHLGANS, T., MEBIUS, R. E., VAN DER WALL, M., KRUSPE, D., ENGLERT, C., LOVAS, A., HU, D., RANDOLPH, G. J., WEIH, F. & HABENICHT, A. J. 2009. Lymphotoxin beta receptor signaling promotes tertiary lymphoid organogenesis in the aorta adventitia of aged ApoE-/- mice. *J Exp Med.,* 206**,** 233-48.

GUERRINI, M. M., OKAMOTO, K., KOMATSU, N., SAWA, S., DANKS, L., PENNINGER, J. M., NAKASHIMA, T. & TAKAYANAGI, H. 2015. Inhibition of the TNF Family Cytokine RANKL Prevents Autoimmune Inflammation in the Central Nervous System. *Immunity,* 43**,** 1174-85.

HARGREAVES, D. C., HYMAN, P. L., LU, T. T., NGO, V. N., BIDGOL, A., SUZUKI, G., ZOU, Y. R., LITTMAN, D. R. & CYSTER, J. G. 2001. A coordinated change in chemokine responsiveness guides plasma cell movements. *J Exp Med.,* 194**,** 45-56.

HESS, E., DUHERON, V., DECOSSAS, M., LÉZOT, F., BERDAL, A., CHEA, S., GOLUB, R., BOSISIO, M. R., BRIDAL, S. L., CHOI, Y., YAGITA, H. & MUELLER, C. G. 2012. RANKL induces organized lymph node growth by stromal cell proliferation. *J. Immunol.,* 188**,** 1245-54.

JARJOUR, M., JORQUERA, A., MONDOR, I., WIENERT, S., NARANG, P., COLES, M. C., KLAUSCHEN, F. & BAJENOFF, M. 2014. Fate mapping reveals origin and dynamics of lymph node follicular dendritic cells. *J Exp Med.,* 211**,** 1109-22. .

KANEMITSU, N., EBISUNO, Y., TANAKA, T., OTANI, K., HAYASAKA, H., KAISHO, T., AKIRA, S., KATAGIRI, K., KINASHI, T., FUJITA, N., TSURUO, T. & MIYASAKA, M. 2005. CXCL13 is an arrest chemokine for B cells in high endothelial venules. *Blood.,* 106**,** 2613-8.

KATAKAI, T. 2012. Marginal reticular cells: a stromal subset directly descended from the lymphoid tissue organizer. *Frontiers in Immunology,* 3**,** 200-6.

KATAKAI, T., SUTO, H., SUGAI, M., GONDA, H., TOGAWA, A., SUEMATSU, S., EBISUNO, Y., KATAGIRI, K., KINASHI, T. & SHIMIZU, A. 2008. Organizer-like reticular stromal cell layer common to adult secondary lymphoid organs. *J. Immunol.,* 181**,** 6189-200.

KNOOP, K. A., BUTLER, B. R., KUMAR, N., NEWBERRY, R. D. & WILLIAMS, I. R. 2011. Distinct developmental requirements for isolated lymphoid follicle formation in the small and large intestine RANKL is essential only in the small intestine. *Am. J. Pathol.,* 179**,** 1861-71.

KONG, Y. Y., YOSHIDA, H., SAROSI, I., TAN, H. L., TIMMS, E., CAPPARELLI, C., MORONY, S., OLIVEIRA-DOS-SANTOS, A. J., VAN, G., ITIE, A., KHOO, W., WAKEHAM, A., DUNSTAN, C. R., LACEY, D. L., MAK, T. W., BOYLE, W. J. & PENNINGER, J. M. 1999. OPGL is a key regulator of osteoclastogenesis, lymphocyte development and lymph-node organogenesis. *Nature,* 397**,** 315-23.

MIONNET, C., MONDOR, I., JORQUERA, A., LOOSVELD, M., MAURIZIO, J., ARCANGELI, M. L., RUDDLE, N. H., NOWAK, J., AURRAND-LIONS, M., LUCHE, H. & BAJENOFF, M. 2013. Identification of a new stromal cell type involved in the regulation of inflamed B cell follicles. *PLoS Biol.,* 11**,** e1001672.

MUELLER, C. G. & HESS, E. 2012. Emerging Functions of RANKL in Lymphoid Tissues. *Frontiers in Immunology,* 3**,** 261-7.

ONDER, L., MORBE, U., PIKOR, N., NOVKOVIC, M., CHENG, H. W., HEHLGANS, T., PFEFFER, K., BECHER, B., WAISMAN, A., RULICKE, T., GOMMERMAN, J., MUELLER, C. G., SAWA, S., SCANDELLA, E. & LUDEWIG, B. 2017. Lymphatic Endothelial Cells Control Initiation of Lymph Node Organogenesis. *Immunity.,* 47**,** 80-92.e4. doi: 10.1016/j.immuni.2017.05.008. Epub 2017 Jul 11.

PABST, O., FORSTER, R., LIPP, M., ENGEL, H. & ARNOLD, H. H. 2000. NKX2.3 is required for MAdCAM-1 expression and homing of lymphocytes in spleen and mucosa-associated lymphoid tissue. *Embo J.,* 19**,** 2015-23.

PASPARAKIS, M., ALEXOPOULOU, L., GRELL, M., PFIZENMAIER, K., BLUETHMANN, H. & KOLLIAS, G. 1997. Peyer's patch organogenesis is intact yet formation of B lymphocyte follicles is defective in peripheral lymphoid organs of mice deficient for tumor necrosis factor and its 55-kDa receptor. *Proc. Natl. Acad. Sci. USA,* 94**,** 6319-23.

PUIMEGE, L., LIBERT, C. & VAN HAUWERMEIREN, F. 2014. Regulation and dysregulation of tumor necrosis factor receptor-1. *Cytokine Growth Factor Rev.,* 25**,** 285-300. doi: 10.1016/j.cytogfr.2014.03.004. Epub 2014 Mar 24.

VONDENHOFF, M. F., GREUTER, M., GOVERSE, G., ELEWAUT, D., DEWINT, P., WARE, C. F., HOORWEG, K., KRAAL, G. & MEBIUS, R. E. 2009. LTbetaR signaling induces cytokine expression and up-regulates lymphangiogenic factors in lymph node anlagen. *J. Immunol.,* 182**,** 5439-45.

WANG, X., CHO, B., SUZUKI, K., XU, Y., GREEN, J. A., AN, J. & CYSTER, J. G. 2011. Follicular dendritic cells help establish follicle identity and promote B cell retention in germinal centers. *J Exp Med.,* 208**,** 2497-510.

WONG, B. R., JOSIEN, R., LEE, S. Y., SAUTER, B., LI, H. L., STEINMAN, R. M. & CHOI, Y. 1997. TRANCE (tumor necrosis factor [TNF]-related activation-induced cytokine), a new TNF family member predominantly expressed in T cells, is a dendritic cell-specific survival factor. *J. Exp. Med.,* 186**,** 2075-80.

XIONG, J., ONAL, M., JILKA, R. L., WEINSTEIN, R. S., MANOLAGAS, S. C. & O'BRIEN, C. A. 2011. Matrix-embedded cells control osteoclast formation. *Nat. Med.,* 17**,** 1235-1241.

Figure legends

Figure 1. Validation of the MRC RANKL knock-out strategy (A) E17.5 inguinal LNs of Ccl19-Cre Rankl flox/flox and control littermates were stained for LECs (mCLCA1), LTi cells (CD4) and RANKL. (B) Adult inguinal LNs of Ccl19-Cre Rankl flox/flox and control littermates were stained for RANKL; nuclear counterstain was DAPI. (C) Gating strategy to identify MRCs and TRCs among FRCs. (D) The proportion (mean ±SD (n=8)) of MRCs (MAdCAM-1+ VCAM-1+ cells) of Ccl19-Cre Rankl flox/flox and control littermates; ns= not significant. (E) Relative Rankl transcription in MRCs and TRCs of Ccl19-Cre Rankl flox/flox and control littermates, mean ±SED (n=3). ND= not detectable.

Figure 2. Stromal RANKL is required for maximal CXCL13 and FDC formation. (A) B and T cell numbers in inguinal (Ing) and brachial (Bra) LNs of Ccl19-Cre Rankl flox/flox and control littermates. (B) Popliteal LNs were stained for the indicated molecules. The scale bars represent 100 µm. (C) Left: Cxcl13 expression was measured by qRT-PCR in different LNs (popliteal, inguinal, brachial and axillary) from different mice (n>5). Each dot represents the mRNA level of a LN. Right: Cxcl13 expression in MRCs sorted from pooled peripheral LNs. Each dot represents the mRNA level of a different experiment. The horizontal bars represent the mean values ±SED. (D) Left: FDC-network formation was assessed in poplital LN sections as the ratio of the CD35+ area over the B220+ area. Each dot represents the value from individual B cell follicles of different LN sections from >3 different mice. The horizontal bars represent the mean values ±SED. Right: The intensity of CD35 staining was determined in the CD35+ area. Each dot represents the value of one CD35+ area from individual B cell follicles of different LN sections of >3 different mice. The horizontal bars are the mean values ±SED. Significance: *= $p<0.05$, **= $p<0.01$, ****= $p<0.0001$, ns= not significant.

Figure 3. RANKL positively controls stromal Tnfr1 expression. (A) Tnfa, Lta, Ltb, Tnfr1 and Ltbr expression was measured by qRT-PCR in different LNs (inguinal, brachial and axillary) from different mice (n>5). Each dot represents the mRNA level of a LN. (B) Tnfr1 and Ltbr expression in MRCs and TRCs sorted from pooled peripheral LNs. Each dot represents the mRNA level of a different experiment. The bars represent the mean values ±SED. Significance: *= $p<0.05$, ****= $p<0.0001$, ns= not significant.

Figure 4. Immunization overcomes RANKL restriction. (A) Immunization protocol. Mice were immunized into the hind leg foodpads and blood drawn at the indicated times. After the final bleeding, the mice were sacrified and the draining popliteal LNs harvested. (B) Seric chicken ovalbumin-specific IgG and IgM was measured by ELISA. Dots represent the different mice and the horizontal bars the mean values. (C) Cxcl13 expression was measured by qRT-PCR in the popliteal LNs. Each dot represents the value of a different mouse. The bars represent the mean values ±SED. (D) Popliteal LNs were stained for the indicated molecules. The scale bars represent 100 µm. (E) Left: FDC-network formation was assessed in the LN sections as the ratio of the CD35+ area over the B220+ area. Each dot represents the value from individual B cell follicles of different LN sections from >5 different mice. The bars represent the mean values ±SED. Right: The intensity of CD35 staining was determined in the CD35+ area. Each dot represents the value of one CD35+ area from individual B cell follicles of different LN sections of >5 different mice. The bars are the mean values ±SED. (F) Popliteal LNs were stained for the indicated molecules. The scale bars represent 100 µm. (G) Tnfr1 and Ltbr expression in popliteal LNs. Each dot represents the mRNA level of a different LN. The bars represent the mean values ±SED. Significance: *= p<0.05, ****= p<0.0001, ns= not significant.

Figure S1. Identification of FDCs by FACS. (A) FACS profiles of FDCs from 3 LNs from WT and KO mice gated as $CD35^+$ $gp38^+$ cells among live $CD45^-$ cells From pooled peripheral LNs. (B) Graphs depicts the mean percentage of FDCs (as identified in panel A) ± SD. Each point represents a different experiment for the WT and KO mice. ns= not significant.

Figure S2. FACS gating of stromal cell subsets and staining of FRCs for TNFR1. FACS profiles of FDCs from 3 LNs from WT and KO mice gated as CD35+ gp38+ cells among live CD45- cells From pooled peripheral LNs. (B) Graphs depicts the mean percentage of FDCs (as identified in panel A) ±SD. Each point represents a different experiment for the WT and KO mice. ns= not significant.

Figure 1

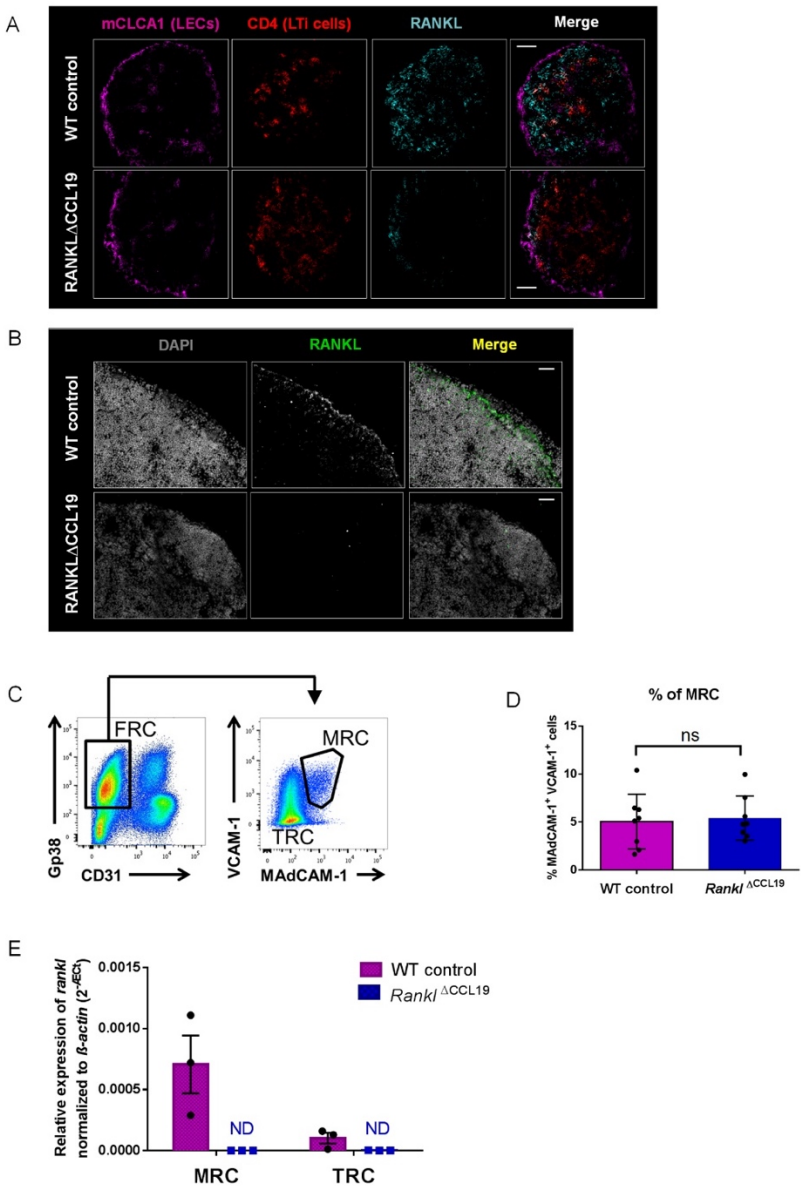

Figure 1. (A) E17.5 inguinal LNs of *Ccl19-Cre Rankl flox/flox* and control littermates were stained for LECs (mCLCA1), LTi cells (CD4) and RANKL. (B) Adult inguinal LNs of *Ccl19-Cre Rankl flox/flox* and control littermates were stained for RANKL; nuclear counterstain was DAPI. (C) Gating strategy to identify MRCs and TRCs among FRCs. (D) The proportion (mean ±SD (n=8)) of MRCs (MAdCAM-1$^+$ VCAM-1$^+$ cells) of *Ccl19-Cre Rankl flox/flox* and control littermates; ns= not significant. (E) Relative *Rankl* transcription in MRCs and TRCs of *Ccl19-Cre Rankl flox/flox* and control littermates, mean ±SED (n=3). ND= not detectable.

Figure 2

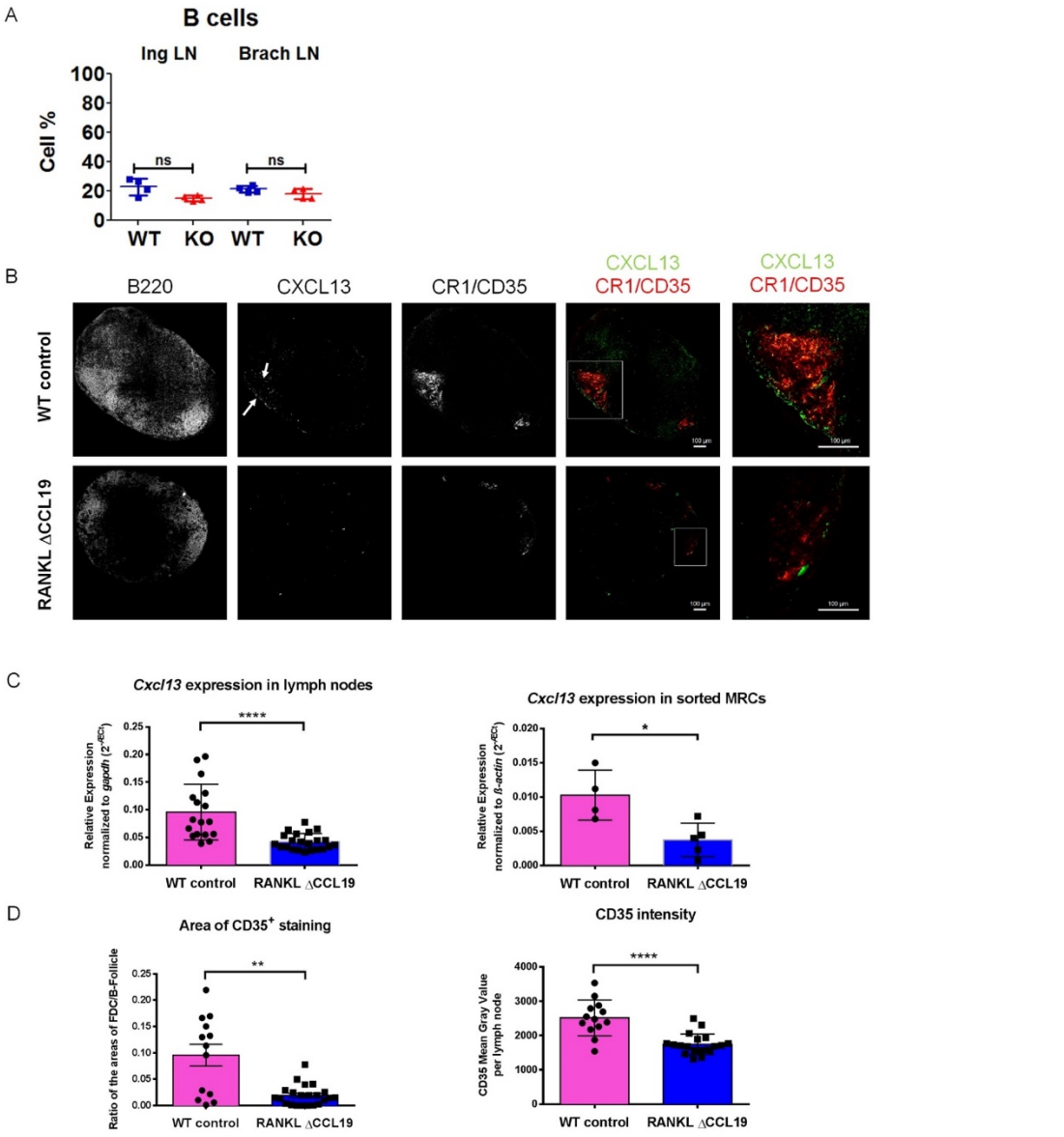

Figure 2. (A) B and T cell numbers in inguinal (Ing) and brachial (Bra) LNs of *Ccl19-Cre Rankl flox/flox* and control littermates.
(B) Popliteal LNs were stained for the indicated molecules. The scale bars
represent 100 µm. (C) Left: *Cxcl13* expression was measured by qRT-PCR in different LNs (popliteal, inguinal, brachial and axillary)
from different mice (n>5). Each dot represents the mRNA level of a LN. Right: *Cxcl13* expression in MRCs sorted from pooled peripheral LNs.
Each dot represents the mRNA level of a different experiment. The horizontal bars represent the mean values ±SED.
(D) Left: FDC-network formation was assessed in poplital LN sections as the ratio of the CD35⁺ area over the B220⁺ area.
Each dot represents the value from individual B cell follicles of different LN sections from >3 different mice.
The horizontal bars represent the mean values ±SED. Right: The intensity of CD35 staining was determined in the CD35⁺ area.
Each dot represents the value of one CD35⁺ area from individual B cell follicles of different LN sections of >3 different mice.
The horizontal bars are the mean values ±SED. Significance: *= p<0.05, **= p<0.01, ****= p<0.0001, ns= not significant.

Figure 3

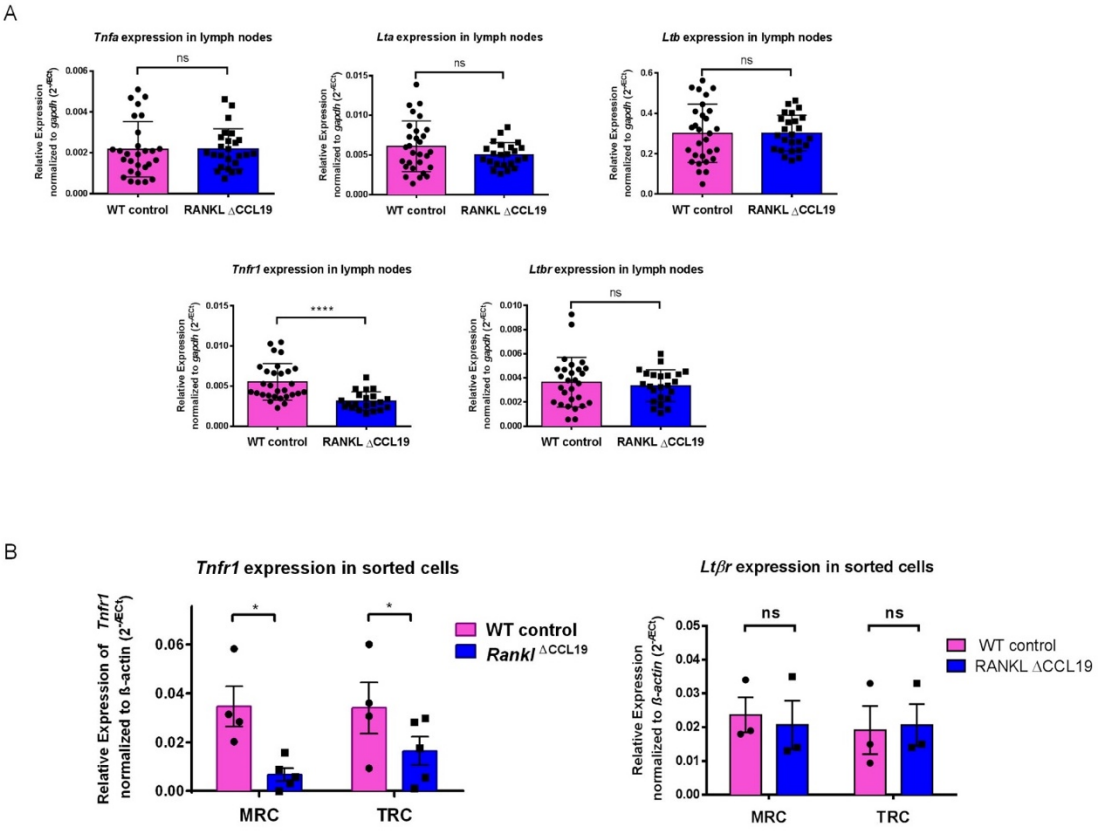

Figure 3. (A) *Tnfa*, *Lta*, *Ltb*, *Tnfr1* and *Ltbr* expression was measured by qRT-PCR in different LNs (inguinal, brachial and axillary) from different mice (n>5). Each dot represents the mRNA level of a LN. (B) *Tnfr1* and *Ltbr* expression in MRCs and TRCs sorted from pooled peripheral LNs. Each dot represents the mRNA level of a different experiment.
The bars represent the mean values ± SED. Significance: *= p<0.05, ****= p<0.0001, ns= not significant.

Figure 4

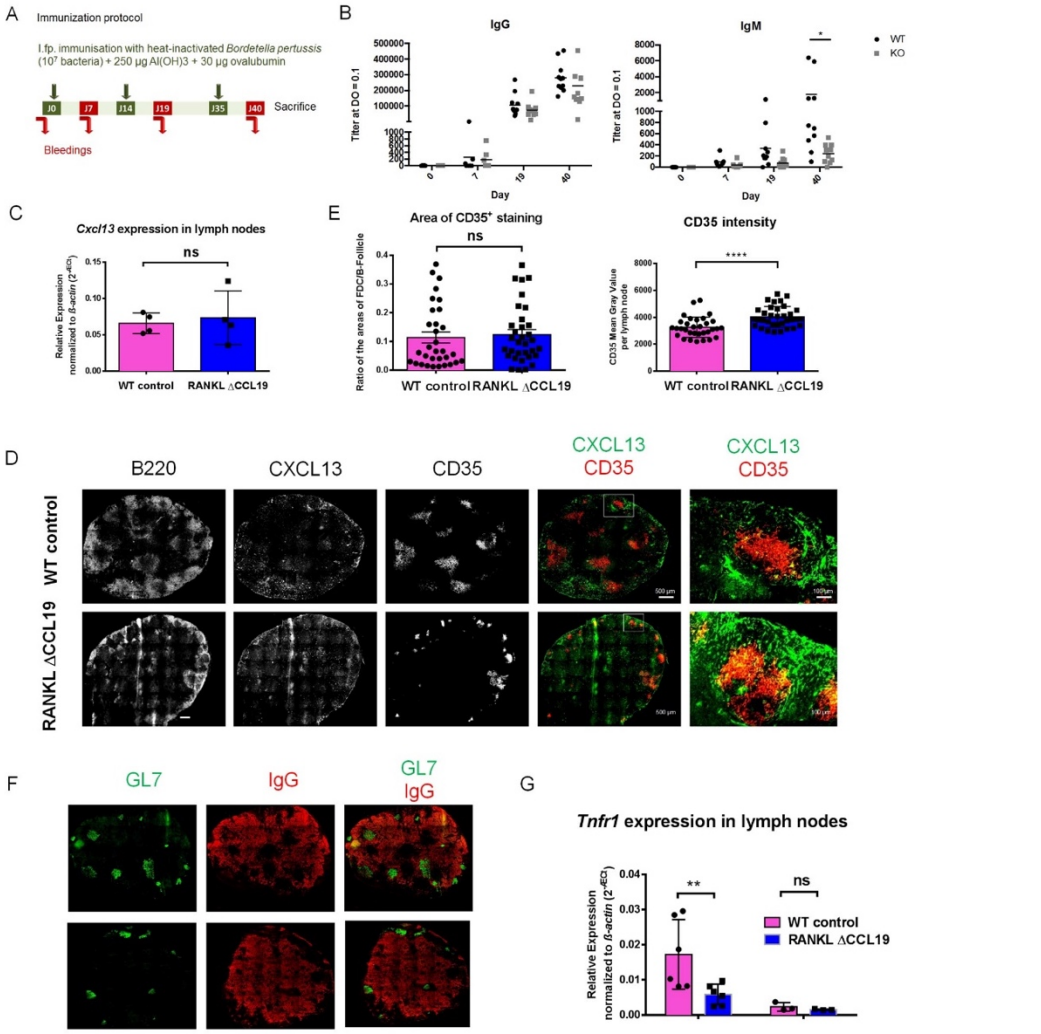

Figure 4. (A) Immunization protocol. Mice were immunized into the hind leg foodpads and blood drawn at the indicated times. After the final bleeding, the mice were sacrified and the draining popliteal LNs harvested. (B) Seric chicken ovalbumin-specific IgG and IgM was measured by ELISA. Dots represent the different mice and the horizontal bars the mean values. (C) *Cxcl13* expression was measured by qRT-PCR in the popliteal LNs. Each dot represents the value of a different mouse. The bars represent the mean values ±SED. (D) Popliteal LNs were stained for the indicated molecules. The scale bars represent 100 µm. (E) Left: FDC-network formation was assessed in the LN sections as the ratio of the $CD35^+$ area over the $B220^+$ area. Each dot represents the value from individual B cell follicles of different LN sections from >5 different mice. The bars represent the mean values ±SED. Right: The intensity of CD35 staining was determined in the $CD35^+$ area. Each dot represents the value of one $CD35^+$ area from individual B cell follicles of different LN sections of >5 different mice. The bars are the mean values ±SED. (F) Popliteal LNs were stained for the indicated molecules. The scale bars represent 100 µm. (G) *Tnfr1* and *Ltbr* expression in popliteal LNs. Each dot represents the mRNA level of a different LN. The bars represent the mean values ±SED.
Significance: *= p<0.05, ****= p<0.0001, ns= not significant.

Figure S1

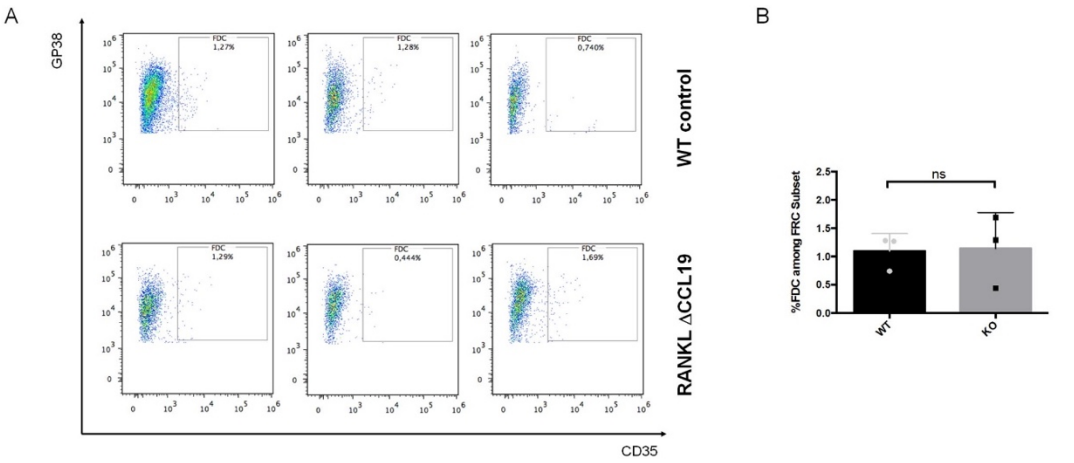

Figure S1. (A) FACS profiles of FDCs from 3 LNs from WT and KO mice gated as $CD35^{+}$ $gp38^{+}$ cells among live $CD45^{-}$ cells From pooled peripheral LNs. (B) Graphs depicts the mean percentage of FDCs (as identified in panel A) ± SD. Each point represents a different experiment for the WT and KO mice. ns= not significant.

Figure S2

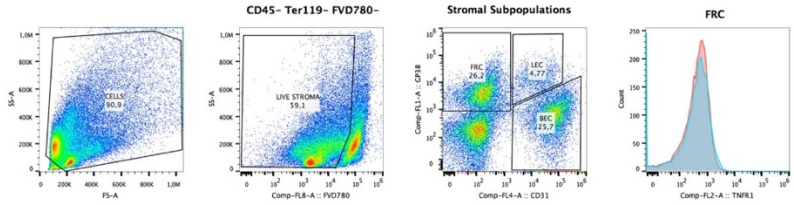

Figure S2. FACS gating of stromal cell subsets and staining of FRCs for TNFR1. FACS profiles of FDCs from 3 LNs from WT and KO mice gated as CD35^{+} gp38^{+} cells among live CD45^{-} cells From pooled peripheral LNs. (B) Graphs depicts the mean percentage of FDCs (as identified in panel A) ± SD. Each point represents a different experiment for the WT and KO mice. ns= not significant.

Table S1: List of primary and secondary antibodies used for flow cytometry and immunofluorescence

Target	Species	Clone	Conjugation	Supplier
CD45	Rat IgG2a	30-F11	APC-CY7	Biolegend
Ter-119	Rat IgG2b	TER-119	APC-CY7	Biolegend
CD31	Rat IgG2a	390	PercP eF710	eBioscience
Gp38	Syrian Hamster IgG	8.1.1	A488	eBioscience
MAdCAM-1	Rat IgG2a	MECA-367	Biotine	eBioscience
VCAM-1	Rat IgG2a	429	APC	Biolegend
CD35	Rat IgG2a	8C12	Biotine	BD
CXCL13	Goat IgG	Polyclonal	Purified	R&D
GL7	Rat IgM	GL7	FITC	BD
CD4	Rat IgG2a	RM4-5	PerCP-Cy5.5 ; APC	BD
mCLCA1	Syrian Hamster IgG	10.1.1	Purified	Andy Farr
RANKL	Rat IgG2a	IK22.5	Purified	Hideo Yagita
CD45R/B220	Rat IgG2a	RA3-6B2	FITC	BD
TNFR1	Goat IgG	Polyclonal	Purified	R&D
TNFR1	Hamster IgG	55R-286	APC	Biolegend
Goat	Donkey		Cy3 ; PE	Jackson
Hamster IgG	Goat		A488; A546	Molecular probes
Rat	Donkey		Cy3	Jackson
Streptavidin			PE	eBiosciences
Streptavidin			AF647	Life technologies

Table S2: List of primers used for qRT-PCR

Name	Sequence
CXCL13 -F	GTATTCTGGAAGCCCATTACAC
CXCL13 -R	CATTTGGCACGAGGATTCACAC
LTα -F	GACTCTCTGGTGTCCGCTTC
LTα -R	CACTGAGGAGAGGCACATGG
LTβ -F	CTGCCCACCTCATAGGCGC
LTβ -R	CGTCCTGCCCCTGTACC
LTβR -F	AAATCCCCCAGAGCCAGGA
LTβR -R	GGTGCCGCTTGAGCAGAGT
RANKL -F	CAGCCATTTGCACACCTCAC
RANKL -R	GTCTGTAGGTACGCTTCCCG
TNFα -F	CGAGTGACAAGCCTGTAGCC
TNFα -R	AAGAGAACCTGGGAGTAGACAAG
TNFR1 -F	ATGTACACCAAGTTGGTAGC
TNFR1 -R	AATATCCTCGAGGCTCTGAGA
GAPDH - F	CCCTTAAGAGGGATGCTGCC
GAPDH - R	TACGGCCAAATCCGTTCACA
Actin-B - F	CACTGTCGAGTCGCGTCCA
Activ-B - R	CATCCATGGCGAACTGGTGG

OTHER CONTRIBUTIONS

Other Contributions

Introduction

Lymph nodes (LNs), like other secondary lymphoid organs (SLOs), are highly organized in order to facilitate the initiation of adaptive immune response. They have an inner T cell zone and cortical B cell follicles. Follicles are lined by the newly discovered marginal reticular cells (MRCs), a stromal subset that constitutively express RANKL and whose function is poorly known. MRCs are in close proximity with lymphatic vessels formed by lymphatic endothelial cells (LECs) and bringing small molecules and antigens to the LN. Antigens are captured by $CD169^{+}$ subcapsular sinus macrophages (SSM) that are intercalated between floor LECs. While the role of RANKL during organogenesis of SLOs is well established, its role in adult LN remains unclear. Hence, our group addressed this question by generating a mouse model deficient for constitutive RANKL in its stromal compartment (MRCs). We asked the question whether LECs are activated by RANKL expressed by MRCs or secreted by activated T cells or keratinocytes.

My colleague, Olga Cordeiro, addressed the question of the heterogeneity of LECs by investigating a new marker, Integrin alpha-IIb (ITGA2B) also known as CD41, that is otherwise expressed by platelets and megakaryocytes. In her work, to which I contributed, the role of RANKL in the activation of LECs and their expression of CD41 was shown. This activation suggests that MRC RANKL would constitutively activate LECs. However, it remains unclear whether RANKL-activation of LECs is direct or indirect. The results of this work are presented in the following article 2.

Article 2

Integrin-alpha IIb identifies murine lymph node lymphatic endothelial cells activated by receptor activator of NF-κB ligand

Olga Cordeiro, Saba Nayar, Mohamed Habbeddine, Farouk Alloush, Mélanie Chypre, Dominik Vonficht, Monique Duval, Burkhard Ludewig, Toby Lawrence, Christopher Buckley, Francesca Barone, Christopher G. Mueller

PLoS One. 2016 Mar 24;11(3):e0151848. doi: 10.1371/journal.pone.0151848

PLOS | ONE

RESEARCH ARTICLE

Integrin-Alpha IIb Identifies Murine Lymph Node Lymphatic Endothelial Cells Responsive to RANKL

Olga G. Cordeiro[1], Mélanie Chypre[1,2], Nathalie Brouard[3], Simon Rauber[1], Farouk Alloush[1], Monica Romera-Hernandez[4], Cécile Bénézech[5], Zhi Li[6], Anita Eckly[3], Mark C. Coles[6], Antal Rot[6], Hideo Yagita[7], Catherine Léon[3], Burkhard Ludewig[8], Tom Cupedo[4], François Lanza[3], Christopher G. Mueller[1]*

1 CNRS UPR 3572, University of Strasbourg, Laboratory of Immunopathology and Therapeutic Chemistry/MEDALIS, Institut de Biologie Moléculaire et Cellulaire, Strasbourg, France, **2** Prestwick Chemical, Blvd Gonthier d'Andernach, Parc d'innovation, 67400, Illkirch, France, **3** INSERM, UMR_S949, Etablissement Français du Sang-Alsace, Faculté de Médecine, Fédération de Médecine Translationnelle, Université de Strasbourg, Strasbourg, France, **4** Department of Hematology, Erasmus University Medical Center, Rotterdam, The Netherlands, **5** BHF Centre for Cardiovascular Science, Queens Medical Research Institute, University of Edinburgh, Edinburgh, United Kingdom, **6** Center for Immunology and Infection, Department of Biology, University of York, York, United Kingdom, **7** Department of Immunology, Juntendo University School of Medicine, Tokyo, 113–8421, Japan, **8** Institute of Immunobiology, Kantonspital St. Gallen, 9007, St. Gallen, Switzerland

* c.mueller@cnrs-ibmc.unistra.fr

Abstract

Microenvironment and activation signals likely imprint heterogeneity in the lymphatic endothelial cell (LEC) population. Particularly LECs of secondary lymphoid organs are exposed to different cell types and immune stimuli. However, our understanding of the nature of LEC activation signals and their cell source within the secondary lymphoid organ in the steady state remains incomplete. Here we show that integrin alpha 2b (ITGA2b), known to be carried by platelets, megakaryocytes and hematopoietic progenitors, is expressed by a lymph node subset of LECs, residing in medullary, cortical and subcapsular sinuses. In the subcapsular sinus, the floor but not the ceiling layer expresses the integrin, being excluded from ACKR4$^+$ LECs but overlapping with MAdCAM-1 expression. ITGA2b expression increases in response to immunization, raising the possibility that heterogeneous ITGA2b levels reflect variation in exposure to activation signals. We show that alterations of the level of receptor activator of NF-κB ligand (RANKL), by overexpression, neutralization or deletion from stromal marginal reticular cells, affected the proportion of ITGA2b$^+$ LECs. Lymph node LECs but not peripheral LECs express RANK. In addition, we found that lymphotoxin-β receptor signaling likewise regulated the proportion of ITGA2b$^+$ LECs. These findings demonstrate that stromal reticular cells activate LECs via RANKL and support the action of hematopoietic cell-derived lymphotoxin.

OPEN ACCESS

Citation: Cordeiro OG, Chypre M, Brouard N, Rauber S, Alloush F, Romera-Hernandez M, et al. (2016) Integrin-Alpha IIb Identifies Murine Lymph Node Lymphatic Endothelial Cells Responsive to RANKL. PLoS ONE 11(3): e0151848. doi:10.1371/journal.pone.0151848

Editor: Jörg Hermann Fritz, McGill University, CANADA

Received: October 29, 2015

Accepted: March 4, 2016

Published: March 24, 2016

Data Availability Statement: All relevant data are within the paper and its Supporting Information files.

Funding: O.C. and M. R.-H. were supported by FP7-MC-ITN No. 289720 "Stroma", M.C. by Prestwick Chemical, S.R. by the German-French University program and F.A. by the IDEX-University of Strasbourg international PhD program. The study has received financial support by the Centre National pour la Recherche Scientifique and the Agence Nationale pour la Recherche (Program "Investissements d'Avenir", ANR-10-LABX-0034 MEDALIS; ANR-11-EQPX-022) to C.G.M. The

funders had no role in study design, data collection and analysis, decision to publish, or preparation of the manuscript. The funder, Prestwick Chemical (commercial company), provided support in the form of salary for author Mélanie Chypre, but did not have additional role in the study design, data collection and analysis, decision to publish, or preparation of the manuscript. The specific roles of the authors are articulated in the 'author contributions' section.

Competing Interests: The commercial affiliation does not alter the authors' adherence to PLOS ONE policies on sharing data and materials.

Introduction

Molecules, cells and pathogens carried by the lymph flow are filtered by lymph nodes (LNs). In these specialized organs, resident immune cells recognize, eliminate and mount an immune response against pathogens. The LECs provide an important structural and functional support to this process by mediating lymph drainage, organizing cellular compartments, regulating the immune response and controlling lymph exit [1]. Lymph first drains into the subcapsular sinus, which comprises an outermost (ceiling-lining) and an inner (floor-lining) lymphatic endothelial layer. Differential expression of the chemokine ACKR4 (also called CCRL1) has recently highlighted structural and functional specialization of these layers [2]. LECs also form the cortical and medullary sinuses that allow distribution of cells and large molecules within different LN compartments and exit into the efferent lymph [3]. Platelet adhesion to lymphatic endothelium mediates blood and lymphatic vessel separation during embryonic development [4].

Integrins play an important role in a variety of biological processes ranging from development, cancer, and inflammation [5]. The large family of transmembrane receptors, composed of α and β subunits, provides structural and functional integrity to connective tissues and organs, mediates cell extravasation from blood and contributes to cell activation. The integrin α2b (ITGA2b, CD41 or glycoprotein IIb) pairs exclusively with integrin β3 (ITGB3, CD61 or glycoprotein IIIa), while the latter can also form a heterodimer with integrin αV (ITGAV, CD51). ITGA2B/ITGB3 is well known for its role in blood clotting through its expression by megakaryocytes and platelets [6]. Upon platelet stimulation, the surface integrin heterodimer becomes activated, binds fibrinogen and von Willebrand factor resulting in platelet aggregation. ITGA2b and ITGB3 are also expressed by embryonic erythroid and hematopoietic progenitor cells arising from the hemogenic endothelium of the conceptus and embryo [7–9]. Although hemogenic endothelium generates ITGA2b$^+$ hematopoietic progenitor cells, these special endothelial cells themselves lack the integrin [7]. Otherwise, blood endothelial cells express a number of integrins, both in the abluminal space to adhere to the basement membrane and in the lumen to recruit leucocytes [5].

The TNF family member RANKL (TNFSF11), alike other member of the protein family such as lymphotoxin-α and β, plays an important role in LN development [10]. It is expressed in the embryo by the hematopoietic lymphoid tissue inducing cells and triggers lymphotoxin production [11]. In a second phase RANKL is expressed by the lymphoid organizer cells of mesenchymal origin [12], which are thought to persist as marginal reticular cells (MRCs) in the adult [13]. The role of RANKL produced by MRCs remains unknown. In a model of skin overexpression RANKL was shown to activate LN lymphatic and blood endothelial cells as well as fibroblastic reticular cells raising the possibility that RANKL of MRCs functions as internal activator of these cells [14].

In this study, we show that a subset of LECs of mouse and human LNs express ITGA2b. In the murine LN the ITGA2b$^+$ LECs are heterogeneously distributed in the medullary and cortical areas as well as in the subcapsular sinus, where only the floor-lining cells carry the integrin. ITGA2b could potentially heterodimerize with ITGB3 to bind ligands, such as fibronectin, but the alternative α-chain, ITGAV, is also present to pair with ITGB3 to anchor the cells to matrix components. In mice overexpressing RANKL the level of ITGA2b increases, while its neutralization or its genetic deletion from MRCs reduce the integrin expression. Similarly, inhibition of lymphotoxin-β receptor signaling negatively affects the proportion of ITGA2b$^+$ LECs. Therefore, ITGA2b is a novel marker for LN LECs constitutively activated by TNF-family members RANKL and lymphotoxin-αβ.

Material and Methods

Mice

C57BL/6, *Itga2b*$^{-/-}$ [15], ACKR4-eGFP transgenic mice (otherwise known as CCRL-1-eGFP) [2], RANK-transgenic [14], and RANKL$^{\Delta Ccl19}$ mice were bred and kept in specific pathogen-free conditions, and all experiments were carried out in conformity to the animal bioethics legislation approved by and according to national guidelines of the CREMEAS (Comité Régional d'Ethique en Matière d'Expérimentation Animale de Strasbourg), permit number AL/02/22/11/11 and AL/03/12/05/12. All efforts were made to minimize suffering. To generate mice with conditional RANKL deficiency in marginal reticular cells (*RANKL*$^{\Delta Ccl19}$), mice containing a single copy of the *Ccl19-cre* BAC transgene [16] were crossed with RANKL$^{f/f}$ (B6.129-Tnfsf11tm1.1Caob/J) mice [17]. For adoptive bone marrow transfer, 6-wk-old mice were lethally irradiated with 9 Gy (Caesium source), and 3 h later they received 5x10^6 bone marrow cells i.v. harvested from *Itga2b*$^{-/-}$ mice. Chimerism was complete by the absence of ITGA2b on platelets.

Preparation of LN Stromal Cells

Stromal cells were prepared from murine peripheral (inguinal, axial and brachial) or mesenteric LNs as previously described [18]. CD45$^+$ and TER119$^+$ cells were depleted using anti-TER119 and anti-CD45 coupled magnetic beads (Miltenyi Biotec). Use of all human tissues was approved by the Medical Ethical Commission of the Erasmus University Medical Center Rotterdam and was contingent on written informed consent from the donor. Stromal cells from human LNs were obtained as described [19].

Flow Cytometry and Cell Sorting

All reactions were performed at 4°C for 20 min in PBS supplemented with 2% FCS and 2.5 mM EDTA. The following antibodies were used for flow cytometry: CD45-APC/CY7 (30-F11, Biolegend), Ter119-APC/CY7 (Ter119, Biolegend), gp38/podoplanin-A488 (8.1.1, Biolegend), CD31-PcPeF710 (390, eBioscience), ITGA2b (APC-conjugated MWReg30, Biolegend, A647-conjugated RAM-2), ITGB3-PE (2C9.G2, Biolegend), glycoprotein subunit IBβ-A647 (RAM-1 [20]), ITGAV-PE (RMV-7, eBioscience), CD3-FITC (145-2C11, BD), CD19-APC (1D3, BD), CD103-PerCP-Cy5.5 (M290, BD), CD11c-PerCP-Cy5.5 (N418, BD), RANK-02 [21] or their isotype controls. Integrin αIIbβ3-PE (JON/A, EMFRET analytics GmbH, Eibelstadt, Germany) was used to stain for the active integrin conformation in tyrode-albumin buffer pH 7.3 (137 mM NaCl, 2,7mM KCl, 12mM NaHCO3, 0.36 mM NaH2PO4, 1mM MgCl2, 2mM CaCl2, 5mM Hepes, 0,35% albumin, 5.55 mM Glucose). Flow cytometry was performed on a Gallios (Beckman-Coulter, Fullerton, CA, USA) or a Fortessa X-20 SORP (BD) and analyzed with FlowJo software (Treestar, Ashland, OR, USA). For flow cytometric analysis of human fetal LNs the following antibodies were used: gp38/podoplanin A488 (NC-08, Biolegend), CD31 Pacific-blue (WM59, Biolegend), CD45 PE-Cy7 (HI30, Biolegend), and mouse anti-Donkey A647 (Life technologies). Primary antibodies were added to the cells for 30 min at 4°C. Then, cells were stained with secondary antibodies for 20 min at 4°C.

Lymphatic Endothelial Cell Culture

LECs were cell-sorted based on gp38 and CD31 expression and cultured in a single drop of endothelial cell growth medium (Lonza) in culture slides (Corning) pre-coated with 5 μg/cm^2 of fibronectin and collagen (Sigma-Aldrich) over-night at 37°C 5% CO_2. The next day, 300 μl of endothelial cell growth medium were added. Cells were fixed in 4% formaldehyde and then

stained for ITGA2b and mCLCA1 with DAPI nuclear counterstain. Images were acquired on a Microscope Zeiss Axio Observer Z1 Confocal LSM780 (Carl Zeiss) with the Carl Zeiss proprietary software Zen and on a spinning disk inverted microscope (Carl Zeiss) with a confocal head Yokogawa CSU and a Metamorph software (Metamorph). Analysis of all microscopic images was done using the open source imageJ-based Fiji distribution.

Immunofluorescence

Organs were embedded in Tissue-Tek O.C.T Compound (Electron Microscopy Science) and frozen in liquid nitrogen. Six to 8 μm sections were cut, fixed in cold acetone and then blocked with 2% BSA. The following antibodies were used: mCLCA1 (hamster mAb 10.1.1), Lyve-1-A488 (ALY7, eBioscience), ITGA2b-APC (MWReg30, Biolegend), Prox-1 (polyclonal goat, R&D Systems), GPIbß (RAM1-A645), MAdCAM-1 (MECA-367, BD-Pharmingen), fibronectin (Rabbit polyclonal, Patricia Simon-Assmann, UMR-S 1109 INSERM, Strasbourg), RANKL (IK22.5, Rat IgG2a, [22]), goat anti-rabbit-A488 (Molecular Probes), goat anti-hamster-A488/A546 (Molecular Probes), donkey anti-rat-Cy3 (Jackson) or streptavidin A546 or A647 (Molecular Probes). Sections were mounted using DAKO mounting medium (Dako, Hamburg, Germany). Images were acquired and treated as noted above.

Transmission Electron Microscopy

ITGA2b^{+} sorted LECs were fixed in 2.5% glutaraldehyde for 1 h and 200 μl blue AccuDrops^{R} beads (BD Biosciences) were added to facilitate cell pellet visualization during the subsequence sample preparation as described [23]. Cells were visualized on a CM120 microscope with biotwin lens configuration operating at 120 kV (FEI, Eindhoven, The Netherlands)

Quantitative Reverse Transcription Coupled Polymerase Chain Reaction (qRT-PCR)

RNA from total LNs and from sorted LECs were extracted with RNeasy kits (Qiagen) and cDNA was synthesized with Maxima First Strand cDNA Synthesis Kit (Thermo Scientific) and Improm-II (Promega) using oligo(dT)15 primers. RT-PCR was performed using Luminaris color HiGreen qPCR Master Mix (Thermo Scientific) using the following primers to amplify ITGA2b: Forward 5'-ATTCCTGTTTAGGACGTTTGGG and Reverse: 5'-TCTTGACTT GCGTTTAGGGC [24] with the housekeeping gene coding for GAPDH (Forward 5'-T GACGTGCCGCCTGGAGAAA and Reverse 5'-AGTGTAGCCCAAGATGCCCTTCAG). Quantitative RT-PCR was run on a Bio-Rad CFX96 thermal cycler, and threshold values (Ct) of the target gene were normalized to GAPDH (ΔCt = CtITGA2b –CtGAPDH). The relative expression was calculated for each sample versus the mean of total 5 day LN ΔCt: ΔΔCt = ΔCtsample– ΔCttotal LN at 5 days; and relative quantification was performed as 2-ΔΔCt.

Immunization

Six-week-old mice were injected in both posterior limbs with 70 μg of chicken ovalbumin, 600 μg aluminium hydroxide (Sigma-Aldrich) and 6x10^{8} heat inactivated *B. pertussis* ml^{-1}. A boost was administrated 2 weeks later. Inguinal and popliteal LN were sampled 4 days later.

Imiquimod Treatment

Adult mice were anesthetized by intraperitoneal injection of ketamine and xylazine (100 μg/g body weight and 10 μg/g body weight, respectively). Back skin or ear skin received 12.5 μg/g (0.1mg/kg body weight) of Toll-like receptor (TLR)-7 agonist imiquimod (Aldara), diluted in

neutral cream (Diprobase) [25]. Back skin hair was trimmed before hair removal with cold wax (Klorane, France). The animals were sacrificed 12h after.

RANKL and Lymphotoxin β Receptor Blockage

The neutralizing anti-RANKL mAb IK22-5 [22] or the rat IgG2a isotype control (BioXell) were administrated s.c. into 6-week old C57BL/6 mice every 3 days (50 μg/ mouse in sterile saline) for two weeks and for 3 consecutive days for the third week. The lymphotoxin β receptor -Ig fusion protein or mIgG1 isotype control (20μg/mouse in sterile saline) were administrated s.c. into 6-week old mice every 3 days for four weeks.

Statistical Analysis

An unpaired two-tailed Student *t*-test and ANOVA with the Bonferroni method were used to determine statistically significant differences. The p values <0.05 were considered statistically significant. GraphPad Prism version 5 for Windows (GraphPad software) was used for the analysis.

Results

LN LECs Express ITGA2b

Microarray gene expression analysis of murine LN stromal cells had revealed transcription of *Itga2b* by LECs but by no other stromal or hematopoietic cells [26]. To study ITGA2b expression by LECs, we prepared stromal cells from peripheral LNs following the same procedure as used in the microarray study. LECs ($gp38^+CD31^+$), fibroblastic reticular cells (FRCs, $gp38^+CD31^-$), blood endothelial cells (BECs, $gp38^-CD31^+$), and pericyte-containing double-negative cells (DNCs, $gp38^-CD31^-$) were identified in the cell suspension (**panel A in S1 Fig**). ITGA2b-specific mAbs (MWReg30 and RAM-2), validated on platelets (**panel B in S1 Fig**), recognized a major subset of LECs and a minor subset of BECs (**Fig 1A and panel A in S1 Fig**). To verify whether the labelling was due to platelets bound to the cells, we exposed them to an antibody specific for glycoprotein subunit GPIbβ (CD42c) that is exclusively carried by megakaryocytes and platelets [20] (**panel B in S1 Fig**). The antibody recognized the minor fraction of BECs but did not interact with LECs (**Fig 1B**). To further assure that LECs were platelet-free, $ITGA2b^+$ LECs were FACS sorted and examined for the adherence of platelets by electron microscopy, however none were found (**panel C in S1 Fig**). To confirm ITGA2b expression, LECs were prepared from mice deficient for ITGA2b [15]. As shown in **Fig 1C**, LECs from heterozygous mice expressed reduced levels of the integrin and LECs from mice with the homozygous deletion fully lacked ITGA2b. We next irradiated WT C57BL/6 mice and adoptively transferred bone marrow from *Itga2b*$^{-/-}$ mice. Six weeks later, circulating platelets were devoid of ITGA2b but LECs still expressed the integrin (**Fig 1D** and **panel A in S2 Fig**). Also the staining for platelets on LN cross-sections did not reveal any presence, whereas platelets were found in the spleen red pulp (**panel B in S2 Fig**). We tested whether the integrin could be detected on FACS-sorted LECs grown in culture. The cells were labelled for ITGA2b and the pan-LEC marker mCLCA1 (recognized by mAb 10.1.1, [27,28]). LECs expressing ITGA2b could be seen, which was found distributed throughout the cell and occasionally concentrated at cell-cell junctions (see arrows) (**Fig 1E**). Finally, to extend this finding to man, human embryonic mesenteric LNs were processed in a similar fashion to obtain the four stromal subsets (**panel C in S2 Fig**). An ITGA2b-reactive mAb that recognized platelets from healthy donors but not from an ITGA2b-deficient Glanzmann donor (**panel D in S2 Fig**)

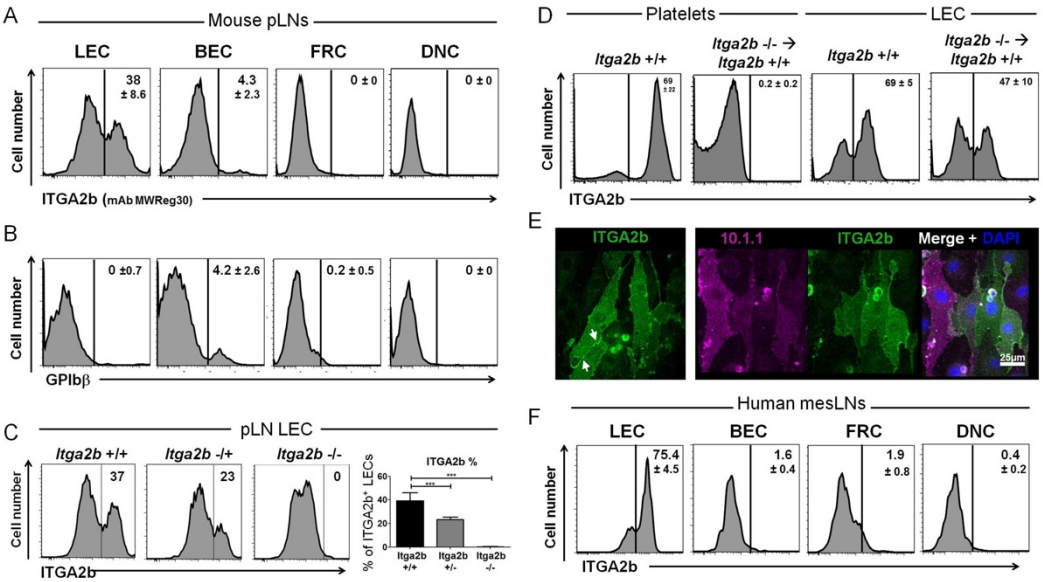

Fig 1. LN LECs express ITGA2b. (A) Flow cytometry histograms display ITGA2b expression by peripheral (p)LN stromal subsets, lymphatic endothelial cells (LEC), blood endothelial cells (BEC), fibroblastic reticular cells (FRC) and the pericyte-containing gp38^{+}CD31^{-} double negative cells (DNC). Peripheral LNs are inguinal, brachial and axial LNs. The percentage ±SD (n = 13) of cells labelled by the mAb is indicated. (B) Histograms of the four stromal cell types incubated with a mAb specific for platelet-restricted GPIBβ. The percentage ±SD (n = 8) of cells labelled by the antibody is indicated. (C) Histograms show ITGA2b expression by LECs of WT mice, but reduced and no expression by LECs isolated from mice heterozygous or homozygous for *Itga2b* genetic deletion. The graph depicts the mean ± SD (n = 9) percentage of ITGA2b^{+} LECs in WT controls and in mice heterozygous or homozygous for the *Itga2b* genetic deletion. (D) Histograms of ITGA2b expression by platelets and LECs in control mice and in mice after adoptive transfer of *Itga2b*$^{-/-}$ bone marrow (n = 8 for adoptive bone marrow transfer, n = 4 for WT mice). The percentage ±SD of ITGA2b^{+} cells is indicted. (E) Confocal fluorescence microscopy images of cell-sorted LECs in culture showing mCLCA1 (mAb 10.1.1) (magenta) and ITGA2b (green) expression. (F) Flow cytometry histograms ±SD (n = 2) display ITGA2b expression within the four stromal subsets of human embryonic mesenteric LN. ***p<0.001.

doi:10.1371/journal.pone.0151848.g001

labelled LECs but not the other stromal subsets (Fig 1F). Taken together, these finding demonstrated that LN LECs, but not other stromal cells, express the ITGA2b integrin.

ITGA2B Is Restricted to LN LEC Subsets

Because only a proportion of LN LECs expressed ITGA2b, we next wished to localize the ITGA2b^{+} LECs in the mouse LN. ITGA2b immunofluorescence on cross-sections together with LEC marker mCLCA1 (10.1.1 mAb) revealed that LECs of the medullary and the cortical area expressed ITGA2b in a heterogenous manner (Fig 2A). Remarkably, the subcapsular sinus ceiling LECs were totally devoid of ITGA2, while its floor counterpart uniformly expressed the integrin. We repeated the immunofluorescence with the lymphatic vessel endothelial hyaluronan receptor (Lyve)-1 and observed again a restricted expression of ITGA2b to a subset of LECs (**panel A in** S3 Fig). Colabelling for Prox-1, the most specific LEC marker, confirmed LEC-restricted ITGA2b staining (**panel B in** S3 Fig). At E18.5, the subcapsular sinus of the embryonic inguinal LNs were not yet formed and was constituted of a single layer of Lyve-1^{+} LECs expressing the integrin to different extents (Fig 2B). To verify its exclusion from the subcapsular sinus ceiling-lining cells, LECs of adult mice that express GFP exclusively in this

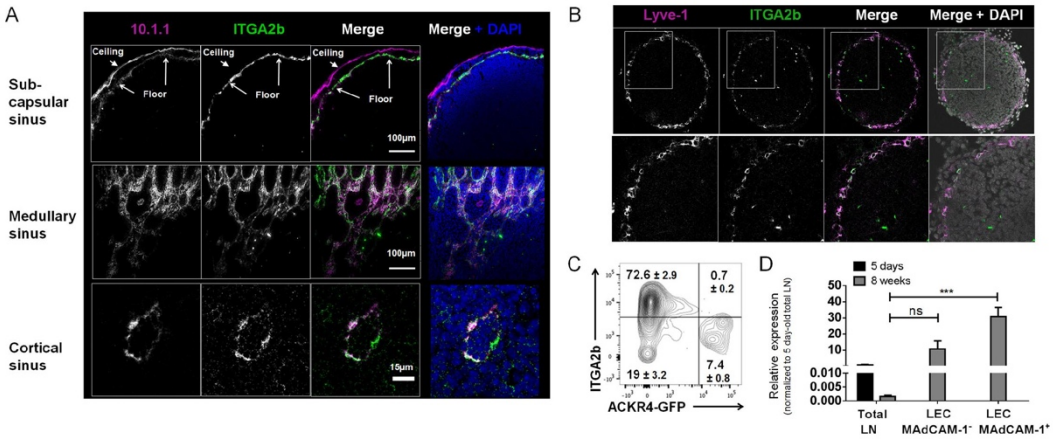

Fig 2. ITGA2b is heterogeneously expressed in the adult and embryonic LN. (A) Confocal microscopy images of an adult inguinal LN probed for ITGA2b together with LEC marker mCLCA1 (mAb 10.1.1) in the subcapsular, the medullary and the cortical sinus. Scale bars are indicated. (B) Confocal microscopy images of an embryonic (E18.5) inguinal LN of ITGA2b and LEC marker Lyve-1. Higher magnification of boxed area is shown below. (C) Flow cytometry counterplot of ITGA2b versus ACKR4 expression by LN LECs of ACKR4-GFP transgenic mice. The percentage ±SD (n = 3) of positive cells is indicated. (D) Mean ± SEM *Itga2b* mRNA expression of total LN from mice aged 5 days and 8 weeks, and of MAdCAM-1$^+$ and MAdCAM-1$^-$ cell-sorted LECs from mice aged 8 weeks. Statistical analysis: ***p<0.001, ns = non significant by one way Anova with the Bonferroni method.

doi:10.1371/journal.pone.0151848.g002

subset [2] were labelled for ITGA2b. Indeed, the ACKR4-GFP$^+$ LECs lacked the integrin (Fig 2C). To verify ITGA2b expression in the floor-lining cells, we sorted LECs based on gp38/CD31 and MAdCAM-1 expression for qRT-PCR analysis. MAdCAM-1 is uniformly carried by the floor-lining subcapsular sinus LECs but not the ceiling counterpart (**panel A in** S4 Fig) and colabelling showed that all MAdCAM-1$^+$ cells express ITGA2b (**panel B in** S4 Fig). MRCs identified by RANKL expression localize close to the LECs but do not carry the integrin (**panel C in** S4 Fig). In whole adult LN, *Itga2b* mRNA was barely detectable, however sorted MAdCAM-1$^+$ and MAdCAM-1$^-$ cells clearly expressed the message (Fig 2D). Sorted LN BECs were devoid of the mRNA (data not shown). This supports its restricted expression in LECs, and in particular the floor-lining MAdCAM-1$^+$ LECs. To determine whether ITGA2b is expressed by non-LN LECs, skin was processed into a cell suspension and LECs were identified as CD45$^-$F4/80$^-$gp38$^+$CD31$^+$ cells. However, we saw no ITGA2b expression by FACS or qRT-PCR, neither in LECs from resting skin, after activation with imiquimod [25] or from RANK-transgenic mice overexpressing RANKL from hair follicles [14,29] (**panel D in** S4 Fig and data not shown). Taken together, the data show that ITGA2b is restricted to subsets of LN LECs.

LEC ITGA2b Is Not Required for Residence in Fibronectin-Rich Environments

To explore the function of ITGA2b for LECs, we first asked whether ITGA2b could heterodimerize with ITGB3 to interact with ligands, such as fibronectin. Indeed, ITGB3 was uniformly expressed by LECs and BECs, while there was little of the β-chain found on FRCs and DNCs (Fig 3A). We next assessed whether there was a correlation between ITGA2b expression and

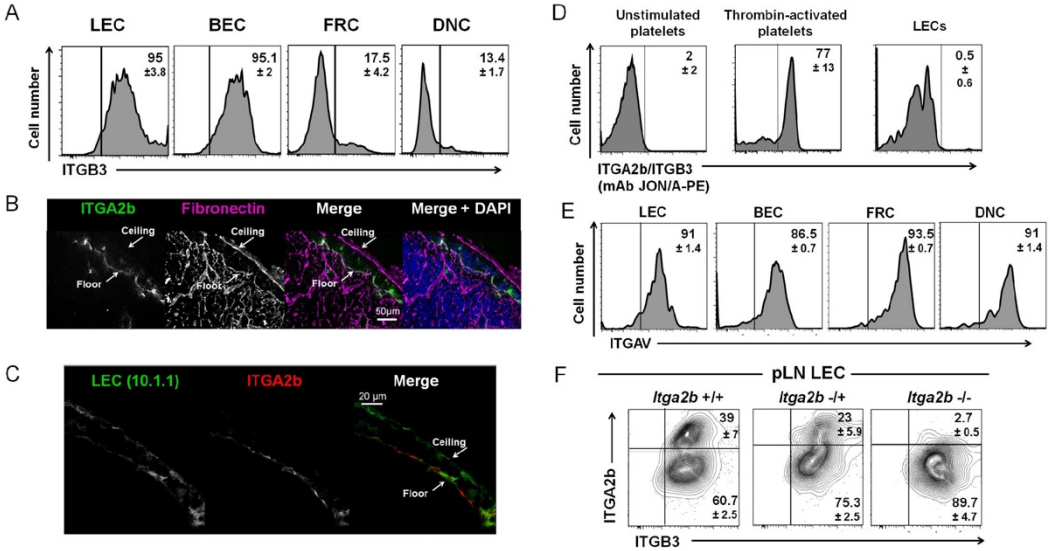

Fig 3. LEC ITGA2b is not required for residence in fibronectin-rich environments. (A) Flow cytometry histograms show the percentage ±SD (n = 4) of LECs expressing ITGB3 by the four stromal subsets. (B) Confocal microscopic images of a LN subcapsular area labelled for fibronectin (magenta) and ITGA2b (green). Nuclear coloration was with DAPI. (C) Confocal high resolution microscopy of the subcapsular area labelled for ITGA2b and mCLCA1 (mAb 10.1.1). (D) Histograms show recognition of the active conformation of the ITGA2b/ITGB3 complex on activated platelets but not on LECs or unstimulated platelets by the PE-conjugated JON/A mAb. (E) Histograms show ITGAV expression ±SD (n = 3) on the stromal subsets. (F) Flow cytometry counterplots of LECs probed for expression of ITGA2b and ITGB3 in *Itga2b*$^{+/+}$, *Itga2b*$^{+/-}$ and *Itga2b*$^{-/-}$ mice (n = 3).

doi:10.1371/journal.pone.0151848.g003

residence in a fibronectin-containing environment. To this end, we stained the LN subcapsular area that contained the ITGA2b^{+} floor-lining and the ITGA2b^{-} ceiling-lining LECs for fibronectin. It was apparent that this extracellular matrix component was present in both sites, demonstrating that the absence of ITGA2b does not prevent LECs to take up position in the fibronectin-containing ceiling (Fig 3B). Further, the positioning of the integrin relative to the sinus luminal or abluminal side was investigated and no preferential location was found (Fig 3C). To explore whether a functional ITGA2b/ITGB3 complex was indeed formed, LECs and, as controls unstimulated and thrombin-activated platelets, were incubated with the phycoerythrin (PE)-conjugated JON/A mAb, which recognizes only the ITGA2b/ITGB3 complex in its activated state, as found on platelets [30,31]. While agonist stimulated platelets were labelled with this mAb, LECs were not recognized (Fig 3D). This suggests that if an ITGA2B/ITGB3 heterodimer is formed on LECs, it is not in a configuration recognized by PE-JON/A and may present a low affinity for its ligands. We therefore asked whether ITGA2b could be substituted by ITGAV to pair with ITGB3. LECs, alike all other stromal cells, expressed ITGAV, suggesting that they could anchor to matrix proteins through ITGAV/ITGB3 (Fig 3E). In platelets (**panel B in S1 Fig**) but not in embryonic hematopoietic stem cells or mast cells [24,32], ITGA2b is required to translocate ITGB3 to the cell surface [15,33], raising the question of whether, in the absence of ITGA2b, ITGB3 would be available to heterodimerize with ITGAV on the cell surface. To assess this issue, we labelled LECs from mice deficient for ITGA2 and observed that

cell surface expression of the ITGB3 was maintained in *Itga2b*$^{-/-}$ mice (Fig 3F). Taken together, ITGA2b is not required for residence of the ceiling LECs in its fibronectin-containing environment, most probably by the formation of an ITGAV/ITGB3 complex that binds with high affinity to this matrix protein.

The ITGA2b^{+} Subset Is Sensitive to Activation by RANKL and Lymphotoxin

We noted that in comparison to peripheral LNs, the proportion of ITGA2b^{+} LECs was higher in mesenteric LNs (Fig 4A). Because mesenteric LNs are stimulated by the intestinal microflora, this evoked the possibility that the heterogenous LN ITGA2b expression reflects differences in cell activation. To test this hypothesis, we administered heat-inactivated *Bordetella pertussis* subcutaneously, and after a secondary immunization, compared ITGA2b expression in draining and non-draining LNs. The proportion of ITGA2b^{+} LECs was markedly increased in response to immunization (Fig 4B), while the other stromal cells remained devoid of the integrin (Fig 4C). The upregulation was not due to platelet adherence to LECs because there was no recognition of LECs by the GPIbβ-specific mAb (Fig 4D). We also tested whether the innate immune stimulus imiquimod (TLR7 ligand) resulted in a similar upregulation. LECs from auricular LNs draining imiquimod or mock-treated ears were analyzed, however, the proportion of ITGA2b^{+} LECs did not rise after application of the TLR-7 ligand (**panel A in** S5 Fig). We have previously observed that RANKL activates LN LECs in a transgenic model of cutaneous RANKL overproduction [14]. Therefore, we determined in these mice whether RANKL affected ITGA2b levels and indeed found that ITGA2b expression was positively regulated by this TNF-family member (Fig 4E). We addressed the question of whether integrin upregulation was due to its externalization to the cell surface. In WT controls, immunolabelling of permeabilized cells revealed a stronger signal compared with the cell surface, however, the signal was identical in the LECs isolated from the transgenic mice (**panel B in** S5 Fig). This suggests that the increased expression of ITGA2b by RANKL stimulation likely involves its translocation from the cytoplasm to the cell membrane. We tested whether the upregulation was accompanied by a rise in transcriptional activity. In comparison with WT controls, there was no major increase in mRNA synthesis in the LEC subsets isolated from the mutant mice (**panel C in** S5 Fig). However, because the proportion of MAdCAM-1^{+} LECs greatly augmented in the transgenic mice (**panel C in** S5 Fig), the increase in ITGA2b expression in these mice is principally the result of an expansion of the MAdCAM-1^{+} subset that naturally expresses more ITGA2b. We next determined if neutralizing RANKL in WT mice led to a downregulation of ITGA2b. Administration of RANKL-blocking mAb caused a significant decrease in ITG2b expression by LECs in comparison to isotype injected controls (Fig 4F). Immunofluorescence on sections confirmed the strong decline of ITGA2b in subcapsular and medullary sinuses (Fig 4G). Because in the LN, RANKL is principally produced by the marginal reticular cells (MRCs) [13], this raised the possibility that MRC RANKL activates LECs resulting in ITGA2b expression. To address this question, we generated mice conditionally deficient for RANKL in MRCs by crossing *Ccl19-cre* mice [16] with *Rankl*$^{f/f}$ mice [17]. These mice were devoid of RANKL expression by MRCs (**panel D in** S5 Fig). Analysis of RANKL$^{\Delta CCL19}$ mice showed that the disappearance of MRC RANKL significantly compromised ITGA2b expression (Fig 4H), supporting a role of RANKL in LEC activation. However, because there was not a complete loss of ITGA2b other factors could contribute to LEC activation. Indeed, approximately 15% of LECs were double positive for RANK and ITGA2b, suggesting that a proportion of LECs reacts to other stimulatory factors (**panel E in** S5 Fig). On the other hand, cutaneous LECs that do not respond to RANKL do not carry any RANK

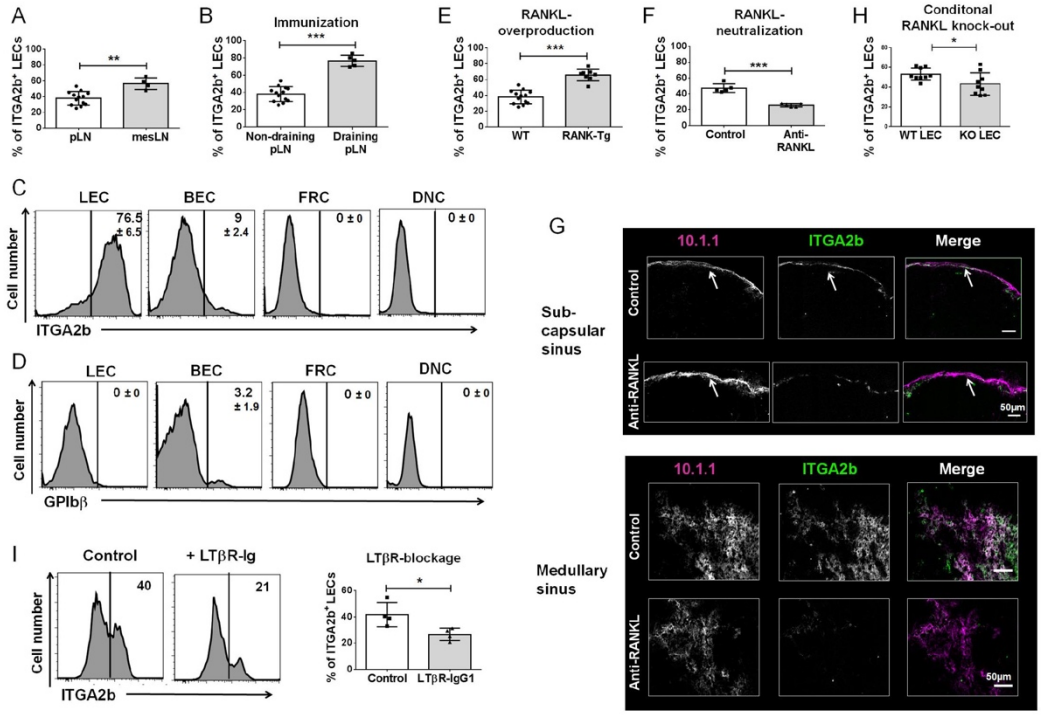

Fig 4. ITGA2b$^+$ LECs are responsive to RANKL and lymphotoxin activation. (A) Mean ± SD (n = 6) percentage of ITGA2b$^+$ LECs of peripheral (p)LNs (inguinal, axial and brachial) versus mesenteric (mes) LNs. (B) Mice were immunized with heat-inactivated *B. pertussis* and LEC ITGA2b expression of draining and non-draining LNs was compared. The graph shows the mean ± SD (n = 6) percentage of ITGA2b$^+$ LECs, revealing increased ITGA2b proportions in response to immunization. (C) Flow cytometry histograms display representative ITGA2b expression ±SD (n = 6) by stromal subsets of inguinal and popliteal LNs draining the immunization site. (D) Histograms show reactivity to anti-GPIBβ labelling of stromal subsets of inguinal and popliteal LNs draining the immunization site. The percentage ±SD (n = 6) of cells labelled by the antibody is indicated. (E) The increase in the proportion of ITGA2b$^+$ pLN LECs from RANK-Tg mice (overproducing soluble RANKL in the skin) compared with LECs of WT controls is shown as mean ± SD (n = 8). (F) Graph shows reduction in the percentage of ITGA2b$^+$ LECs upon RANKL neutralization (mean ± SD, n = 5). (G) Confocal microscopy imaging in inguinal LN subcapsular and medullary sinuses of ITGA2b expression (green) by LECs (10.1.1, magenta) after RANKL-neutralization or after administration of isotype-control antibody. (H) Mean ± SD (n = 9) percentage of ITGA2b$^+$ LECs from mice with conditional deficiency of RANKL in marginal reticular cells (KO) versus WT littermate controls. (I) Histograms of ITGA2b expression of LECs from mice treated with LTβR-Ig or IgG1 control. The graph depicts the mean ± SD (n = 3) percentage of ITGA2b$^+$ LECs. *p<0.5, **p < 0.01, ***p < 0.001.

doi:10.1371/journal.pone.0151848.g004

(**panel F in** S5 Fig). In light of similar activities of RANKL and lymphotoxin αβ (LT) [10,34] and the expression of the LTβ receptor (R) by LECs [35], we asked whether also LT regulated ITGA2b expression. Therefore, mice were treated with soluble LTβR-Ig to inhibit LTβR signaling [36]. We found that this treatment likewise reduced ITGA2b (Fig 4I). Taken together, ITGA2b is a novel marker for subsets of LN LECs that respond to activation by TNF-family members RANKL and LT.

Discussion

In this study we show that ITGA2b is expressed by a subset of LN LECs in the subcapsular, cortical and medullary sinus. This subset is also marked by MAdCAM-1. The ITGA2b$^+$ population is sensitive to stimulation by the TNFSF members RANKL and LT.

ITGA2b is known to be carried by megakaryocytes and platelets as well as by hematopoietic stem and progenitor cells in the embryo and the adult [7–9,37]. Here we show for the first time that LN LECs also carry this integrin. A number of studies had analyzed ITGA2b expression using different experimental approaches, including a genetic reporter system to mark ITGA2b-expressing cells by β-galactosidase [7–9]. However, these reports, which investigated whole embryos, the embryonic aorta-gonad-mesonephros region, spleen, thymus and bone marrow, did not analyze LNs. Although platelets interact with endothelial cells in the embryo during separation of blood and lymphatic systems [4], the following observations exclude the possibility that ITGA2b expression by LEC is the result of platelet contamination: (i) the platelet glycoprotein subunit Iβ was not detected on LECs, (ii) electron microscopy did not reveal platelets adhering to the cells, (iii) ITGA2b-deficient platelets lacked surface ITGB3, yet the β-chain was expressed by LECs of *Itga2b*$^{-/-}$ mice, (iv) after adoptive transfer of *Itga2b*$^{-/-}$ bone marrow resulting in the repopulation of ITGA2b$^-$ platelets, the integrin was still expressed by LECs and (vi) *Itga2b* mRNA was amplified from sorted LECs. The related BECs were devoid of the integrin, irrespective of the site of residence or the presence of stimulatory signals. This is supported by an early report noting the absence of ITGA2b in the blood endothelial cell line bEnd3 [38].

LN LECs and BECs uniformly expressed ITGB3 and ITGAV, while only a subset of LECs also carried ITGA2b. Both α-chains pair with ITGB3 and recognize similar matrix proteins, such as fibronectin, fibrinogen, von Willebrand factor and vitronectin, which raises the question of the necessity of the ITGA2b chain. This is in contrast to platelets that predominantly express ITGA2b to ensure platelet aggregation. Indeed, although ITGA2b was expressed by LECs in embryonic LNs, its absence had no discernible impact on LN development. In addition, those LECs that naturally lack ITGA2b are still capable of taking up residence in the fibronectin-rich subcapsular sinus. Further, the absence of polarization towards the luminal or the abluminal side does not point to a predominant function in cell-cell interaction or cell-extracellular matrix contact. It is likely that LECs rendered genetically deficient for ITGA2b function normally, since the migration of tissue-derived dendritic cells to the LN cortex of ITGA2b-deficent mice was unperturbed (data not shown). Although we observed a reduction in the number of B cells, it cannot be excluded that this defect was the result of a loss of ITGA2b from platelets (data not shown). Indeed, a minor defect in LN structuring during development was seen in mice lacking platelet CLEC-2 [39]. Further investigation into the specific role of ITGA2b for LEC function will await the generation of mice with conditional deletion of ITGA2b in these cells. Inside-out signaling of platelets results in a conformation change of ITGA2b/ITGB3 to increase affinity for its ligands. This conformation is detected by the PE-conjugated JON/A mAb. LECs were not recognized by the antibody indicating either that ITGA2b does not pair with ITGB3 or that the complex is not in the same configuration as that found on platelets. On the other hand, to our knowledge, this mAb has only been used successfully on activated platelets and may not be a suitable reagent to probe for the ITAG2b/ITGB3 heterodimer on other cells. It is also noteworthy that although bone marrow-derived mast cells express ITGA2b and ITGB3, no binding to fibrinogen was seen, and, paradoxically, cell adhesion to fibronectin increased in ITGA2b-deficient cells [24]. It should also be noted that the densities of the α and β chains are at least 10-fold higher on platelets owing to their approximately 10-fold smaller size with roughly equal mean fluorescence intensities, resulting in greatly increasing the avidity.

ITGA2b was carried by the subcapsular floor-lining LECs but absent from its ceiling equivalent. Interestingly, this expression pattern was shared with MAdCAM-1. Hence, MAdCAM-1$^+$ LECs displayed the highest *Itga2b* transcriptional activity. In addition, there was a heterogenous expression of ITGA2b in the medullary and the cortical sinuses. Skin LECs were devoid of the integrin on protein and mRNA levels in all conditions tested. Difference in tissue versus secondary lymphoid organ LECs is supported by other examples, such as Sphingosine-1-phosphate [3], found expressed by LN LECs, or ITGA9 [40] that is carried exclusively by vessel LECs. In view of its uniform expression by the subcapsular floor-lining LECs, their juxtaposition to the RANKL-expressing MRCs, and the finding that RANKL upregulates MAdCAM-1 expression [14], we reasoned that RANKL may control ITGA2b synthesis. Using overexpression and neutralization / genetic deletion, we showed that RANKL positively regulates the proportion of ITGA2b$^+$ LECs. The finding that conditional deficiency of RANKL from MRCs lowers ITGA2b expression to the same extent as RANKL neutralization concords with the idea that MRC RANKL is the main LN RANKL source and identifies a cellular target for the stromal cell-produced RANKL. However, in the absence of definite proof that RANKL activates ITGA2b transcription we cannot completely rule out the possibility that RANKL stimulates the expansion of the ITGA2b$^+$ subset. Two elements suggested that RANKL is not the exclusive ITGA2b regulatory factor: (i) RANKL neutralization or genetic deletion do not eliminate its expression and (ii) only a proportion of ITGA2b$^+$ LECs express RANK. Lymphotoxin and RANKL share not only biological functions (requirement for secondary lymphoid organ formation), signaling (canonical and non-canonical NF-κB pathways) but also receptor expression by LECs, so that it appeared rational to investigate the impact of LTβR blockage. Indeed, administration of LTβR-Ig also led to reduced ITGA2b expression. It is therefore likely that both RANKL and LT contribute to the expression of this integrin by LECs and that its upregulation in response to immunization is the consequence of stimulatory factors including RANKL produced by primed T cells and LT expressed by activated B and T cells. The finding that imiquimod had no effect on ITGA2b may therefore reflect a failure to stimulate RANKL and LT synthesis. Further work is necessary to determine whether other stimuli such as TNF-α or T and B cell-released cytokines also impact on ITGA2b expression by LN LECs. Beyond the question of its function for LN LECs, the ITGA2b integrin sheds a new light on the heterogeneity of LECs and their response to activation signals.

Supporting Information

S1 Fig. (A) Left: Flow cytometry dot plot profiles displaying the gating strategy for stromal cell identification in CD45/Ter119-depleted LN cell suspensions. Right: Flow cytometry histograms show ITGA2b expression by the four stromal subsets using the RAM-2 mAb. The percentage ±SD (n = 6) of cells labelled by the antibody is indicated. (B) Validation of MWReg30 and RAM.2 (anti-ITGA2b antibodies), RAM.1 (anti-GPIbβ antibody) and 2C9.G2 (anti-ITGB3 antibody) in WT and knock-out animals. Expression of ITGA2b and ITGB3 was seen on platelets from *Itgab2*$^{+/+}$ mice but not on platelets from *Itgab2*$^{-/-}$ mice. GPIbβ was present on platelets of both mice. (C) FACS sorting of Itga2b$^+$ LECs. Plots for sorting and post-sort analyses are represented. Sorted cells were then viewed by transmission electron microscopy. Eight representative images of LECs are shown together with an image of platelets with the same magnification.
(TIF)

S2 Fig. (A) Microscopy images of a LN of mouse that was lethally irradiated and had received *Itgab2*$^{-/-}$ bone marrow, labelled for ITGA2b (clone MWReg30) and the LEC marker mCLCA1 (mAb 10.1.1). (B) Staining of spleen and LN sections for platelets using the platelet-specific

glycoprotein GPIbβ (mAb RAM.1) together with LEC marker mCLCA1 (mAb 10.1.1). RP = red pulp. (C) Flow cytometry dot plot profiles displaying the gating strategy for stromal cell identification from human embryonic mesenteric LN. (D) The histogram displays ITGA2b expression (SDF.2 mAb) on human healthy donor platelets but not on platelets from a patient with Glanzmann's thrombasthenia. Representative image of over 10 donors.
(TIF)

S3 Fig. (A) Confocal microscopy images of an inguinal LN, showing the medullary and the subcapsular sinus LECs labelled with anti-Lyve-1 and anti-ITGA2b mAbs. Images are representative of 2 different experiments. (B) Upper: Images of the medullary region stained for ITGA2b and nuclear Prox-1. Lower: Images of the subcapsular sinus from a LN of a mouse expressing GFP under the control of the Prox-1 promoter.
(TIF)

S4 Fig. (A) Confocal microscopy images of a LN subcapsular sinus showing MAdCAM-1 expression by the floor-lining but not the ceiling-lining LECs marked with the 10.1.1 mAb. (B) Images show overlapping staining of subcapsular sinus LECs for mCLCA1 (mAb 10.1.1), MAdCAM-1 (MECA-367) and ITGA2b (MWReg30). The flow cytometry profile shows double labelling of LECs with ITGA2b and MAdCAM-1. (C) Confocal microscopy images of a LN subcapsular sinus labelled for MAdCAM-1 and RANKL. (D) Flow cytometry of mouse skin: upper dot plot panels depict the gating strategy for skin LECs; lower panels show the histograms for ITGA2b expression ± SD (n = 3) of skin LECs from control mice, imiquimod-treated skin and from RANK-transgenic skin (overexpressing RANKL in the hair follicles).
(TIF)

S5 Fig. (A) Histograms show ITGA2b expression of auricular LN LECs from mice non-treated or after 2 or 4 day topical application of imiquimod on ears. Graph depicts the levels (geometric mean of fluorescence) of ITGA2b expression (mean ±SD, n = 3–4). (B) Histograms show LEC ITGA2b expression on the cell surface or on the cell surface and in the cytoplasm for WT and RANK-Tg mice. The graphs show the expression levels of the integrin in LECs after cell surface or intracellular/cell surface labelling. The data for WT mice are of 8 mice and for Tg mice are of 4 mice. (C) Graphs show mean ± SEM (n = 6) *Itga2b* mRNA expression of total LN, MAdCAM-1$^+$ and MAdCAM-1$^-$ LECs from WT and RANK-Tg mice (left) normalized with respect to WT 5 day LNs. Right: Graph shows the mean ± SD (n = 10) percentage of MAdCAM-1$^+$ LECs in WT and RANK-Tg mice measured by flow cytometry. (D) Confocal microscopy images of WT and RANKL$^{\Delta Ccl19}$ inguinal LNs, showing the subcapsular sinus area labelled for mCLCA1 (red) and RANKL (green). The RANKL$^{\Delta Ccl19}$ LN is devoid of RANKL expression. Representative of 4 mice. (E) Counterplot of LN LECs double stained for ITGA2b and RANK expression. Graph bar (n = 6) shows the percentage of LECs expressing both ITGA2b and RANK. (F) Histograms show RANK expression by LECs and BECs from skin and LNs. The percentage of ITGA2b$^+$ cells is indicated. Graph shows their mean ± SD (n = 6) percentages. ns = not significant, $^*p<0.5$, $^{**}p < 0.01$, $^{***}p < 0.001$.
(TIF)

Acknowledgments

The authors would like to thank Monique Duval and Delphine Lamon for mouse care, and Andy Farr (University of Washington, Seattle, USA) for mAb 10.1.1, the Biogen Idec Inc. for lymphotoxin reagents, Taija Mäkinen (Uppsala, Sweden) for lymph nodes from Prox1-CreERT2;R26-mTmG mice, the IGBMC microarray / sequencing and the cell sorting facilities

and Sophie Guillot (Institut Pasteur, Paris) for *B. pertussis*. O.C. and M. R.-H. were supported by FP7-MC-ITN No. 289720 "Stroma", M.C. by Prestwick Chemical, S.R. by the German-French University program and F.A. by the IDEX-University of Strasbourg international PhD program. The study has received financial support by the Centre National pour la Recherche Scientifique and the Agence Nationale pour la Recherche (Program "Investissements d'Avenir", ANR-10-LABX-0034 MEDALIS; ANR-11-EQPX-022) to C.G.M.

Author Contributions

Conceived and designed the experiments: CGM FL CL OGC MC NB. Performed the experiments: OGC MC NB SR FA MRH CB ZL AE. Analyzed the data: OGC MC NB SR FA MRH CB ZL CGM MCC TC AE. Contributed reagents/materials/analysis tools: MCC AR HY BL FL TC. Wrote the paper: CGM FL OGC MC.

References

1. Tewalt EF, Cohen JN, Rouhani SJ, Engelhard VH (2012) Lymphatic endothelial cells—key players in regulation of tolerance and immunity. Front Immunol 3:305.: 1–6.
2. Ulvmar MH, Werth K, Braun A, Kelay P, Hub E, Eller K, et al. (2014) The atypical chemokine receptor CCRL1 shapes functional CCL21 gradients in lymph nodes. Nat Immunol 15: 623–630. doi: 10.1038/ni.2889 PMID: 24813163
3. Schwab SR, Cyster JG (2007) Finding a way out: lymphocyte egress from lymphoid organs. Nat Immunol 8: 1295–1301. PMID: 18026082
4. Bertozzi CC, Schmaier AA, Mericko P, Hess PR, Zou Z, Chen M, et al. (2010) Platelets regulate lymphatic vascular development through CLEC-2-SLP-76 signaling. Blood 116: 661–670. doi: 10.1182/blood-2010-02-270876 PMID: 20363774
5. Lowell CA, Mayadas TN (2012) Overview: studying integrins in vivo. Methods Mol Biol 757: 369–397. doi: 10.1007/978-1-61779-166-6_22 PMID: 21909923
6. Lefkovits J, Plow EF, Topol EJ (1995) Platelet glycoprotein IIb/IIIa receptors in cardiovascular medicine. N Engl J Med 332: 1553–1559. PMID: 7739710
7. Mitjavila-Garcia MT, Cailleret M, Godin I, Nogueira MM, Cohen-Solal K, Schiavon V, et al. (2002) Expression of CD41 on hematopoietic progenitors derived from embryonic hematopoietic cells. Development 129: 2003–2013. PMID: 11934866
8. Emambokus NR, Frampton J (2003) The glycoprotein IIb molecule is expressed on early murine hematopoietic progenitors and regulates their numbers in sites of hematopoiesis. Immunity 19: 33–45. PMID: 12871637
9. Ferkowicz MJ, Starr M, Xie X, Li W, Johnson SA, Shelley WC, et al. (2003) CD41 expression defines the onset of primitive and definitive hematopoiesis in the murine embryo. Development 130: 4393–4403. PMID: 12900455
10. Mueller CG, Hess E (2012) Emerging Functions of RANKL in Lymphoid Tissues. Frontiers in Immunology 3: 261–267. doi: 10.3389/fimmu.2012.00261 PMID: 22969763
11. Yoshida H, Naito A, Inoue J, Satoh M, Santee-Cooper SM, Ware CF, et al. (2002) Different cytokines induce surface lymphotoxin-alphabeta on IL-7 receptor-alpha cells that differentially engender lymph nodes and Peyer's patches. Immunity 17: 823–833. PMID: 12479827
12. Sugiyama M, Nakato G, Jinnohara T, Akiba H, Okumura K, Ohno H, et al. (2012) Expression pattern changes and function of RANKL during mouse lymph node microarchitecture development. Int Immunol 24: 369–378. doi: 10.1093/intimm/dxs002 PMID: 22354913
13. Katakai T, Suto H, Sugai M, Gonda H, Togawa A, Suematsu S, et al. (2008) Organizer-like reticular stromal cell layer common to adult secondary lymphoid organs. J Immunol 181: 6189–6200. PMID: 18941209
14. Hess E, Duheron V, Decossas M, Lézot F, Berdal A, Chea S, et al. (2012) RANKL induces organized lymph node growth by stromal cell proliferation. J Immunol 188: 1245–1254. doi: 10.4049/jimmunol.1101513 PMID: 22210913
15. Zhang J, Varas F, Stadtfeld M, Heck S, Faust N, Graf T (2007) CD41-YFP mice allow in vivo labeling of megakaryocytic cells and reveal a subset of platelets hyperreactive to thrombin stimulation. Exp Hematol 35: 490–499. PMID: 17309829

16. Chai Q, Onder L, Scandella E, Gil-Cruz C, Perez-Shibayama C, Cupovic J, et al. (2013) Maturation of lymph node fibroblastic reticular cells from myofibroblastic precursors is critical for antiviral immunity. Immunity 38: 1013–1024. doi: 10.1016/j.immuni.2013.03.012 PMID: 23623380

17. Xiong J, Onal M, Jilka RL, Weinstein RS, Manolagas SC, O'Brien CA (2011) Matrix-embedded cells control osteoclast formation. Nat Med 17: 1235–1241. doi: 10.1038/nm.2448 PMID: 21909103

18. Link A, Vogt TK, Favre S, Britschgi MR, Acha-Orbea H, Hinz B, et al. (2007) Fibroblastic reticular cells in lymph nodes regulate the homeostasis of naive T cells. Nat Immunol 8: 1255–1265. PMID: 17893676

19. Onder L, Narang P, Scandella E, Chai Q, Iolyeva M, Hoorweg K, et al. (2012) IL-7-producing stromal cells are critical for lymph node remodeling. Blood 120: 4675–4683. doi: 10.1182/blood-2012-03-416859 PMID: 22955921

20. Perrault C, Moog S, Rubinstein E, Santer M, Baas MJ, de la Salle C, et al. (2001) A novel monoclonal antibody against the extracellular domain of GPIbbeta modulates vWF mediated platelet adhesion. Thromb Haemost 86: 1238–1248. PMID: 11816713

21. Chypre M, Seaman J, Cordeiro OG, Willen L, Knoop KA, Buchanan A, et al. (2016) Characterization and application of two RANK-specific antibodies with different biological activities. Immunol Lett 171:5–14. doi: 10.1016/j.imlet.2016.01.003 PMID: 26773232

22. Kamijo S, Nakajima A, Ikeda K, Aoki K, Ohya K, Akiba H, et al. (2006) Amelioration of bone loss in collagen-induced arthritis by neutralizing anti-RANKL monoclonal antibody. Biochem Biophys Res Commun 347: 124–132. PMID: 16815304

23. Eckly A, Strassel C, Cazenave JP, Lanza F, Leon C, Gachet C (2012) Characterization of megakaryocyte development in the native bone marrow environment. Methods Mol Biol 788:175–92. doi: 10.1007/978-1-61779-307-3_13 PMID: 22130708

24. Berlanga O, Emambokus N, Frampton J (2005) GPIIb (CD41) integrin is expressed on mast cells and influences their adhesion properties. Exp Hematol 33: 403–412. PMID: 15781330

25. Voisin B, Mairhofer DG, Chen S, Stoitzner P, Mueller CG, Flacher V (2014) Anatomical distribution analysis reveals lack of Langerin+ dermal dendritic cells in footpads and tail of C57BL/6 mice. Exp Dermatol 23: 354–356. doi: 10.1111/exd.12373 PMID: 24629018

26. Malhotra D, Fletcher AL, Astarita J, Lukacs-Kornek V, Tayalia P, Gonzalez SF, et al. (2012) Transcriptional profiling of stroma from inflamed and resting lymph nodes defines immunological hallmarks. Nat Immunol 13: 499–510. doi: 10.1038/ni.2262 PMID: 22466668

27. Ruddell A, Mezquita P, Brandvold KA, Farr A, Iritani BM (2003) B lymphocyte-specific c-Myc expression stimulates early and functional expansion of the vasculature and lymphatics during lymphomagenesis. Am J Pathol 163: 2233–2245. PMID: 14633598

28. Furuya M, Kirschbaum SB, Paulovich A, Pauli BU, Zhang H, Alexander JS, et al. (2010) Lymphatic endothelial murine chloride channel calcium-activated 1 is a ligand for leukocyte LFA-1 and Mac-1. J Immunol 185: 5769–5777. doi: 10.4049/jimmunol.1002226 PMID: 20937843

29. Duheron V, Hess E, Duval M, Decossas M, Castaneda B, Klöpper JE, et al. (2011) Receptor Activator of NF-kB (RANK) stimulates the proliferation of epithelial cells of the epidermo-pilosebaceous unit. Proc Natl Acad Sci USA 108: 5342–5347. doi: 10.1073/pnas.1013054108 PMID: 21402940

30. Bergmeier W, Schulte V, Brockhoff G, Bier U, Zirngibl H, Nieswandt B (2002) Flow cytometric detection of activated mouse integrin alphaIIbbeta3 with a novel monoclonal antibody. Cytometry 48: 80–86. PMID: 12116368

31. Wang Y, Jobe SM, Ding X, Choo H, Archer DR, Mi R, et al. (2012) Platelet biogenesis and functions require correct protein O-glycosylation. Proc Natl Acad Sci U S A 109: 16143–16148. doi: 10.1073/pnas.1208253109 PMID: 22988088

32. Boisset JC, Clapes T, Van Der Linden R, Dzierzak E, Robin C (2013) Integrin alphaIIb (CD41) plays a role in the maintenance of hematopoietic stem cell activity in the mouse embryonic aorta. Biol Open 2: 525–532. doi: 10.1242/bio.20133715 PMID: 23789102

33. Hodivala-Dilke KM, McHugh KP, Tsakiris DA, Rayburn H, Crowley D, Ullman-Cullere M, et al. (1999) Beta3-integrin-deficient mice are a model for Glanzmann thrombasthenia showing placental defects and reduced survival. J Clin Invest 103: 229–238. PMID: 9916135

34. Kong YY, Yoshida H, Sarosi I, Tan HL, Timms E, Capparelli C, et al. (1999) OPGL is a key regulator of osteoclastogenesis, lymphocyte development and lymph-node organogenesis. Nature 397: 315–323. PMID: 9950424

35. Cohen JN, Tewalt EF, Rouhani SJ, Buonomo EL, Bruce AN, Xu X, et al. (2014) Tolerogenic properties of lymphatic endothelial cells are controlled by the lymph node microenvironment. PLoS ONE 9: e87740. doi: 10.1371/journal.pone.0087740 PMID: 24503860

36. Ettinger R, Browning JL, Michie SA, van Ewijk W, McDevitt HO (1996) Disrupted splenic architecture, but normal lymph node development in mice expressing a soluble lymphotoxin-beta receptor-IgG1 fusion protein. Proc Natl Acad Sci USA 93: 13102–13107. PMID: 8917551

37. Gekas C, Graf T (2013) CD41 expression marks myeloid-biased adult hematopoietic stem cells and increases with age. Blood 121: 4463–4472. doi: 10.1182/blood-2012-09-457929 PMID: 23564910

38. Nieswandt B, Echtenacher B, Wachs FP, Schroder J, Gessner JE, Schmidt RE, et al. (1999) Acute systemic reaction and lung alterations induced by an antiplatelet integrin gpIIb/IIIa antibody in mice. Blood 94: 684–693. PMID: 10397735

39. Benezech C, Nayar S, Finney BA, Withers DR, Lowe K, Desanti GE, et al. (2014) CLEC-2 is required for development and maintenance of lymph nodes. Blood 123: 3200–3207. doi: 10.1182/blood-2013-03-489286 PMID: 24532804

40. Bazigou E, Xie S, Chen C, Weston A, Miura N, Sorokin L, et al. (2009) Integrin-alpha9 is required for fibronectin matrix assembly during lymphatic valve morphogenesis. Dev Cell 17: 175–186. doi: 10.1016/j.devcel.2009.06.017 PMID: 19686679

Supplemental Figure 1 (related to Figure 1)

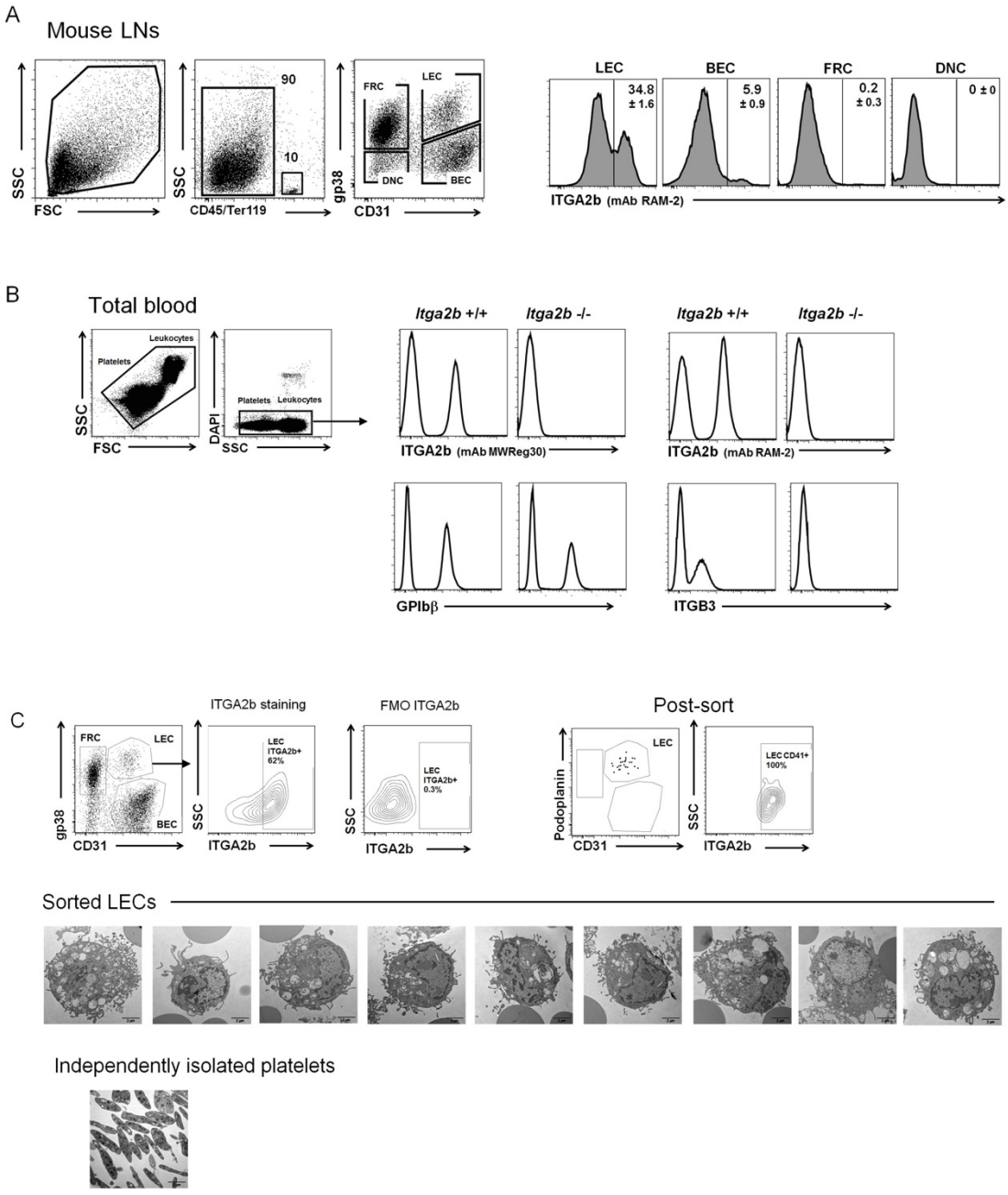

Supplemental Figure 2 (related to Figure 1)

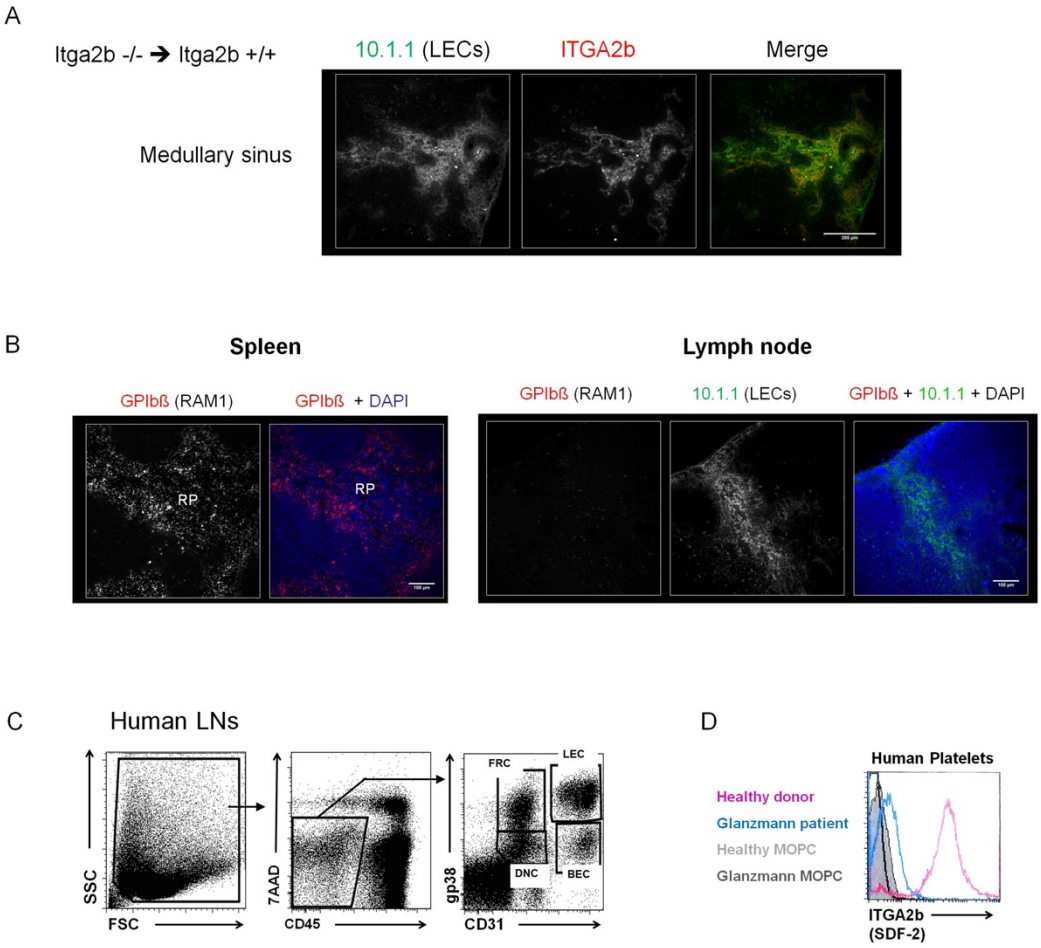

Supplemental Figure 3 (related to Figure 2)

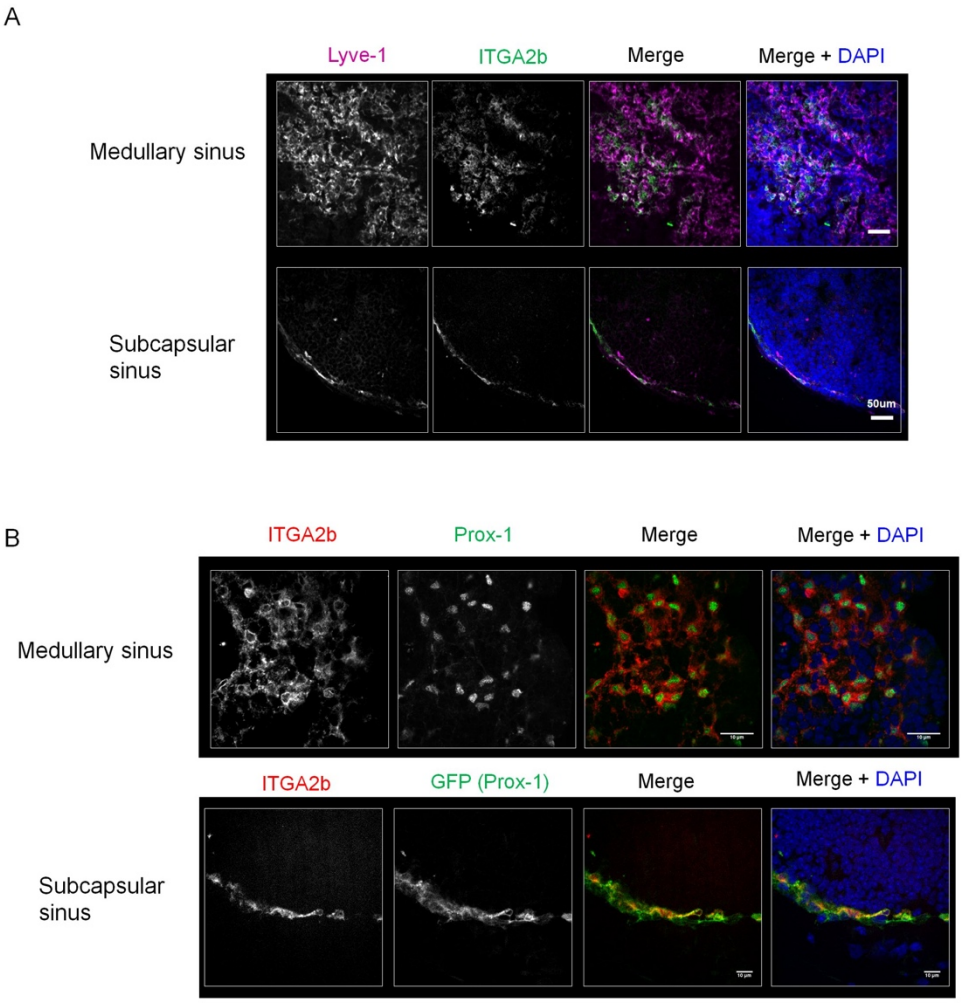

Supplemental Figure 4 (related to Figure 2)

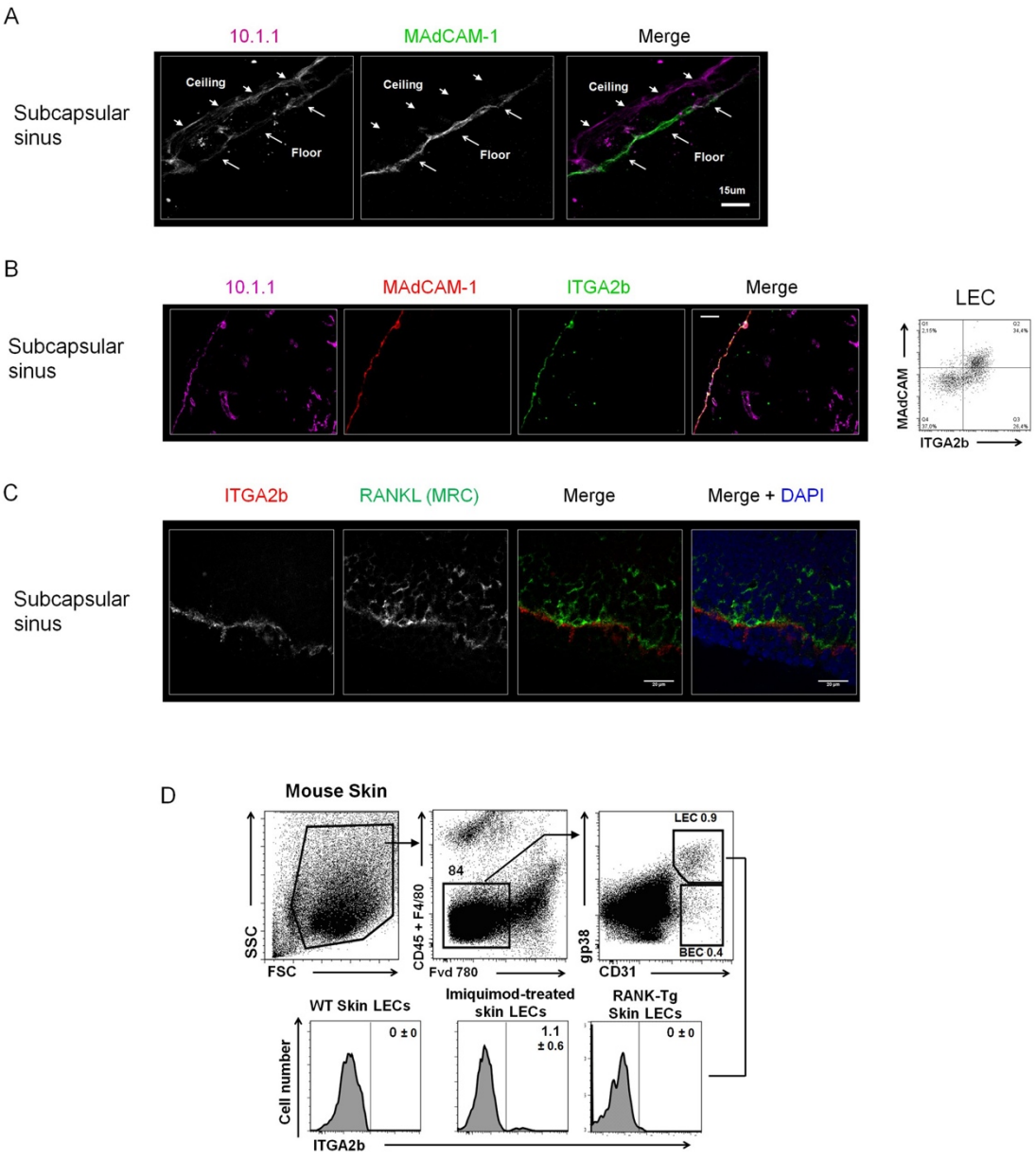

Supplemental Figure 5 (related to Figure 4)

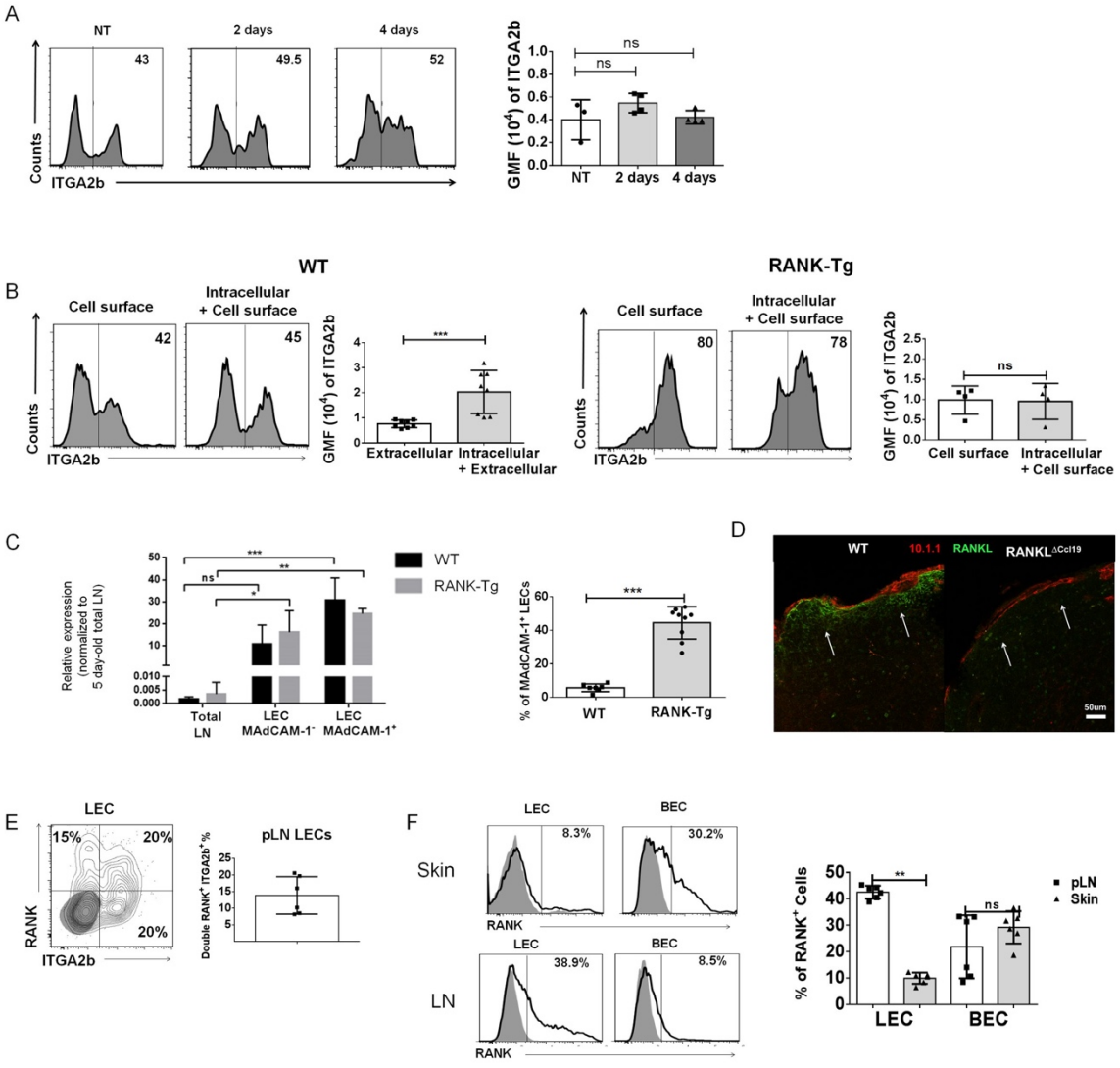

PERSPECTIVES AND CONCLUSIONS

Perspectives and Conclusions

1. Preliminary results and perspectives

1.1. LTβR regulates RANKL signaling in LNs

Since MRC RANKL is implicated in B cell follicle architecture regulation and IgM production, it is of interest to address the question of the molecular signals that regulate RANKL. LT signaling is known to be essential for B cell follicle homeostasis by controlling both FDC network and CXCL13 expression (see chapter 3). In addition, we showed that TNFR1 in the MRCs is also under control of RANKL which raises the question about an LTbR-RANKL-TNFR1 axis. Moreover, LTβR stimulation of embryonic mLN cell extracts with agonist antibodies leads to RANKL and VCAM-1 upregulation suggesting a regulatory role of LTβR on these molecules (*1*). In order to investigate the role of LTβR in RANKL regulation, we treated C57BL6/J mice with LTβR-Fc as described by Rennert and collaborators (*2*). Skin-draining LNs were harvested for qRT-PCR of RANKL, TNFR1 and CXCL13 mRNA of LTβR-Fc-treated and control mice (Figure P-1).

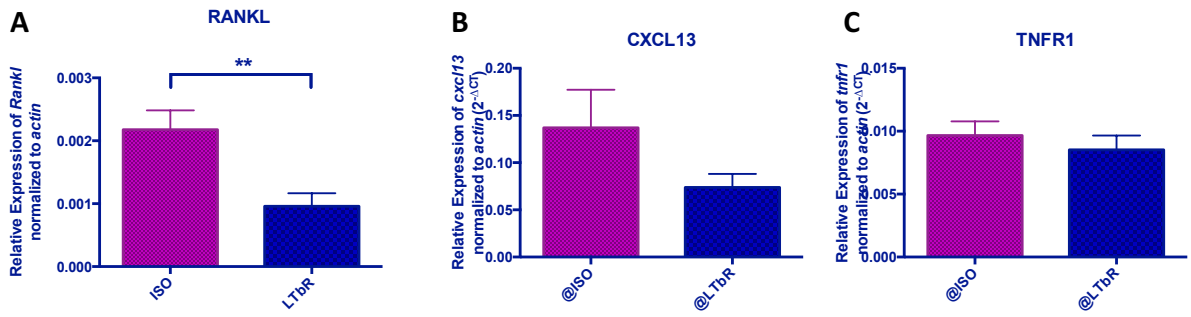

Figure P-1: Ltβr regulates Rankl and Cxcl13 expression but not Tnfr1. *Relative gene expression in c57BL6/J mice treated or not with anti-LTβR-Fc. Gene expression is normalized to actin, mean ±SEM, n=5. (A) significant down-regulation of Rankl in treated mice; (B) Cxcl13 down-regulation in treated mice is not statistically relevant; (C) Tnfr1 expression is unchanged. Mann-Whitney, significant p value <0,05, ** <0,001.*

We observed a significant down-regulation of RANKL in LNs of treated mice, CXCL13 showed a tendency of reduction, while TNFR1 was unchanged. These results show a regulation of MRC-RANKL by LT signaling. In order to confirm these observations, B cell

follicle staining could be performed by immunofluorescence. Moreover, an agonist treatment could be done on fibroblastic cell lines or MRCs in culture.

On the other hand, TNFR1 was not affected by LTβR blockade. Still, we showed in article 1 that TNFR1 is under RANKL control; and here we show that RANKL is under positive control by LTβR. One explanation for this discrepancy could be that the alterations of TNFR1 expression by RANKL only operate during embryogenesis / early postnatal days and not in the adult (LTbR agonist was administrated to adults). Once the Tnfr1 transcription regulatory mechanisms have been primed by embryonic RANKL the loss of RANKL (indirectly via LTbR blockage, or directly by RANKL-specific mAbs) would have no effect. Still, we cannot dismiss the possibility that the levels of RANKL or its duration are not sufficient to provoke Tnfr1 downregulation.

In order to better understand the role of LTβR in RANKL and TNFR1 signaling in the B cell follicle, we are experimenting with a new mouse model with LTβR deficiency in stroma. Since LTβR total mice do not develop LN, we want to specifically target stromal LTβR by crossing CCL19-Cre mice with LTβR knock in mice. We will study the incidence of this LTβR deficiency on RANKL expression, B cell follicle and B cell affinity maturation. Furthermore, complementation assay with recombinant RANKL could be performed in order to rescue the phenotype.

1.2. Functional relevance of reduced TNFR1 expression by RANKL-deficient MRCs in the regulation of MRC and FDC function

The role of TNFR1 in B cell follicle maintenance has been previously demonstrated (3). During my PhD, I showed that TNFR1 expression in B cell follicle is regulated by RANKL. In order to validate that the reduced TNFR1 expression is alone responsible for the observed phenotypes, we could try to complement it by administrating recombinant TNFα or by transferring lymphocytes from mice that overexpress TNFα. We expect thus to specifically (over)stimulate TNFR1 signaling and thus compensate for reduced TNFR1 expression and hence a normalization of CXCL13 expression and FDC formation. The B cells would therefore form distinct B cell follicles.

1.2.1. Complementation with recombinant TNFα

In order to test in vivo the RANKL-mediated TNFR1 expression for CXCL13 production and FDC formation, complementation test with increasing doses of recombinant TNFα (1, 10, 100 ng/kg) every 3 days would be performed on neonatal RANKL$^{\Delta CCL19}$ mice (*4*). At the age of 4 weeks, the expression of CXCL13 and the formation of FDCs will be analyzed by immunofluorescence and qRT-PCR. The choice of new-born mice is justified by their active engagement in B cell recruitment and FDC differentiation to constitute their LNs.

1.2.2. Lymphocyte transfer from TNF-overexpressing mice

Furthermore, a collaboration established by my PhD advisor and Jorge Caamano, University of Birmingham, UK would allow us to obtain TNF$^{\Delta ARE/+}$ mice. These mice express increased levels of TNFα under basal conditions, due to mutation in the gene causing a higher stability of its mRNA. TNF$^{\Delta ARE/+}$ B cells would be purified from LNs using standard negative-selection procedures and injected into newborn MRC$^{\Delta RANKL}$ mice. Both mice strains are on the same genetic background (C57BL/6) permitting B cell transfer without rejection. Newborn mice will receive different numbers of B cell (1 000, 10 000, 100 000 or 1 000 000) by a single intravenous i.v. injection. As control, wt B cells (not-overexpressing TNFα) will be transferred to MRC$^{\Delta RANKL}$ mice.

1.3. T cell RANKL and the humoral immune response

We showed that stromal RANKL is essential for B cell follicle stability in the steady state and for IgM secretion after an immune challenge. Because T cell RANKL does not play an essential role in the priming of DCs and the polarization of T cells, it is of interest to ask whether it regulates GC formation and Ig secretion. In order to address this question, we generated a mouse model in which RANKL is knocked out in T cells by crossing RANKL$^{flox/flox}$ mice (*5*) with mice containing a single copy of Cre-recombinase under the control of LCK (lymphocyte-specific protein tyrosine kinase) promoter (*6*). We injected mice with an immunization mix as described in figure P-2. KO mice were still able to form germinal centers.

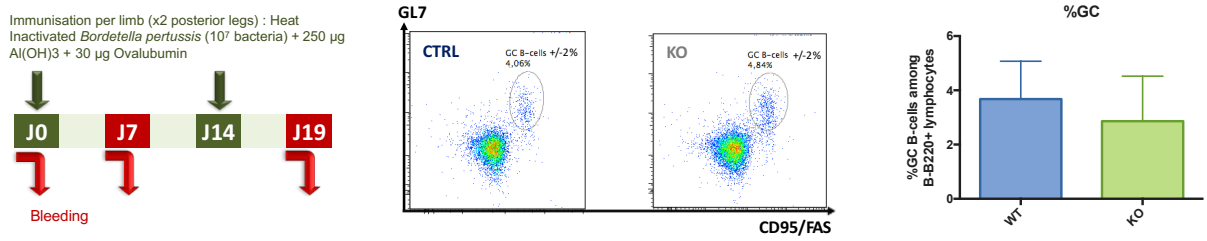

Figure P-2: RANKL$^{\Delta LCK}$ mice (deficient for RANKL in their T cells) normally form GCs. *(Left) Immunization protocol: mice were immunized into the hind leg footpads and blood drawn under the indicated times. (Middle) Dot plots showing the percentage of GC (GL7+ CD95+) B cells (B220+) in KO and control mice. (Right) Proportion ±SD of GC B cells among the B cell population (n=3), difference is not statistically relevant: p> (Mann-Whitney).*

Moreover, we performed 5-month immunization experiments with several boosts as described in figure P-3 in order to study the incidence of T cell RANKL deficiency on the long-term humoral immune response. IgM and IgG levels were measured at different times by OVA-ELISA. IgM levels in one experiment of three were significantly decreased after the second boost. This low level of IgM can be also seen in another experiment, but without statistical significance. On the other hand, IgG levels seem not to be affected which is concordant with a normal GC observed by flow cytometry. Hence, this result raises the question about a redundancy of T cell RANKL that allows the organism to overcome the deficiency.

In order to better understand the role of RANKL under immune activation, it would be necessary to eliminate both the stromal and the T cell RANKL sources by generating a chimeric mouse carrying such a double RANKL deficiency. RANKL$^{\Delta MRC}$ mice could be irradiated and bone marrow from RANKL$^{\Delta LCK}$ mice could be adoptively transferred. The mouse immune system would then be challenged as above in order to survey B cell follicle and GC formation as well as the long-term immune response.

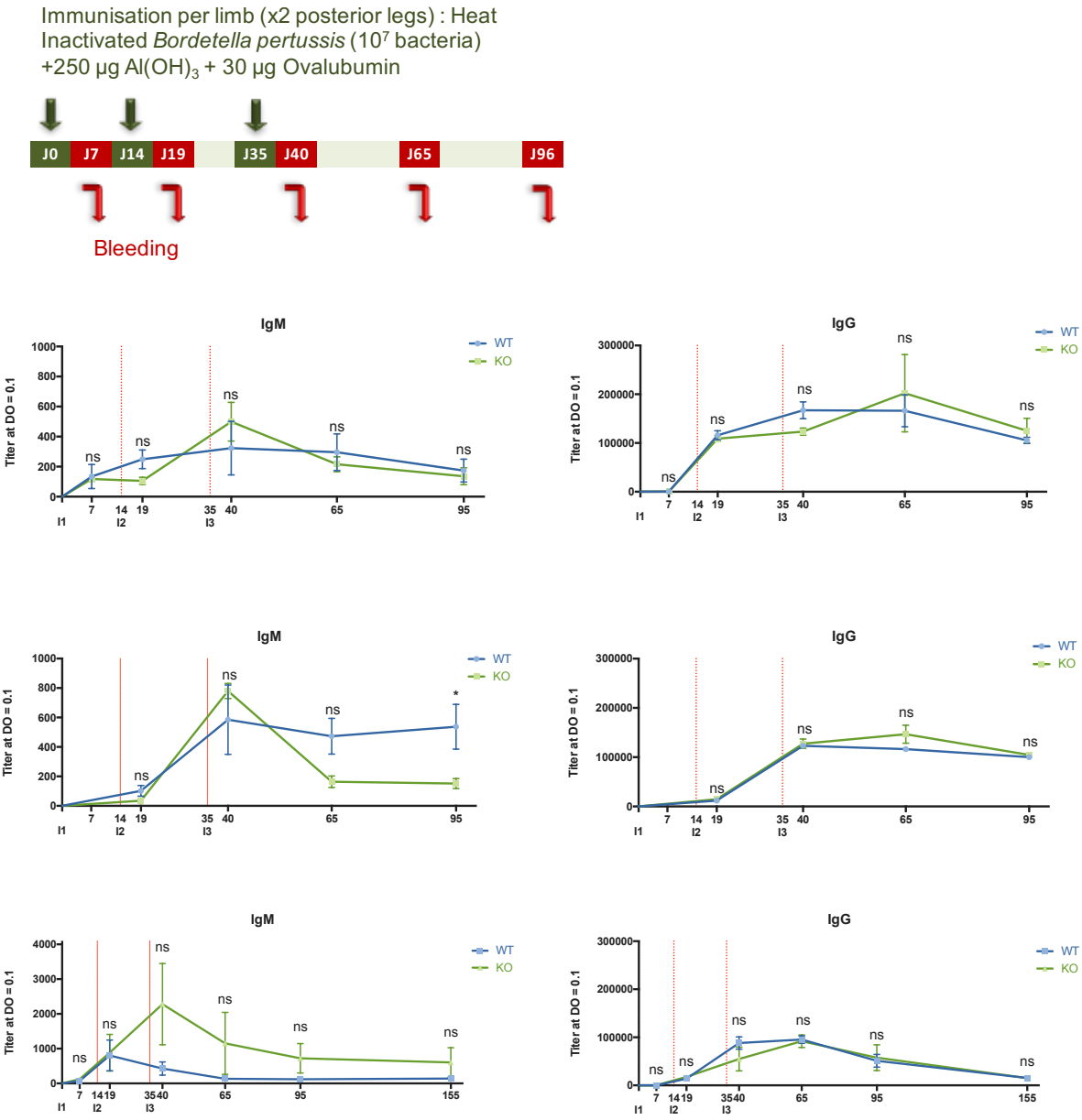

Figure P-3: T cell RANKL deficiency does not affect Ig secretion by B cells. *(Top) Immunization protocol: RANKL$^{\Delta LCK}$ mice were immunized into the hind leg footpads and blood drawn under the indicated times. (Bottom) Seric-chicken ovalbumin-specific IgG and IgM were measured by ELISA. Each graph represents an experiment conducted on 3 mice of each genotype. Statistical significance was tested (Mann-Whitney); p-values < 0.05 were considered as significant. *p <0.05, ns: non-significant.*

1.4. Potential role of LECs in immune homeostasis

1.4.1. RANKL signaling in LN stroma does not occur in an autocrine manner

As we showed in article 1, RANKL drives stromal activation. To address the question of whether this occurs in an autocrine manner by activating stromal RANK, we tested for the expression of RANK mRNA in FRCs. We also included LECs and BECs in the analysis. We found by qPCR that FRCs (TRC and MRCs) do not express RANK while both LEC and BEC do (Figure P-4). This shows that stromal cells cannot be directly activated by RANKL. This also makes the existence of an autocrine loop proposed for LTOs unlikely (7).

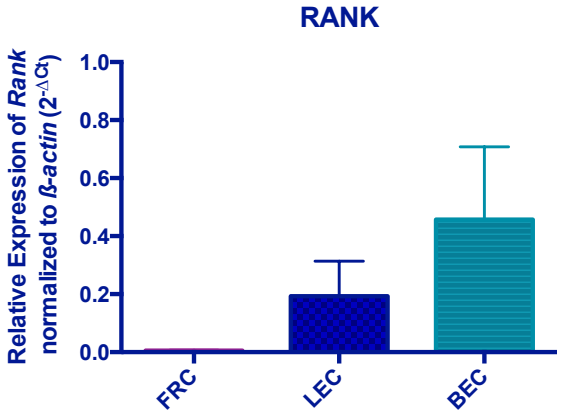

Figure P-4: RANK expression in different stromal subsets. *qRT-PCR has been performed on sorted stromal cells from C57BL6/J mice. PCR has been performed using the following primers: Forward 5'TGCGTGCTGCTCGTTCCA-3' and Reversve 5'- ACCGTCCGAGATGCTCATAAT-3'. Rank expression is not detectable in FRC subset (including MRCs) while it is clearly expressed in LECs and BECs.*

1.4.2. Role of LEC-RANK in RANKL-mediated immune homeostasis

These findings together with our data published in article 2, strongly support a direct activation of LECs by stromal RANKL. To show this experimentally *in vivo*, we generated mice deficient for RANK specifically in LECs by crossing $RANK^{flox/flox}$ mice (8) with Prox-1 cre ERT2 mice (9) to obtain a $RANK^{\Delta Prox\text{-}1}$ mouse. Since Cre-recombinase is under control of tamoxifen, we set up the condition of tamoxifen administration to efficiently delete RANK in LECs (Figure P-5). A loss of CXCL13 and FDCs in this LEC-RANK KO would mean that RANKL ensures B cell follicle maintenance through its interaction with RANK on LECs. If this were the case, we would then also measure TNFR1 expression.

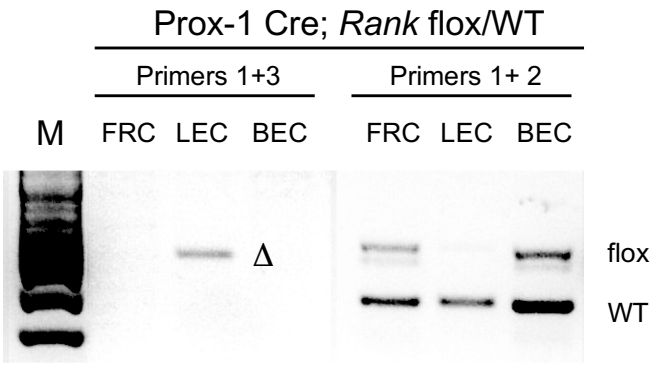

Figure P-5: Deletion of exon 2 and 3 of* the *Rank gene in genomic DNA of sorted LECs of RANK$^{\Delta Prox\text{-}1}$ mice after tamoxifen injection. *8-week old mice were injected with 3 mg of tamoxifen for 4 consecutive days then LECs were sorted and gDNA extracted. Two PCR reactions were performed using the protocol described by Rios and collaborators* **(8)**. *Primers 1 and 2 amplify a 469 bp fragment from the floxed locus and a 290 bp fragment from wt locus. Primers A and 3 amplifies a fragment of 392 bp resulting from the deletion of the floxed region by Prox1-cre recombinase.*

2. Conclusions

LNs are an important site of the adaptive immune response. They are highly organized and compartmentalized organs in order to optimize immune cell activity. Stromal cells, which are not of hematopoietic origins have been shown to play a crucial role for LNs in embryogenesis, in the steady state and during the immune response. Stroma is constituted of 2 major categories: endothelial cells and fibroblastic reticular cells. A newly identified fibroblastic reticular cell subtype (called MRCs) is not yet well characterized. Its localization between the B cell follicle and the capsular lymphatic sinus suggest a role of these cell in the homeostasis on the cortical area of the LN. MRCs express RANKL, a TNFSF member known to be essential for LN development and organogenesis. During my PhD, I aimed at studying the role of RANKL expressed by MRCs for the B cells and the humoral immune response.

I showed that MRCs express both RANKL and CXCL13, a chemokine known for its role in B cell chemotaxis. Furthermore, I showed that MRCs do not express RANK, and so there is no autocrine loop for RANK/RANKL signaling on MRCs. I studied a mouse model where RANKL is conditionally knocked-out in MRCs and found that the lack of RANKL leads to downregulation of stromal TNFR1 expression. Stromal TNFR1 is known to be crucial for B cell follicle formation and maintenance by signaling CXCL13 expression and FDC differentiation. Strikingly, the TNFR1 downregulation is still detectable after repeated immunizations suggesting a stable modification of the transcription regulatory elements. Many unclear zones need to be elucidated concerning the mechanism of regulation of stromal TNFR1 by RANKL, especially the cell type that expresses RANK and that mediates the RANKL-effects. One potential candidate cell is the LEC because it expresses RANK and responds to MRC RANKL and is localized next to the MRCs. Our next step will be to test this hypothesis using the $RANK^{\Delta Prox1}$. Moreover, to demonstrate that TNFR1 downregulation has functional consequences on TNFα/LTα signaling and is alone responsible for the observed phenotypes caused by the loss of RANKL, complementation studies with TNFα/LTα could be conducted.

In order to unveil the molecular and cellular mechanisms that govern RANKL expression by MRCs a role of LTβR signaling appears likely. Preliminary LTβR-blockade experiments in adult mice support this hypothesis. To go further, we generated a mouse model in which

LTβR is knocked-out in LN stroma. The incidence of this knock-out on B cell follicle, MRC RANKL and LEC activation will need to be studied.

Taken together, we can propose the following model of regulation of B cell-associated stroma in the steady state in the LN: MRCs express RANKL that binds RANK on LECs. LECs provide MRCs with TNFα that binds TNFR1 on MRCs and enhances CXCL13 expression in order to attract B cells. Further B cells provide in return MRCs with LTα1β2 that enhances LTβR signaling and so RANKL expression and differentiation into FDCs (Figure P-5).

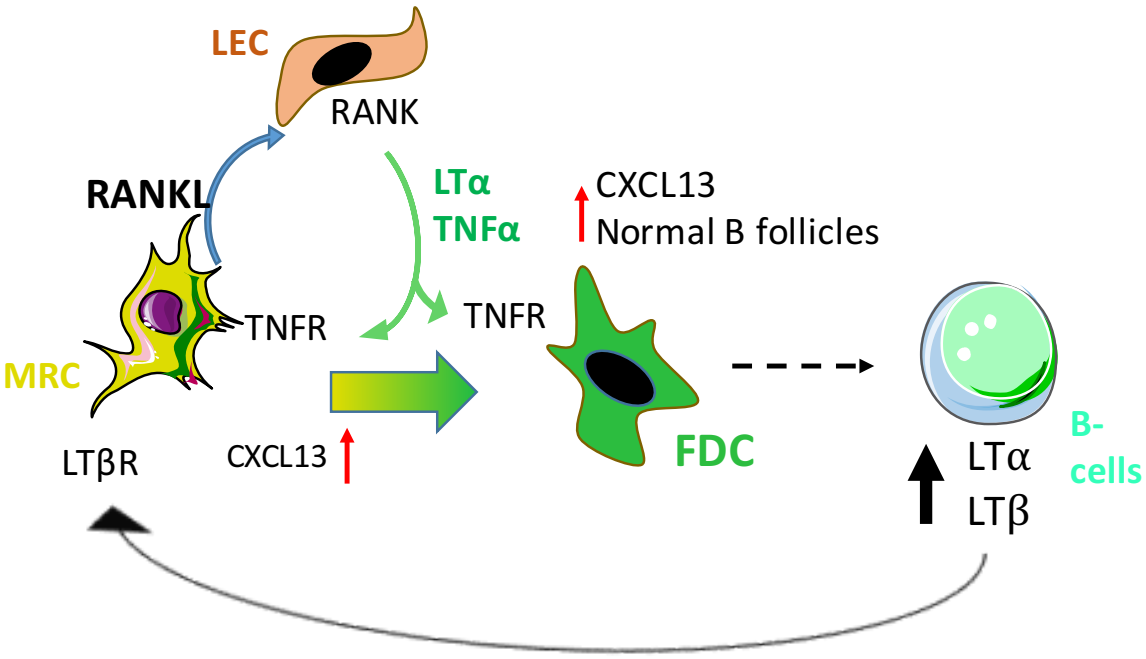

Figure P-5: schematic representation of our hypothesis concerning RANKL place in the B cell follicle homeostasis regulation and maintenance. *MRC express RANKL that binds RANK on LECs. LECs provide MRCs with TNFα that binds TNFR1 on MRCs and FDCs and enhances CXCL13 expression in order to attract B cells. B cells provide in return MRCs with LTα1β2 that enhances LTbR signaling and so RANKL expression.*

Under immune stimulatory conditions, we have shown that neither stromal RANKL nor T cell RANKL deficiency separately affect IgG secretion. Moreover, GC formation and B cell follicles appear normally formed suggesting the presence of a recovery mechanism that would implicate RANKL from other sources or compensatory other TNF(R)SF. Strikingly, IgM secreted after a two boosts are significantly decreased in stromal RANKL-KO and low TNFR1 expression by stroma is maintained. These findings suggest that some aspects of RANKL restriction on B cells is maintained that would implicate TNFR1 signaling.

3. Bibliography

1. M. F. Vondenhoff *et al.*, LTbetaR signaling induces cytokine expression and up-regulates lymphangiogenic factors in lymph node anlagen. *J. Immunol. Baltim. Md 1950*. **182**, 5439–5445 (2009).

2. P. D. Rennert, D. James, F. Mackay, J. L. Browning, P. S. Hochman, Lymph node genesis is induced by signaling through the lymphotoxin beta receptor. *Immunity*. **9**, 71–79 (1998).

3. M. Pasparakis *et al.*, Peyer's patch organogenesis is intact yet formation of B lymphocyte follicles is defective in peripheral lymphoid organs of mice deficient for tumor necrosis factor and its 55-kDa receptor. *Proc. Natl. Acad. Sci. U. S. A.* **94**, 6319–6323 (1997).

4. L. Huys *et al.*, Type I interferon drives tumor necrosis factor-induced lethal shock. *J. Exp. Med.* **206**, 1873–1882 (2009).

5. J. Xiong *et al.*, Matrix-embedded cells control osteoclast formation. *Nat. Med.* **17**, 1235–1241 (2011).

6. Y. Takahama *et al.*, Functional competence of T cells in the absence of glycosylphosphatidylinositol-anchored proteins caused by T cell-specific disruption of the Pig-a gene. *Eur. J. Immunol.* **28**, 2159–2166 (1998).

7. E. Hess *et al.*, RANKL induces organized lymph node growth by stromal cell proliferation. *J. Immunol. Baltim. Md 1950*. **188**, 1245–1254 (2012).

8. D. Rios *et al.*, Antigen sampling by intestinal M cells is the principal pathway initiating mucosal IgA production to commensal enteric bacteria. *Mucosal Immunol.* **9**, 907–916 (2016).

9. E. Bazigou *et al.*, Genes regulating lymphangiogenesis control venous valve formation and maintenance in mice. *J. Clin. Invest.* **121**, 2984–2992 (2011).

*****

Farouk ALLOUCHE

Role of RANKL in the differentiation of B cell associated stroma in secondary lymphoid organs

Résumé

RANKL (ligand du récepteur activateur de NF-KB) est un membre de la famille des TNF dont la signalisation passe par RANK et qui joue un rôle important dans la régulation immunitaire. Chez l'adulte, RANKL est exprimé constitutivement par des cellules réticulaires marginales (MRC) des ganglions lymphatiques. Comme les MRCs sont physiquement proches des lymphocytes B (LB) et ont été proposé d'être des précurseurs de cellules dendritiques folliculaires (FDC), RANKL pourrait jouer un rôle dans la différenciation du stroma associé aux LB et dans la réponse humorale. Afin de mieux comprendre la fonction de RANKL exprimé par les MRC, nous avons généré des souris déficitaires pour RANKL dans les cellules stromales. Nous avons constaté que la formation du follicule B était perturbée ainsi que le réseau FDC. Bien que RANKL ne soit pas requis pour la formation des MRC, il est nécessaire pour l'expression de la chimiokine CXCL13 par ces mêmes cellules. Parmi les TNFRSF dont la signalisation est requise pour l'expression de CXCL13 et la différenciation des FDC, le TNFR1 était significativement réduit dans les cellules stromales des souris dépourvues de RANKL stromal. Ainsi, RANKL pourrait constituer une nouvelle cible thérapeutique contre les immunopathologies des LB en agissant sur son stroma.

Mots Clefs : RANKL, ganglion lymphatique, MRC, follicule B, CXCL13, TNFR1

Résumé en anglais

RANKL (receptor activator of NF-κB ligand), a member of the TNF family that signals via RANK, plays an important role for immune regulation. In the adult, RANKL is constitutively expressed by marginal reticular cells (MRCs) of the lymph nodes. Because MRCs are positioned in close vicinity to B cells and may be precursors of follicular dendritic cells (FDCs), RANKL could play a role in the differentiation of B cell-associated stroma and the humoral immune response. In order to better understand the role of RANKL expressed by the MRCs, we generated mice with conditional RANKL deficiency in the stromal compartment. We found that the B cell follicle structure was disrupted and FDC network formation was reduced. Although RANKL was not required for MRC formation, it was necessary for the expression of B cell attracting chemokine CXCL13. Among the TNFRSF members known to control CXCL13 expression and FDC formation, we found that TNFR1 was significantly reduced in the RANKL cKO mice. Thus, RANKL may present a novel therapeutic strategy against B cell-mediated immunopathologies by acting on its stroma.

Keywords : RANKL, lymph node, MRC, B cell follicle, CXCL13, TNFR1